UNCLASSIFIED

AD NUMBER
AD882771
LIMITATION CHANGES
TO: **Approved for public release; distribution is unlimited.**
FROM: **Distribution authorized to DoD only; Specific Authority; MAR 1971. Other requests shall be referred to Army Aviation Systems Command, Attn: AMSAV-R-F, PO Box 209, St. Louis, MO 63166.**
AUTHORITY
usaavscom ltr, 12 nov 1973

THIS PAGE IS UNCLASSIFIED

AD882771

AD882771L

AD_____
RDTE PROJECT NO. 1X141807D174
USAAVSCOM PROJECT NO. 69-11
USAASTA PROJECT NO. 69-11

ENGINEERING FLIGHT TEST
AH-1G HELICOPTER (HUEYCOBRA)

D D C
RECEIVED
APR 26 1971
A

MANEUVERING LIMITATIONS

FINAL REPORT

RICHARD B. LEWIS, II
PROJECT OFFICER/ENGINEER

EDWARD E. BAILES
PROJECT ENGINEER

RANDY D. McCLELLAN
ENGINEER

JOHN D. CLAXTON
CPT, TC
US ARMY
PROJECT PILOT

MARVIN W. BUSS
PROJECT PILOT

WILLIAM J. CONNOR
CW4, AV
US ARMY
PROJECT PILOT

JOHN A. JOHNSTON
LTC, TC
US ARMY
PROJECT PILOT

MARCH 1971

This document may be further distributed by any holder only with specific prior approval of the CG, USAAVSCOM, ATTN: AMSAV-R-E, PO Box 209, St. Louis, Missouri 63166.

US ARMY AVIATION SYSTEMS TEST ACTIVITY
EDWARDS AIR FORCE BASE, CALIFORNIA 93523

DISCLAIMER NOTICE

The findings of this report are not to be construed as an official Department of the Army position unless so designated by other authorized documents.

DDC AVAILABILITY NOTICE

US military agencies may obtain copies of this report directly from DDC. Other qualified users shall request through the Commanding General, US Army Aviation Systems Command (USAAVSCOM), ATTN: AMSAV-R-F, PO Box 209, St. Louis, Missouri 63166.

REPRODUCTION LIMITATIONS

Reproduction of this document in whole or in part is prohibited except with permission obtained through the Commanding General, USAAVSCOM, ATTN: AMSAV-R-F, PO Box 209, St. Louis, Missouri 63166. DDC is authorized to reproduce the document for United States Government purposes.

DISPOSITION INSTRUCTIONS

Destroy this report when it is no longer needed. Do not return it to the originator.

TRADE NAMES

The use of trade names in this report does not constitute an official endorsement or approval of the use of the commercial hardware and software.

PRECEDING PAGE BLANK-NOT FILMED

RDTE PROJECT NO. 1X141807D174
USAAVSCOM PROJECT NO. 69-11
USAASTA PROJECT NO. 69-11

ENGINEERING FLIGHT TEST

AH-1G HELICOPTER (HUEYCOBRA)

MANEUVERING LIMITATIONS

FINAL REPORT

RICHARD B. LEWIS, II
PROJECT OFFICER/ENGINEER

EDWARD E. BAILES
PROJECT ENGINEER

RANDY D. McCLELLAN
ENGINEER

JOHN D. CLAXTON
CPT, TC
US ARMY
PROJECT PILOT

MARVIN W. BUSS
PROJECT PILOT

WILLIAM J. CONNOR
CW4, AV
US ARMY
PROJECT PILOT

JOHN A. JOHNSTON
LTC, TC
US ARMY
PROJECT PILOT

MARCH 1971

[redacted] the CG, USAAVSCOM, ATTN: AMSAV-R-F, PO Box 209, St. Louis, Missouri 63166.

US ARMY AVIATION SYSTEMS TEST ACTIVITY
EDWARDS AIR FORCE BASE, CALIFORNIA 93523

ABSTRACT

The AH-1G helicopter maneuvering limitations flight test program was conducted at Edwards Air Force Base, California, between 13 March and 4 May 1970. The purpose of the test program was to study in detail the characteristics of maneuvering flight and to identify any limitations required to improve flight safety. The program included investigation of steady-state turns, three types of return-to-target maneuvers, and simulated operational maneuvers. Repeated instances of untorquing of the tail rotor retention nut were encountered during flight and constituted a safety-of-flight deficiency. Four shortcomings were noted: 1) undesirable cyclic control force characteristics, 2) transient torque surge, 3) insufficient main rotor rpm overspeed margin, 4) lateral stability and control augmentation system instability. It was concluded that the maneuvering characteristics of the AH-1G are generally excellent and are suitable for operational use. A number of maneuvering characteristics should be emphasized during pilot training, and the information should be incorporated into the operator's manual. Several additions to the cockpit instrumentation are proposed, and further maneuverability testing is recommended.

TABLE OF CONTENTS

Page

INTRODUCTION

Background 1
Test Objectives 1
Description 1
Scope of Test 2
Methods of Test 3
Chronology 3

RESULTS AND DISCUSSION

General 4
Turning Performance 5
Bank Angle Versus Load Factor 6
Energy Maneuverability 9
Load Parameters During Banked Turns 10
Return-to-Target Maneuvers 12
Operational Maneuverability 16
Longitudinal Control Force Characteristics 16
Lateral Stick Position During Turns 16
Altitude Loss During Dive Recovery 16
Transient Torque Surge 17
Engine Torque Oscillation 17
Vibration Characteristics 18
RPM Increase with Angle of Attack 18
Cyclic Control Force Feedback 19
Normal Acceleration Cues 20
Lateral SCAS Instability 20
Miscellaneous 20
USAAVLABS Maneuvers 20
Tail Rotor Retention Nut Untorquing 21

CONCLUSIONS

General 24
Deficiencies and Shortcomings Affecting
Mission Accomplishment 24
Flight Characteristics 24
Instruments 25
Miscellaneous 25

Page

RECOMMENDATIONS 27

APPENDIXES

I. References 28
II. Basic Aircraft Information and Operating Limits 30
III. Data Reduction Methods 38
IV. Instrumentation 46
V. Test Data 56
VI. Distribution 84

INTRODUCTION

BACKGROUND

1. Operational experience with the AH-1G HueyCobra helicopter has revealed a number of phenomena associated with maneuvering flight. These characteristics include: transient engine torque changes during high roll rate maneuvers, cyclic control force feedback at high load factors, and inadequate altitude margins to recover from high g turns at low airspeeds. However, no *cautions* presently exist in the operator's manual (ref 1, app I) with regard to acceptable bank angles, normal load factors, roll rates, sideslip angles and/or maneuver control displacements. To better understand these phenomena, their interrelationships, and their impact on safety of flight, the US Army Aviation Systems Command (USAAVSCOM) requested (ref 2) that the US Army Aviation Systems Test Activity (USAASTA) investigate AH-1G maneuvering characteristics. The test plan (ref 3) was submitted in November 1969.

TEST OBJECTIVES

2. The primary objective of this engineering flight test was to identify limitations on bank angle, normal load factor, roll rate, sideslip angle and/or maneuver control displacement of the AH-1G helicopter, and to develop suitable methods for their presentation in the operator's manual. To accomplish the primary objective, it was necessary to develop new techniques for testing and data analysis. In addition, the test program presented the opportunity for USAASTA to gather comprehensive maneuvering data suitable for future analytical study.

3. Specifically, this test program was designed to identify the maximum steady-state turning capability of the AH-1G helicopter. Tests were performed to define, in terms of airspeed and/or altitude loss, the energy exchange associated with exceeding this capability. Finally, a series of simulated operational maneuvers was investigated to identify any limiting condition.

DESCRIPTION

4. The AH-1G is a derivative of the UH-1 series helicopter, redesigned for use in armed helicopter missions. The configuration features a narrow fuselage with tandem seating. A two-bladed, teetering "door hinge" main rotor and a two-bladed, delta-three hinged, teetering tail rotor are employed. No stabilizer bar is used; instead, a three-axis stability and control augmentation system (SCAS) is provided to improve the aircraft's flying qualities. The flight controls are hydraulically boosted, mechanical and irreversible. Conventional controls are provided the pilot, and the copilot/gunner has sidearm cyclic and collective controls. An electrically operated force trim system is provided to the cyclic and directional controls to

provide artificial feel and control centering. The elevator is synchronized with the longitudinal cyclic control. An integral chin turret and a stub wing having four external store stations are provided, making various armament configurations possible. The pilot fires the wing stores and can fire the chin turret only when it is in the stowed position. The copilot/gunner operates the turret weapons and can also fire the wing stores in an emergency. The wing stores can be jettisoned by the pilot or the gunner. The power plant is a Lycoming T53-L-13 turboshaft engine rated at 1400 shaft horsepower (shp) at sea-level (SL) static conditions. The engine is derated to 1100 shp at a 324-rpm main rotor speed because of the maximum torque limit of the helicopter's main transmission. The maximum gross weight (grwt) of the AH-1G is 9500 pounds. More detailed aircraft information and the operating limits of the helicopter are presented in appendix II.

5. The test helicopter, S/N 66-15247, was an early prototype AH-1G. Its empty weight in a clean configuration with test instrumentation was 5880 pounds with a center-of-gravity (cg) location at fuselage station (FS) 204.3 inches. An instrumented main rotor was provided by the Bell Helicopter Company (BHC) and was used to measure blade bending moments and loads in the rotating controls.

SCOPE OF TEST

6. The AH-1G maneuvering limitations program consisted of 22 test flights totaling 17.5 productive flight hours. A total of 31.3 flight hours were accumulated. Testing was conducted in the vicinity of Edwards Air Force Base (AFB), California, between 13 March and 4 May 1970. A majority of the testing was conducted in the heavy hog configuration (TAT-102 chin turret and two XM159 rocket pods on each stub wing). To assess the effect of drag, the clean configuration (TAT-102 turret and no wing stores) was also tested. Only the aft cg condition was tested since previous AH-1G test experience showed it to be the most critical for maneuver investigations. The effects of altitude and rotor tip Mach number were not determined. Main rotor speed was maintained at 324 rpm during maneuver entries and at the steady-state maneuver conditions. Three pilots flew each set of tasks to provide information on pilot variability.

7. The scope of test and its relationship to the test objectives are detailed in reference 3, appendix I, and in the Results and Discussion section of this report. One additional test flight was added to provide data for the US Army Aviation Materiel Laboratories (USAAVLABS) maneuverability study (ref 4).

8. The test program was conducted within the limits as established by the safety-of-flight release issued by USAAVSCOM (ref 5, app I). All tests were performed and supported by USAASTA personnel. Throughout the test program, sensitive test instrumentation was employed to record main rotor and control system loads, cockpit vibrations, control requirements, flapping angles, and aircraft attitudes.

9. The USAAVSCOM comments (ref 6, app I) to the draft test plan suggested avoidance of tests at load factors less than 1.0g. Recent tests conducted by BHC provide considerable data on maneuvering characteristics at less than 1.0g (ref 7). Because of the extensive build-up effort and tests required just to confirm the BHC results, maneuvering limitations at less than 1.0g were not included in the scope of these tests.

METHODS OF TEST

10. The test methods that were used for these tests are described in the Results and Discussion section of this report. Data reduction methods are described in appendix III. Tests were conducted in calm air to minimize the influence of atmospheric turbulence on the test data.

11. The data were obtained primarily from oscillograph records. Limited additional data were hand recorded by the flight test engineer and ground observers. A detailed listing of the test instrumentation, with the locations, ranges, desired accuracies, sensitivities, readability and calibration standard deviations of the sensors, is presented in appendix IV.

CHRONOLOGY

12. The chronology of the AH-1G maneuvering limitations test program is as follows:

Test request received	2	September	1969
Test plan submitted		November	1969
Test plan approved	12	December	1969
Instrumentation installation initiated	12	January	1970
Safety-of-flight release received	31	January	1970
Testing initiated	13	March	1970
Testing completed	4	May	1970
Advance copy of report submitted		December	1970

RESULTS AND DISCUSSION

GENERAL

13. The AH-1G maneuvering limitations test program was conducted in three parts: 1) steady-state turns, 2) return-to-target maneuvers, 3) simulated operational maneuvers. Repeated instances of untorquing of the tail rotor retention nut were encountered, and constituted a safety-of-flight deficiency. Four shortcomings were noted: 1) undesirable cyclic control force characteristics, 2) transient torque surge, 3) insufficient main rotor overspeed margin, 4) lateral SCAS instability.

14. During the first portion of the test program, the maximum AH-1G sustained load factor was defined for constant-speed, fixed-altitude, coordinated turns. This maximum sustained turning capability was then incrementally exceeded to determine performance at higher levels of aircraft total energy. Altitude and airspeed were individually decreased, trading off the vehicle's potential and kinetic energy. At a 9000-pound grwt and a 3000-foot density altitude (H_D), the AH-1G can sustain approximately 1.5g's in a level turn with full power (red line torque pressure). By decelerating or descending, a 2.0g turn can be sustained. It was found that the concept of energy maneuverability can be employed to normalize the power, speed and thrust data. Further, many load parameters displayed well-defined trends as functions of speed and equivalent thrust. The classical relationship between normal load factor (n) and bank angle (ϕ) ($n = 1/\cos\phi$) was found to be inaccurate, and substantially higher bank angles were required.

15. In the second part of the test program, three types of simulated return-to-target maneuvers were studied: 1) teardrop turns at constant altitude; 2) decelerating climbs, turns, and dives back to the target while not penetrating below the entry altitude; 3) teardrop turns with height loss allowed in order to minimize the return time. The vehicle kinematics, piloting tasks, vibration and load characteristics encountered were studied. It was found that return-to-target times varied substantially with pilot technique. The decelerating, climbing turn was clearly shown to be the fastest method of returning to a point target. In addition, that method resulted in the lowest vibration levels experienced by the crew and may offer some operational advantages.

16. During the final portion of the test program, a series of simulated combat maneuvers was investigated. Included were simulated gunnery runs, simulated ground fire evasion, terrain-following flight, and rapid roll and pitch rates while maneuvering in close proximity to the ground. Although the flight characteristics mentioned in paragraph 13 were in evidence during these flights, the maneuverability characteristics of the AH-1G are considered satisfactory for operational use. Adequate control of aircraft attitudes and rates is available to permit nap-of-the-earth maneuvering and terrain-following flight. The aircraft can be maneuvered adequately to accomplish the required operational tasks without encountering control force feedback or torque or rotor speed surging. When these

characteristics are encountered, the required reduction in maneuver rate or engine power is small and does not reduce the operational capability. The maneuvering characteristics of the AH-1G helicopter are generally excellent and are suitable for operational use.

17. Several recent USAASTA test programs have been performed to investigate certain aspects of AH-1G maneuvering performance and handling qualities. To avoid duplication of effort, maximum use was made of previous data. These data included rotor loads information obtained during the stabilized night sight test program (refs 8 and 9, app I); performance, handling qualities, and vibration information from the Phase D airworthiness and flight qualification test program (refs 10 through 12); and turning performance and dive recovery information gathered during Phase D supplementary tests (ref 13).

TURNING PERFORMANCE

18. During the first portion of the test program, the basic stability, control, performance, vibration and structural loads characteristics of the AH-1G were investigated during controlled, steady-state turns. Each of three pilots was asked to execute windup turns (holding both altitude and airspeed constant) while incrementally increasing bank angle for each new test point until the maximum allowable engine torque was reached. Data were recorded at each stabilized point. Both right and left turns were executed, although each pilot performed most turns in only one direction. Two gross weights (approximately 8000 and 9200 pounds) were studied to establish dependence of maneuvering parameters on equivalent thrust (the product of normal acceleration and gross weight). Figure A illustrates the V-n diagram achieved.

19. Next, the turning performance was determined for conditions exceeding the steady-state capability of the aircraft by utilizing excess potential or kinetic energy. The first method, utilizing potential energy, was to fly constant load factor, constant airspeed turns at constant (red line) engine power and attain increased load factor with increasing rate of descent (R/D). The second method was to fly constant load factor, constant altitude turns at constant engine power and attain increased load factor by decelerating. The piloting task for this latter maneuver was very difficult because of the rapid increase in deceleration required with increasing load factor, the very high turn rates at the lower airspeeds (less than 80 knots indicated airspeed (KIAS)), and the rapidly changing bank angle, load factor and airspeed relationships during the maneuver. Considerable flight time was required to gather these data. Several practice runs were needed by each pilot before acceptable performance was achieved; and even then, a much higher than normal number of data runs were aborted and restarted because of unacceptable condition deviations. Figure A shows the resulting maneuver performance.

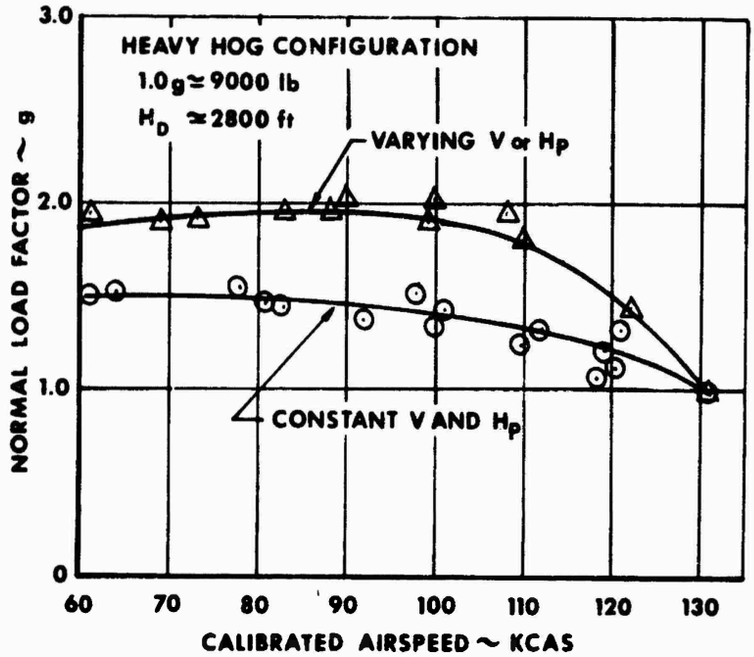

Figure A. Test V-n Diagram.

Bank Angle Versus Load Factor

20. Following initial examination of the data, it became evident that the theoretical relationship between normal acceleration and bank angle ($n = 1/\cos \phi$) was not confirmed by the test data. Figure B illustrates that substantially higher bank angles were required than the simple theory predicts. Review of the main rotor flapping angle data indicated that lateral flapping varied no more than 1 degree between level flight and 2g's. Hence, it was concluded that flapping was not the cause of the high measured bank angles. Accuracy of the cg normal accelerometer (approximately 0.01g, equivalent to 1.2 degrees at a 2.0g load factor) and the roll attitude gyro (approximately 0.5 degree) could not have caused the large shift in measured bank angle per g. The absence of a reliable means of measuring main rotor thrust (para 31) prevented cross-checking the cg normal acceleration data. Large damping capacitors in the rate gyro circuits complicated cross-checking the roll attitude data. However, careful examination of the data supports consistently higher bank angles. Reference 13, appendix I, also shows bank angle data considerably higher than the $n = 1/\cos \phi$ theory requires.

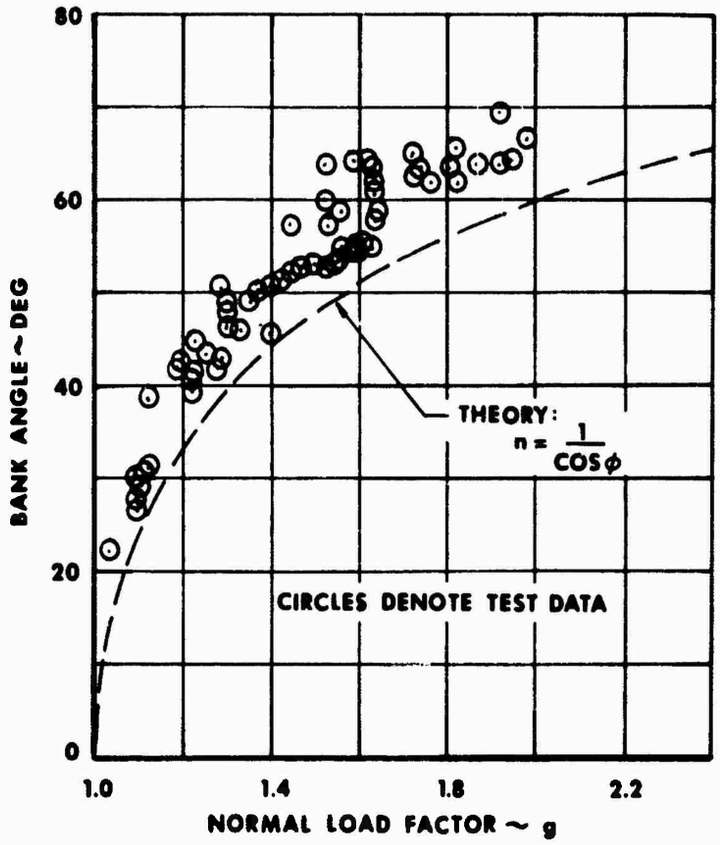

Figure B. Bank Angle and Normal Load Factor Relationships.

21. The above discrepancy between bank angle data and theory was reported in reference 14, appendix I. Reference 15 subsequently suggested that the following analysis be applied to define the relationship of normal load factor and aircraft attitudes. Coordinated flight actually requires only that the ball of the turn-and-bank indicator be centered. This requires a zero net side force in the body axis system. Because of aerodynamic side-force characteristics, this can occur in the presence of some sideslip. In addition, the analysis discussed in paragraph 20 neglects both angle of attack and pitch attitude. If these terms are taken into consideration, analysis (app III) yields:

$$n \cos \phi = \cos \theta \quad \cos^2 \phi + \cos \theta \frac{\sin^2 \phi}{1 + K}$$

$$+ \frac{\sin \phi \quad \tan \beta \quad \sin \theta}{1 + K}$$

Where: $K = \dfrac{\tan \theta \quad \tan \alpha}{\cos \phi}$

θ = Pitch attitude

β = Sideslip angle

α = Angle of attack

At 2g's and 100 knots true airspeed (KTAS), the above analysis indicates that each degree of nose-down angle of attack requires approximately one additional degree of bank angle. Similarly, 1 degree of nose-down pitch requires 0.2 degree of increased bank angle. Pitch attitude is the least sensitive with 1 degree of nose-down pitch requiring 0.1 degree of additional bank angle.

22. A comparison of the test data and the more elaborate theory is presented in figure 1, appendix V. The large scatter band relative to the range of test values indicates that additional test data and analysis may be required for better correlation.

23. At present, the operator's manual employs the simple relationship of paragraph 20 in presenting maneuver data and is incorrect. Therefore, the data of figure B should be substituted. In addition, the turn radii cited in the operator's manual presuppose an instantaneous and constant load factor throughout a turn. Reference 13, appendix I, presents detailed test data on turning performance which should be included in the operator's manual.

24. Throughout the test program, the attitude indicator installed in the test aircraft exhibited excessive precession during maneuvers. The errors in bank and pitch attitude were as much as 30 degrees. This instrument is unacceptable for use in a highly maneuverable helicopter such as the AH-1G. A modification work order (MWO) number 55-1520-221-30/19 was established to provide an improved attitude indicating system for AH-1G helicopters. This MWO was not incorporated on the test aircraft. Because of the high degree of maneuverability available and flight maneuvers required during tactical operations (some in limited visibility conditions during day and/or night), an accurate, reliable attitude indicating system is essential for flight safety. This attitude indicating system MWO should be evaluated by USAASTA for confirmation of instrument capability and performance.

Energy Maneuverability

25. The analytical process which relates maneuver capability to the rate of change of energy is termed "energy maneuverability." It provides a means of normalizing maneuvering performance in the same frame of reference as level flight performance. Instead of measuring only thrust, engine power and speed, the normal load factor, rate of climb (R/C), acceleration and rotor energy must also be specified. The latter are converted into equivalent thrust and equivalent power. Equivalent thrust (T_{equiv}) is the product of normal load factor (n) and gross weight (W) ($T_{equiv} = nW$). Equivalent power (P_{equiv}) is the combination of engine power and the time rate of change of kinetic energy, potential energy, and rotational energy:

$$P_{equiv} = P_{eng} - mV\frac{dV}{dt} - W\frac{dh}{dt} - I\Omega\frac{d\Omega}{dt}$$

Where: P_{eng} = Engine power (lb-ft/sec)

m = Aircraft mass (slugs)

V = True airspeed (ft/sec)

$\frac{dV}{dt}$ = Acceleration (+) or deceleration (-) (ft/sec^2)

$\frac{dh}{dt}$ = Rate of climb (+) or sink (-) (ft/sec)

I = Main rotor inertia (slug-ft^2)

Ω = Main rotor rotational frequency (rad/sec)

Advance ratio (μ) is true airspeed (V) divided by main rotor tip speed (ΩR) ($\mu = V/\Omega R$). Using the above terms, maneuvering performance can be plotted along with level-flight data. The higher thrust and power levels reflect both load factor and energy exchange. An expanded discussion of energy maneuverability, as it applies to rotary wing aircraft, is presented in reference 16, appendix I.

26. Equivalent power and thrust data for the AH-1G are summarized in figure 2, appendix V. The data are a composite of 10 flights during which altitude and airspeed were varied individually. Depending on the manner in which each data point was achieved, different trim attitudes were present. As a consequence, considerable scatter was noted in the raw data. However, well-defined loci of minimum powers required to achieve a given speed and equivalent thrust were evident. Figure 2 presents these minimum equivalent powers. It is emphasized that trim conditions other than those required to reproduce the data in figure 2 will induce higher equivalent power requirements.

27. An analysis of the energy maneuverability data revealed the following:

a. Equivalent main rotor thrust, equivalent power, and advance ratio appear to be valid scaling parameters for the family of data obtained.

b. Power divergence accompanying rotor stall is quite gradual, as is seen by the spacing of adjacent equivalent thrust increments.

c. The characteristic trends (shapes and curvatures) of nonmaneuvering data (thrust coefficient (C_T), power coefficient (C_P), and μ) continue to hold for maneuvering performance.

28. The power required for level flight, obtained as a base-line reference during these tests, was consistently 26 horsepower (hp) higher than the data reported in reference 11, appendix I. Efforts were made to reconcile this discrepancy; however, no solution was found. The aircraft and engine and engine calibrations were identical. One difference in instrumentation was that, for this test, a differential pressure transducer was used to record engine torque; while in the testing reported in reference 11, two absolute pressure gages were used to record output and reservoir pressures. In addition, data were recorded continuously on an oscillograph during this test; while the former data were recorded from aircraft-type instruments mounted in a photopanel.

29. The energy maneuverability data in figure 2, appendix V, can be used to develop sink rate and deceleration associated with maneuvering flight when power required exceeds power available. If available power is known, it is possible to plot either rate of descent required to sustain constant airspeed and load factor or deceleration required to sustain constant altitude and load factor. These data are plotted for one gross weight and for maximum power setting in figures 3 and 4.

Load Parameters During Banked Turns

30. Loads measured in the rotor and control system are shown versus speed and aircraft load factor in figures 5 through 14, appendix V. Data are plotted for main rotor thrust link axial load, main rotor flapwise bending moment at radial station 46, main rotor chordwise bending moment at radial station 135, rotating pitch link axial load, and longitudinal push rod axial load. Both mean values and peak-to-peak oscillatory amplitudes are presented. Because of the large amount of data and the corresponding manpower requirements, no attempt was made to harmonically analyze the load data. The data were obtained from two gross weight values (approximately 8000 and 9100 pounds) but are plotted at discrete values of equivalent thrust. The data and fairings employed are in good agreement with references 9 and 17, appendix I. It is noteworthy that all the parameters correlate well with equivalent thrust. Any effects of drag between the two configurations tested are masked by data scatter.

31. The main rotor thrust link restrains the main transmission to the airframe structure. The transmission is also dynamically isolated at five points through Lord mounts. It should be noted that the control linkages provide additional load paths between rotor and airframe. The mean thrust link load data are shown in figure 5, appendix V. The mean axial thrust link load did not equal the airframe weight (excluding main rotor and transmission) during steady level flight. No ratio of increased indicated thrust link load to aircraft normal load factor was evident in maneuvering flight. Furthermore, as speed increased, main rotor thrust should have increased slightly. The mean thrust link axial load reached a maximum below 105 KTAS and diminished as airspeed was increased. The variation in mean thrust link load with speed and normal acceleration indicated that both the isolators (Lord mounts) and the control rods were transmitting some variable fraction of the total rotor thrust to the airframe. Examination of the peak-to-peak thrust link axial loads (fig. 6) shows a marked increase at speeds above and below 85 KTAS. The vibratory amplitude was frequently 50 percent of the mean load. This would tend to reduce the validity of the thrust link as an indication of steady main rotor thrust. It is concluded that the thrust link is not a useful means of measuring AH-1G total thrust and that some other approach (such as flap bending in the blade root region) should be developed.

32. Main rotor flapwise bending moment data at radial station 46 are shown in figures 7 and 8, appendix V. The flapwise bending moment data show good grouping with respect to equivalent thrust. An S-shape is noted in both the mean and peak-to-peak moment values, with maxima around 80 to 85 KTAS and minima near 100 KTAS. Both mean and vibratory moments rise uniformly with normal load factor, and only moderate scatter is noted with respect to the data fairings shown. The peak-to-peak moment levels diverge sharply upward in the vicinity of V_H, the maximum speed for level flight (about 130 KTAS for the heavy hog configuration).

33. Main rotor chordwise bending moment data at radial station 135 are presented in figures 9 and 10, appendix V. The mean values are only moderately dependent on airspeed. Peak-to-peak levels are lowest at the lowest airspeeds tested, rise to a plateau in the 95 to 125 KTAS region, and then rise again as V_H is approached. Like the flapwise bending moment data, the chordwise bending moments correlate well with equivalent thrust. In the case of the mean chordwise data, this is to be expected since the interrelationships between equivalent thrust and equivalent power (hence torque, hence steady chordwise bending) have been established (para 26).

34. Rotating pitch link axial load data are shown in figures 11 and 12, appendix V. The mean values are highest around 105 KTAS and become less with increasing or decreasing airspeeds. The oscillatory loads rise slightly with increasing airspeed. These data also correlate well with equivalent thrust.

35. Longitudinal push rod axial load data are presented in figures 13 and 14, appendix V. The mean values are nominally insensitive to variations in airspeed but are strongly influenced by load factor. Oscillatory values exhibit pronounced minima between 85 and 95 KTAS, diverge sharply in the vicinity of V_H, and are also strongly influenced by normal load factor. Again, the equivalent thrust parameter serves to correlate these data.

36. Three additional load parameters were recorded during the test program: 1) main rotor flapwise bending moment at radial station 60, 2) main rotor drag brace axial load, 3) lateral push rod axial load. They were considered to be of secondary importance and were not reduced or presented because of manpower and schedule limitations.

RETURN-TO-TARGET MANEUVERS

37. During the second portion of the AH-1G maneuvering limitations test program, a series of return-to-target maneuvers was investigated. Three different maneuvers were performed by each of three pilots to determine pilot technique and vehicle constraints influencing the time required to return over a point target and, also, the overall aircraft behavior during a complex, highly transient maneuver. The maneuver patterns were flown over flat terrain having an orthogonal system of dirt roads with intersections every statute mile A ground vehicle was positioned at the reference crossroad, and two ground observers recorded time from the instant the aircraft passed directly overhead until it completed the return-to-target maneuver. These observations were averaged for each run. In addition, the pilot was instructed to count down as he approached the point. This was monitored via radio and corresponded closely to the ground observers' track of the aircraft. Tests were conducted in calm air (winds less than 5 knots) to reduce the influence of wind. Several turns were flown on reciprocal headings to further check the influence of wind. Limited data and pilot observations from a flight in winds greater than 5 knots confirmed that wind is a significant factor. Consequently, the test results reported herein are valid only for calm air conditions. Only right turns were tested since data from the Bell Model 209 evaluation (ref 18, app I) had indicated no effect of direction on level teardrop turns. Phase D tests (ref 13), however, indicated that right return-to-target maneuvers at high gross weights could be accomplished 10 to 20 percent faster than left turning maneuvers. A few check points during this test program confirmed the latter findings. The effects of gross weight were checked by performing the same maneuvers at the beginning and end of each flight. No perceptible influence was noted for gross weight variations of as much as 1000 pounds. The data presented in reference 18 also showed no effect of gross weight, although reference 13 reported a small gross weight influence.

38. The pilot instructions for the three types of turns were given as indicated below. Each type of turn was accomplished at entry airspeeds of 60, 75, 90, 105 and 120 KIAS. Ground-observed times and oscillograph data were recorded during each turn.

a. *Level return-to-target or teardrop turn:* "Perform a turn at constant altitude and fly over the entry point on any heading in the minimum amount of time."

b. *Diving return-to-target:* "Perform a turn, descend as desired during the maneuver, and fly over the entry point in the minimum amount of time. Restrict height loss to approximately 1000 feet."

c. *Climbing return-to-target or climbing pedal turn:* "Perform a turn, climbing first and then diving, as desired, to fly over the entry point at the entry altitude in the minimum amount of time."

39. The selection of right versus left turns was influenced by the transient rotor torque characteristics associated with rapid roll rates at high airspeeds. Transient torque increases are experienced with left roll rates, and torque decreases accompany right roll rates (ref 19, app I). For high-power, high-airspeed entry conditions, right turn entries were less demanding than left turn entries because the engine torque tended to decrease with the right roll. However, the recovery from the maximum performance right turns (involving left roll) required considerable pilot effort and attention to avoid an overtorque condition and excessive rotor rpm droop. The recovery task from right turns (rapid left roll at high collective and power settings) was much more difficult and demanding than a left rolling entry task. There could be even more difference for lower-powered entry conditions. It was concluded that left return-to-target maneuvers require less pilot effort and may be preferred for operational use.

40. Return-to-target times for each maneuver are shown for individual pilots in figure 15, appendix V, and for each maneuver in figure 16. For clarity the data in figure 15 are averaged for each pilot while all test data points are shown in figure 16. The typical test sequence was for each pilot to perform each maneuver at a given entry speed, then repeat this procedure at the next higher speed, and so on.

41. The level teardrop turns were accomplished with each of the three pilots using slightly different techniques.

a. Pilot number one initiated the maneuver with coordinated cyclic and collective inputs to achieve a steep banked attitude which was limited by maximum power and vibration. Altitude control throughout the maneuver required considerable pilot attention. During the entry, there was a strong tendency to overbank and lose altitude. During the acceleration phase, the pilot felt a strong urge to dive toward the target. All turns were made with coordinated directional control; the pilot did not care to establish a yaw by using uncoordinated pedal inputs. This technique resulted in the fastest return-to-target time at low entry speeds but was noticeably slower at speeds greater than 95 knots calibrated airspeed (KCAS).

b. The technique used by pilot number two was to initiate a roll rate when the entry point was passed. The collective was lowered as the desired bank attitude was approached, and aft cyclic was applied to establish the turn rate and deceleration flare. When the airspeed reached approximately 70 KIAS, the collective was increased until maximum engine torque was applied. The rollout heading was reached at very nearly the same time as maximum torque was applied, and the aircraft was accelerated toward the entry point. Only moderate load factors were applied during deceleration and turn because of the rapid increase in pilot workload required to control aircraft attitude, turn rate and rotor rpm as the load factor was increased. This technique resulted in the slowest return-to-target times at low entry speeds.

c. The technique used by pilot number three was to rapidly roll into a 65- to 75-degree bank attitude. Aft cyclic was used to increase load factor as the bank was established. The collective was increased to establish maximum power. The entry roll rate and load factor during the turn were pilot limited at a tolerable (but high) vibration level. Both load factor and bank angle were maintained as the airspeed decreased to approximately 70 KIAS. At this point, the bank attitude and load factor were reduced in a manner such that constant turn rate and airspeed were maintained. The roll attitude was then leveled, and the aircraft was accelerated toward the entry point. Aircraft attitudes and rates were easily controlled throughout the turn maneuver as long as the airspeed was not allowed to decrease below 60 KIAS. At lower airspeeds, the control task increased very rapidly; and on two occasions, the aircraft "fell through" the turn and developed a high sink rate. The sink rate resulted from an inability to maintain sufficient load factor at the high bank attitude. At low airspeeds, less than 60 KIAS, the turn rate resulting from a 1.5 to 2.0g banked turn is very fast, and the control task is difficult. The maximum transient load factors (approximately 2.5g's) were achieved only for airspeeds greater than 100 KIAS. This third pilot's technique produced the fastest return-to-target times at the high entry speeds.

42. It should be noted that considerable differences in return-to-target times were achieved by different pilots. A standard deviation of 1.01 seconds was calculated for the level turns. From a statistical viewpoint, this represents a very large scatter band. The influence of technique on the teardrop turn must be considered when applying this maneuver as a standard of aircraft agility. Further, the large variations seen in the test results degrade precise quantitative comparisons of maneuvering performance.

43. The diving return-to-target maneuvers produced the largest time variations for each pilot and between each of the pilots. The measured standard deviation was 1.57 seconds. The quickest return times were obtained by pilot number three using a similar deceleration technique as for the level turn maneuver, followed by a steep angle dive toward the entry point. Pilot number one also used a technique similar to the level turn but restricted the rate of sink to control altitude lost in the turn. This pilot felt that improved return times could be achieved by permitting greater altitude loss. Pilot number two maintained a higher airspeed (equal to or greater than the entry airspeed) throughout the maneuver and relied on the

maximum load factor to tighten the turn. This technique was not only much slower but also resulted in much higher vibration levels experienced by the crew. The small difference in return-to-target times between level and diving turns indicates that very little was gained by exchanging potential energy for airspeed during the acceleration back to the entry point.

44. The climbing return-to-target maneuvers were accomplished with the least variation in technique by the three pilots. The resulting performance and standard deviation (0.33 second) also displayed close agreement. Each maneuver was begun with an aft cyclic input to establish a steep decelerating climb. At a suitable lower airspeed (40 to 60 KIAS), the aircraft was abruptly turned using lateral cyclic and directional pedals. The turn terminated in a steep dive, and full power was applied to accelerate back over the entry point. This maneuver was the quickest and easiest to accomplish for each of the three pilots. Only moderate load factors were required during the maneuver, and vibration level never became a problem.

45. Several general observations are made with regard to pilot performance and applicability of these return-to-target maneuvers:

a. The longest return times were achieved by a pilot whose maneuvers, although coordinated, were qualitatively assessed to result in the most severe vibrations and g levels encountered during this phase of the program.

b. The shortest return times were achieved by a recently assigned combat pilot whose maneuvers were intentionally highly uncoordinated but qualitatively resulted in low vibrations and loads.

c. Intermediate results were achieved by a second pilot whose maneuvers were highly coordinated.

d. It should be stressed that these return-to-target maneuvers are not likely to be used frequently during combat operations since combat maneuvers usually demand that the target be kept in sight. However, it is believed that they may be valid measures of qualitatively comparing the idealized maneuvering capability, providing pilot technique is specified. Because of the large scatter evident in return-to-target times, the validity of quantitative comparisons of aircraft performing these maneuvers must be carefully considered. It is suggested that the climbing turn replace the level teardrop turn if a single maneuver is to be used to define minimum time to return to target.

e. Further maneuverability testing should include investigation of wind effects on return-to-target performance. In addition, the differences and similarities between idealized and operational maneuvering should be quantitatively studied.

OPERATIONAL MANEUVERABILITY

46. The final portion of the test program involved a series of free-form maneuvers designed to cover all aspects of combat maneuverability. The pilots were instructed to tax the aircraft as strenuously as they felt was operationally realistic, and data were recorded throughout the flights. Maneuvers included diving gunnery runs, rapid heading changes, simulated ground fire evasion, terrain-following flight, and so forth. A number of the handling qualities and vehicle performance characteristics are worthy of mention and are discussed in the following paragraphs.

Longitudinal Control Force Characteristics

47. Foremost among the complaints regarding maneuvering handling qualities were the longitudinal control force characteristics. As reported in reference 10, appendix I, the high cyclic breakout forces, combined with a low stick force gradient, increase the pilot effort to precisely control the aircraft in all flight regimes and are considered to detract from the overall mission suitability of the aircraft. These characteristics restricted the pilot's ability to control airspeed in non-steady maneuvers where many other factors had to be simultaneously observed or controlled. Similar tasks exist in the operational environment. Consequently, the longitudinal control force characteristics constitute a shortcoming, correction of which is desired for improved mission accomplishment.

Lateral Stick Position During Turns

48. Several pilots reported inconsistent lateral stick positions during turning maneuvers. Only very small rightward stick displacements were required for significant load factor changes as airspeed decreased. Similar phenomena had been previously noted in the AH-1G Phase D tests (ref 10, app I). The time history data obtained in the present test program revealed that the aircraft was decelerating, and the stick positions were in the correct sense and magnitude to reflect the static lateral trim characteristics. Flight data recorded during constant speed and altitude turns revealed no unusual lateral stick characteristics.

Altitude Loss During Dive Recovery

49. Flight tests of performance during dive recovery were not conducted during this test program since ample data were available in reference 13, appendix I. However, the subject was considered qualitatively, and an attempt was made to correlate several pertinent related experiences. Numerous field units have reported ground strikes occurring during diving pullouts. Engineering tests were conducted in addition to the AH-1G Phase D effort (ref 13) to define dive recovery performance. Those results substantiate information provided in the operator's manual. Aviation unit commanders have reported the need to periodically reemphasize the kinematics of diving pullouts to assigned aviators. It appears that continued emphasis on this subject is needed by AH-1G pilots.

50. Discussions with aviators and examination of existing test data indicate that several contributing factors tend to aggravate the diving pullout maneuver:

a. The low drag of the AH-1G permits quite rapid longitudinal acceleration and high rates of descent during the dive. At increased rates of descent, the height loss during dive recovery is increased.

b. The AH-1G possesses neutral static longitudinal stability near the limit airspeed (V_L) (ref 10, app I). Speed control in the dive is, therefore, difficult.

c. Target fixation during dives can also contribute to untimely pilot reaction. The pilot must be cautioned to disregard the target once he descends to the prescribed height required for recovery.

d. Experience obtained during USAASTA testing indicates that substantial misimpressions of aircraft altitude can exist even within a controlled, semi-static test environment. The possibility of misjudging aircraft height is probably greater in the combat environment. A radar altimeter display, perhaps coupled with an aural warning signal, could reduce the errors in height assessment.

e. High-speed attack helicopters can benefit from even greater load factor capability than the AH-1G. Reduced height loss during pullouts would be a major benefit. Increases in both transient and sustained maneuver capability could be effectively utilized in future generations of Army aircraft.

Transient Torque Surge

51. The transient torque surge accompanying left lateral cyclic inputs and resultant left roll rates is discussed in the operator's manual (ref 1, app I). A more detailed technical discussion appears in reference 19. Torque surges as high as 10 to 15 psi can accompany rapid left lateral inputs. This characteristic is familiar to AH-1G pilots and is apparently tolerable even though it results in high pilot workload when flying is done at high power settings. A majority of operational flying is done at or below a 70-percent engine torque which allows an adequate margin for left turns. The 70-percent torque level also results in tolerable delay times in the event of engine failure at high dive airspeeds (ref 9). The torque surge does, however, restrict return-to-target and other turning maneuvers. It is, therefore, a shortcoming for which correction is desirable. Since the transient torque surge is an inherent rotor characteristic, a simple fix does not appear to exist.

Engine Torque Oscillation

52. When power setting is increased to near the engine topping limit, noticeable oscillations in engine output torque (±1 to 2 percent) are encountered. As illustrated in the time histories (figs. 17, 18 and 19, app V), the main rotor rpm and peak-to-peak chordwise bending at radial station 135 also exhibit this oscillatory characteristic. The oscillations occur for both slow and rapid torque increases and tend to persist following torque reduction to a power setting below

that at which they were encountered. The frequency is 1.3 Hertz (Hz), and the response is nominally of constant amplitude. The magnitudes of the engine torque surge (±100 to 200 in.-lb) and main rotor speed variation (±0.4 to 0.7 rpm) are consistent with the inertial relationship ($Q = I\ d\Omega/dt$). The engine speed oscillation is assumed to be caused by the engine governor. While the oscillation does not detract from mission accomplishment, it does constitute an annoyance to the pilot, and its existence should be noted in the operator's manual.

Vibration Characteristics

53. Vibration levels at the copilot station tended to decrease with increasing normal load factor up to an equivalent thrust of approximately 10,000 pounds. This trend is consistent with the findings of the AH-1G Phase D program where the worst vibrations occurred at light gross weight and high speed (ref 12, app I). During the most extreme maneuvers, however, the vibration increased sharply, indicating the onset of rotor stall. The peak vibration levels encountered were vertical with a high four-per-rotor-revolution (4/rev) harmonic content. No quantitative information is presented because manual reading and Fourier-analysis of the vibration data would have significantly delayed the report.

54. During pullouts from dives and during high g turns, the vibration levels and g forces in the front cockpit were so high that manipulation of switches and writing were restricted. During a flight with a photographer in the front cockpit, difficulty was encountered in attempting to take motion pictures during maneuvers. In the combat situation, effective target tracking and firing may be similarly restricted. Consequently, effective weapons deployment of the AH-1G is reduced during maneuvering flight. A stabilized gun sight or computer-assisted fire control system would improve the AH-1G's ability to deliver weapons fire during maneuvering.

RPM Increase with Angle of Attack

55. The maximum angle-of-attack capability of the AH-1G during pull-ups is severely restricted by a rapid build-up of rotor rpm. Pilot workload to control rpm is frequently excessive. The power-off upper rotor speed limit (339 rpm) is marked with a red line on the aircraft instruments and is interpreted by the pilot as a not-to-exceed rotor speed. The 339-rpm limit allows less than a 5-percent overspeed from the normal operating value of 324. This small margin is considered a design shortcoming. The military specification for structural design requirements for helicopters (ref 20, app I) requires a 25-percent margin between design maximum and power-on limit rotor speed. A minimum margin of 10-percent between design maximum and limit operating rpm should be specified for Army helicopters.

56. A consequence of the rpm increase with increased angle of attack is a limitation on the thrust vectoring capability. While this is inherent in all rotary wing vehicles, it is most pronounced in aircraft such as the AH-1G, in which the maximum rotor speed is restricted. As a result, the deceleration capability is limited. All of the project pilots felt that increased deceleration capability would greatly improve the

AH-1G's maneuverability. This opinion is consistent with the benefits quantitatively recorded during the return-to-target tests using uncoordinated flight techniques (para 45b). It is interesting to note that such an important item as low drag can detract from the maneuverability of a high-performance attack vehicle. Both the low-drag fuselage profile and the restricted attitude vectoring capability limit performance. Speed brakes or other deceleration devices could greatly improve the deceleration capability which is essential to the attack mission.

Cyclic Control Force Feedback

57. Frequent occurrences of control force feedback were recorded by project pilots during maneuvering flight. Reference 13, appendix I, states that this feedback occurs during symmetrical pullouts as a discernible function of equivalent thrust, with light feedback occurring between 16,500 and 17,000 pounds and heavy feedback between 17,500 and 18,000 pounds. During these tests, feedback was investigated during banked turns and other nonsymmetrical maneuvers. It was not possible to consistently repeat the test conditions where the feedback was experienced, and no identifiable feedback boundary or region was found.

58. The control force feedback in the AH-1G occurs at both moderate and high airspeeds, torque settings and load factors. The feedback is usually interpreted by the pilot as an indication of the onset of rotor stall, and his instinctive reaction is to "ease off" the maneuver condition. If feedback is, in fact, a valid cue to rotor stall, it is a useful pilot signal.

59. Two time history plots showing stick force feedback occurrence appear as figures 20 and 21, appendix V. It is seen that both longitudinal and lateral control force feedback on the order of ±5 to 7 pounds are experienced. The initial build-up appears to be triggered by large right lateral control inputs (75 to 80 percent of full travel) and then sustained by an aft stick displacement (approximately 30 percent). It is further noted that an oscillatory stick displacement accompanies the force feedback during most of the time. This displacement is considered to cause the force since the pilot tends to restrain the movement of the stick.

60. In an attempt to trace the feedback through the control system to the rotor, the following observations were made:

a. Feedback is large when chordwise vibratory loads are high. Flapwise vibratory loads appear to be unrelated to control force feedback.

b. Longitudinal push-rod vibratory loads (nonrotating) are consistently high during occurrence of feedback. However, neither lateral push-rod (nonrotating) nor pitch link (rotating) oscillatory loads appear to be related to the control force feedback.

c. Since the rotor was not instrumented for torsional bending moment, conclusions regarding the existence of moment stall are not possible.

61. Because of the absence of clearly defined rotor and control system loads which may have caused feedback, the possibility exists that it is triggered by airframe vibration or servo instabilities. The lack of conclusive evidence as to the origin of the control force feedback phenomenon highlights the need for additional analysis and further testing.

Normal Acceleration Cues

62. Although the pilot is effectively informed of the maneuver limits of the AH-1G by vibration, control force feedback, and general aircraft feel, it was determined during these tests that a normal acceleration indicator (g meter) was a very useful and desirable instrument. With a well-positioned easy-to-read g meter installed on the pilot instrument panel, the maximum turn and pull-up performance of the AH-1G was easier to accurately predict and utilize. A g meter is desirable for installation on all AH-1G helicopters for the above reasons. More important, however, is the requirement for accurate normal acceleration information during weapons firing maneuvers. It is essential for accuracy that weapons be fired in 1.0g, zero-sideslip flight with the noncompensating sighting system used in the AH-1G. Small deviations in normal acceleration cause large undershoot or overshoot firing errors with all normally used aircraft dive angles. It is recommended that a g meter be installed in all AH-1G helicopters. Its sensor should be located as near as possible to the mid cg position to reduce Coriolis acceleration effects. The area behind the pilot's seat would accomodate a load factor sensor.

Lateral SCAS Instability

63. The data in figures 20 and 21, appendix V, illustrate the presence of an unstable oscillation in the lateral SCAS which occurred when step-type lateral control inputs were made. The natural frequency is approximately 0.78 Hz, and oscillations are noticeable in the lateral SCAS displacement (±40 to 80 percent of full authority), roll rate (±10 to 25 deg/sec) and, to a very slight degree, roll attitude (±2 to 4 degrees). Generally, the pilot was not aware of the occurrence of this phenomenon, probably because of its low frequency. The aircraft's response was, however, noticeable to observers on the ground. Additional testing would be required to better define the mechanisms triggering the instability. In particular, it would be of interest to determine if the instability is a forced or free oscillation. The lateral SCAS instability is an unnecessary characteristic and is a shortcoming for which correction is desired.

MISCELLANEOUS

USAAVLABS Maneuvers

64. On the recommendation of USAAVSCOM, the original scope of test for the AH-1G maneuvering limitations project was expanded to provide limited test data for USAAVLABS. Principal investigators from USAASTA and USAAVLABS agreed that data would be provided on maneuvers where vertical flight path displacement

was accomplished by longitudinal cyclic pitch control inputs. The maneuvers that were performed consisted of inputting aft cyclic control in varying degrees to initiate a climb. Several g levels were achieved; and for each g level, the method of control input was varied. The maneuvers were terminated by rolling to the right. This was done to avoid fractional load factors which would result in loss of control effectiveness.

65. Figures 22 and 23, appendix V, illustrate representative test results. The pilot was instructed to vary control input techniques to maximize the vertical displacement of the flight path. The nominal entry conditions for all test points were the heavy hog configuration, a 9250-pound grwt, a 200-inch aft cg, 120 KIAS, and a 5500-foot H_D.

66. Figure 22, appendix V, represents a 1.4g pull-up with a slow longitudinal input; figure 23 represents a 1.7g pull-up. Higher load factors resulted in more rapid establishment of the climb. Approximately 2.5 seconds elapsed between control input and the development of an essentially steady rate of climb. If a 0.7-second recognition lag is assumed (ref 4, app I), approximately 850 feet of ground distance is required to clear a 100-foot obstacle at 1.7g's and a 120-KIAS entry speed.

67. It is noted that the blade bending moment data generated during these pull-up maneuvers do not generalize in the same manner as the turning data reported in paragraphs 32 and 33. Of particular interest is the relative insensitivity of flapwise peak-to-peak blade bending to load factors below 1.25g's, high sensitivity up to about 1.5g's, and nominal insensitivity as the load factor increases above 1.5g's. Further analysis is required to determine if banked turn and pull-up maneuver data can be generalized in some common format.

68. The sensitivity of the altitude measuring trace was set for previous portions of the test program, rather than for these data. Consequently, the recorded altitudes were difficult to read and analyze. The altimeter lags were negligible because of the transducer and short plumbing paths employed. However, excessive rates of climb were indicated for these data, and caution should be exercised in their interpretation.

Tail Rotor Retention Nut Untorquing

69. Repeated instances of untorquing of the AH-1G tail rotor retention nut occurred during the return-to-target and operational maneuverability portions of this test program. Three different Army aviators experienced this occurrence. In the most critical instance, the nut torque was reduced from 400 in.-lb to less than 100 in.-lb following approximately 30 minutes of flight. Typically, 100 to 200 in.-lb of torque loss were encountered during 1-hour flights by each aviator. USAASTA submitted an Equipment Improvement Recommendation (EIR), number 396199, on 28 April 1970, and an Equipment Performance Report (EPR), number SAVTE-001, on 10 July 1970, (ref 21, app I) describing in detail the untorquing incidents, inspection and maintenance procedures employed, and additional information relating to the tail rotor retention nut untorquing.

70. The untorquing occurred during return-to-target maneuver flights and during simulated combat maneuvering tests. The flights included all three types of return-to-target maneuvers previously mentioned. Typically, the test gross weight was 9250 pounds in the heavy hog configuration, although untorquing also occurred at a lighter gross weight (8500 pounds). A majority of the flying was done between 60 and 120 KIAS at an average density altitude of 3000 feet. Deceleration to near zero airspeed was required during some turning maneuvers. Substantial "uncoordination" was employed during maneuvers, and abrupt pedal inputs at low airspeeds were made. Load factors encountered during maneuvers typically ranged between 2 and 2.5g's. Most turns were made to the right. Normal operating rpm was 324, and both rpm and engine torque limits specified in the operator's manual were observed. Tail rotor retention nut torque decreased during almost every flight.

71. After the first instance of untorquing, discovered during a routine inspection, a thorough inspection procedure was initiated for succeeding flights. Following each flight, the nut torque was checked by applying a tightening torque with a 100 to 500 in.-lb range torque wrench, and the safety wire was then secured. Since steel shims were used, no axial compression was noted. The nut and shaft were then torque-painted with a magic marker (photo 1). All nuts had approximately one thread disengaged when fully tightened because of the requirement for proper spacing between the tail rotor and the pylon (measured between the blade tip at maximum flapping and collective pitch and the rear pylon fairing). To determine if the nut were faulty, a replacement was made, but the untorquing incidents persisted. All nuts were subsequently hardness tested and found to measure 30 on the Rockwell "C" scale. The tail drive gearbox gear wear patterns were checked regularly and showed no evidence of high horsepowers. In addition, no occurrences of teetering stop pounding were reported by the pilots, nor were any evident from the surface condition of the teetering stops.

72. The repeated occurrence of tail rotor retention nut untorquing, under varied maneuvering conditions with different aviators, is considered a flight safety deficiency. However, since confirmed reports of this untorquing have been confined to USAASTA experience, it is recommended that further action on this deficiency be delayed pending confirmation from operational units, BHC data, or continuing occurrences at USAASTA.

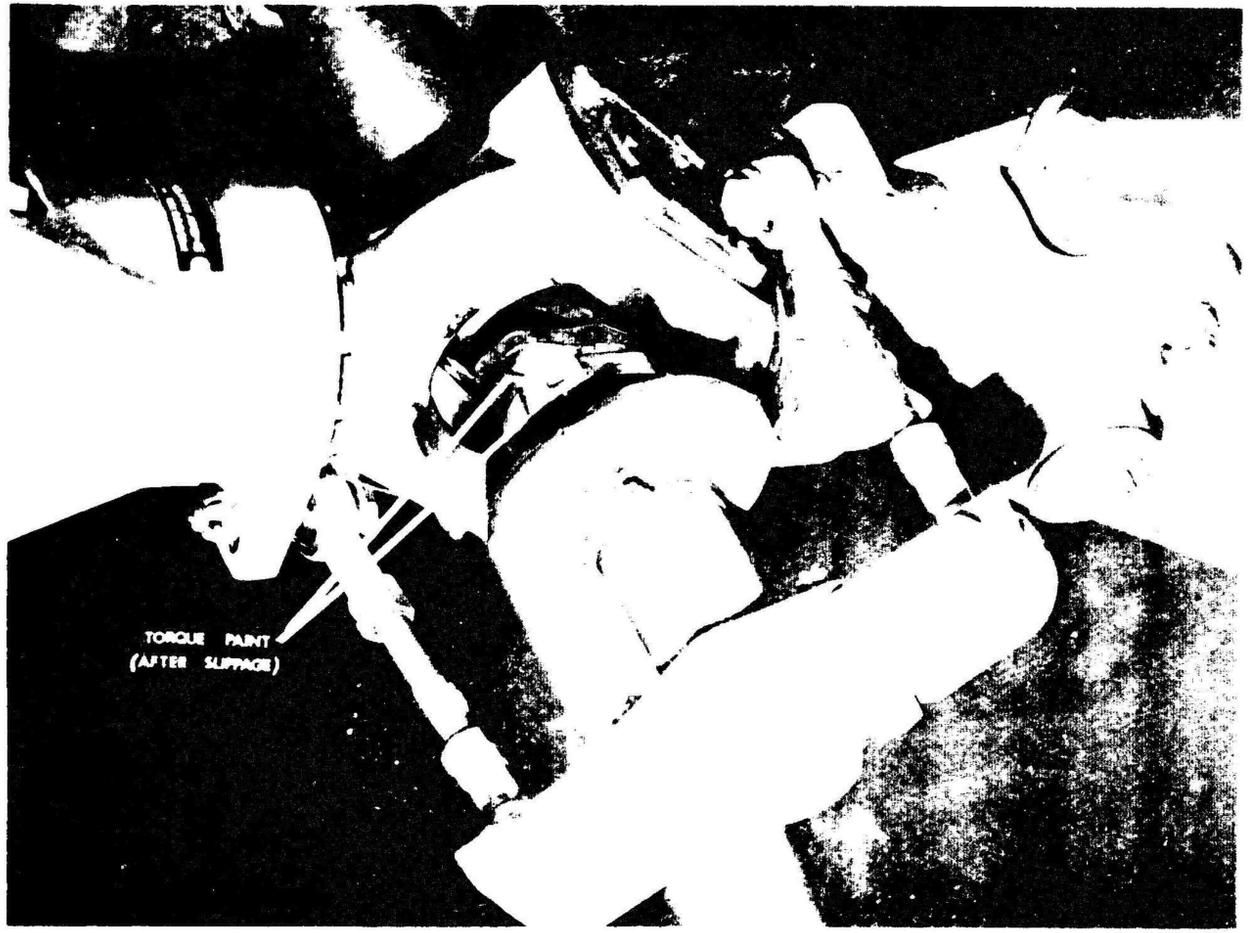

Photo 1. Tail Rotor Retention Nut.

CONCLUSIONS

GENERAL

73. The maneuvering characteristics of the AH-1G are generally excellent and are suitable for operational use. No cautions or limitations to bank angle, normal load factor, roll rate, sideslip angle, or maneuver stick displacement are required for operation within the test flight envelope. Adequate control exists at all tested maneuver conditions.

DEFICIENCIES AND SHORTCOMINGS AFFECTING MISSION ACCOMPLISHMENT

74. The untorquing of the tail rotor retention nut during flight is a safety-of-flight deficiency (para 72). If confirmatory reports of untorquing are obtained from operational units, contractor test data, or further USAASTA experience, corrective action will be required.

75. Correction of the following shortcomings is desirable for improved mission accomplishment:

a. The undesirable longitudinal control force characteristics which degrade effective speed control (para 47).

b. The transient torque surge encountered at high left roll rates, compensation for which requires high pilot workload (para 51).

c. The insufficient main rotor overspeed margin which requires excessive pilot compensation during maneuvers (para 55).

d. The low-frequency lateral SCAS instability which occurs during banking maneuvers (para 63).

FLIGHT CHARACTERISTICS

76. The following characteristics of the AH-1G should be emphasized during pilot training:

a. Higher bank angles than predicted by simple theory are required for a given normal load factor (para 20).

b. Return-to-target times are strongly influenced by pilot technique (paras 41 and 42).

c. The climbing turn is the quickest of the three methods tested to return to a point target in the AH-1G (para 44).

d. Lateral stick positions required in turns are influenced by deceleration and reflect static trim characteristics (para 48).

e. Altitude loss during dive recovery is complicated by the low drag and neutral static longitudinal stability near V_L and is subject to judgment errors induced by target fixation and altitude misjudgment (para 50).

f. Torque oscillation occurs when the engine is at topping power (para 52).

g. High vibration restricts copilot/gunner functioning during maneuvers (para 54).

h. The most rapid vertical flight path displacements are produced by the highest normal load factors (para 66).

INSTRUMENTS

77. The following instrumentation would contribute to improved AH-1G operational maneuver capability:

a. An improved attitude display (para 24).

b. The addition of a radar altimeter (para 50d).

c. Incorporation of a stabilized weapons sight and/or computer-assisted fire control system (para 54).

d. The addition of a g meter (para 62).

MISCELLANEOUS

78. The operator's manual requires the following revisions:

a. Show test data instead of theoretical bank angle versus load factor and turning radii (para 23).

b. Modify chapter 8 to discuss the items listed in paragraph 76.

79. Energy maneuverability appears to be a valid method for presenting maneuvering test data (para 27).

80. Measured load parameters in banked turns displayed well-defined trends as functions of speed and normal load factor (para 30).

81. The thrust link is not satisfactory for the measurement of total rotor thrust (para 31).

82. Return-to-target times are imperceptibly influenced by gross weight but strongly affected by wind (para 37).

83. Left return-to-target maneuvers may be preferable to right turns for operational use because of transient torque characteristics (para 39).

84. The large variations encountered in return-to-target performance degrade the return-to-target maneuver as a quantitative measure of comparative maneuverability (para 45d).

RECOMMENDATIONS

85. The safety-of-flight deficiency (para 74) should be corrected on a high-priority basis if confirmatory reports of other occurrences are obtained.

86. The shortcomings (para 75) should be corrected at the earliest convenience.

87. During pilot training, emphasis should be placed on the maneuvering characteristics noted in paragraph 76.

88. Recommended changes to the AH-1G instruments (para 77) should be considered.

89. The AH-1G operator's manual should be revised according to paragraph 78.

90. USAASTA should test the improved attitude indicating system provided by MWO 55-1520-221-30/19 (para 24).

91. Pilot technique should be specified when attempting to compare aircraft maneuverability (paras 42 and 45d).

92. The climbing turn should be used if a single maneuver is to be used to define minimum time to return to target (para 45d).

93. Further maneuvering test programs should include investigation of wind effects on return-to-target performance and should seek to quantitatively define the differences between idealized and operational maneuvering (para 45e).

94. Future generations of Army aircraft should be designed with even higher load factor capability than the AH-1G (para 50e).

95. A minimum rotor overspeed margin of 10 percent should be provided in all future designs (para 55).

96. Improved deceleration capability for high-speed rotary wing aircraft should be considered (para 56).

97. Maneuvering test programs should be initiated for other current Army aircraft.

APPENDIX I. REFERENCES

1. Technical Manual, TM 55-1520-221-10, *Operator's Manual, Army Model AH-1G Helicopter*, April 1969.

2. Letter, USAAVSCOM, AMSAV-R-F, 2 September 1969, subject: Request for Test, Bank Angle Limitations of the AH-1G.

3. Test Plan, USAASTA, Project No. 69-11, *Engineering Flight Test, AH-1G Helicopter (HueyCobra), Maneuvering Limitations*, January 1970.

4. Draft Statement of Work, USAAVLABS, SAVFE-AA, "Analysis of Maneuverability Effects on Rotor/Wing Design Characteristics."

5. Message, USAAVSCOM, AMSAV-R-F, Unclas, 30 January 1970, subject: Safety of Flight Release, Project No. 69-11.

6. Letter, USAAVSCOM, AMSAV-R-F, 12 December 1969, subject: AH-1G Helicopter (HueyCobra), Maneuvering Limitations.

7. Final Report, Bell Helicopter Company, No. 209-099-309, *Results of the Flight Test Investigation of the Reduced G Maneuver in the AH-1G Helicopter*, October 1969.

8. Final Report, USAASTA, Project No. 69-01, *Airworthiness and Flight Characteristics, AH-1G Helicopter with Stabilized Night Sight (SNS), Phase I*, December 1969.

9. Final Report, USAASTA, Project No. 69-01, *Airworthiness and Flight Characteristics, AH-1G Helicopter with Stabilized Night Sight (SNS), Phase II*, August 1970.

10. Final Report, USAASTA, Project No. 66-06, *Engineering Flight Test, AH-1G Helicopter (HueyCobra), Part I, Handling Qualities*, October 1970.

11. Final Report, USAASTA, Project No. 66-06, *Engineering Flight Test, AH-1G Helicopter (HueyCobra), Part II, Performance*, April 1970.

12. Final Report, USAASTA, Project No. 66-06, *Engineering Flight Test, AH-1G Helicopter (HueyCobra), Part III, Vibration Characteristics*, October 1970.

13. Final Report Addendum, USAASTA, Project No. 66-06, "Engineering Flight Test, AH-1G Helicopter (HueyCobra), Part II, Performance," Unpublished.

14. Technical Paper, American Helicopter Society, Richard B. Lewis II, No. 472, *HueyCobra Maneuvering Investigations*, June 1970.

15. Letter, Bell Helicopter Company, C. L. Livingston, 7 July 1970, subject: Computation of Turning Flight.

16. Technical Paper, Southwest Region of the American Helicopter Society, C. L. Livingston, *Maneuverability Prediction*, December 1966.

17. Final Report, Bell Helicopter Company, No. 209-099-041, *Specification for Flight Load Survey on the Model AH-1G Helicopter*, 18 July 1966.

18. Final Report, USAAVNTA, Project No. 65-30, *Engineering Flight Evaluation of the Bell Model 209 Armed Helicopter*, May 1966.

19. Technical Article, C. L. Livingston and M. R. Murphy, *Flying Qualities Considerations in the Design and Development of the HueyCobra*, Journal of the American Helicopter Society, Vol. 14, No. 1, January 1969.

20. Military Specification, MIL-S-8698(ASG), *Structural Design Requirements, Helicopters*, 2 February 1958.

21. Equipment Performance Report, USAASTA, SAVTE-001, "AH-1G Turning Limitations," 10 July 1970.

22. Textbook, Bernard Etkin, *Dynamics of Flight, Stability and Control*, John Wiley and Sons, Inc., New York, 1967.

APPENDIX II. BASIC AIRCRAFT INFORMATION AND OPERATING LIMITS

AIRFRAME

Rotor System

1. The 540 "door hinge" main rotor assembly is a two-bladed, semi-rigid, underslung feathering-axis type rotor. The assembly consists basically of two all-metal blades, blade grips, yoke extensions, yoke trunnion, and rotating controls. Control horns for cyclic and collective control input are mounted on the trailing edge of the blade grip. Trunnion bearings permit rotor flapping. The blade grip-to-yoke extension bearings permit cyclic and collective pitch action.

Tail Rotor

2. The tail rotor is a two-bladed, delta-hinge type employing preconing and underslinging. The blade and yoke assembly is mounted to the tail rotor shaft by means of a delta-hinge trunnion. Blade pitch angle is varied by movement of the tail rotor control pedals. Power to drive the tail rotor is supplied by a takeoff on the lower end of the main transmission.

Transmission System

3. The transmission is mounted forward of the engine and coupled to the engine by a short drive shaft. The transmission is basically a reduction gear box which transmits engine power at reduced rpm to the main and tail rotors by means of a two-stage planetary gear train. The tranmission incorporates a free-wheeling clutch unit at the input drive. This provides a disconnect from the engine in case of a power failure to allow the aircraft to make an autorotational landing.

Synchronized Elevator

4. The synchronized elevator, which has an inverted airfoil section, is located near the aft end of the tail boom and is connected by control tubes and mechanical linkage to the fore and aft cyclic control system. Fore and aft movements of the cyclic control stick produce a change in the synchronized elevator attitude.

Control Systems

5. A dual hydralic control system is provided for the cyclic and collective controls. The directional controls are powered by a single servo cylinder which is operated by system number 1. The hydraulic system consists of two hydraulic pumps, two reservoirs, relief valves, shut-off valves, pressure warning lights, lines, fittings, and manual dual-tandem servo actuators incorporating irreversible valves. Tandem power cylinders incorporating closed-center four-way manual servo valves and irreversible valves are provided in the lateral, fore and aft cyclic and collective

control system. A single power cylinder incorporating a closed-center four-way manual servo valve is provided in the directional control system. The cylinders contain a straight-through mechanical linkage.

Force Trim

6. Magnetic brake and force gradient devices are incorporated in the cyclic control and directional pedal controls. These devices are installed in the flight control system between the cyclic stick and the hydraulic power cylinders and between the directional pedals and the hydraulic power cylinder. The force trim control can be turned off by depressing the left button on the top of the cyclic stick. The gradient is accomplished by springs and magnetic brake release assemblies which enable the pilot to trim the controls as desired.

Cyclic Control Stick

7. The pilot and gunner cyclic stick grips each have a force trim switch and a SCAS release switch. The pilot cyclic stick has a built-in operating friction. The cyclic control movements are transmitted directly to the swash plate. The fore and aft cyclic control linkage is routed from the cyclic stick through the SCAS actuator, to the dual boost hydraulic actuator, and then to the right horn of the fixed swash plate ring. The lateral cyclic is similarly routed to the left horn.

Collective Pitch Control

8. The collective pitch control is located to the left of the pilot and is used to control the vertical mode of flight. Operating friction can be induced into the control lever by hand-tightening the friction adjuster. The pilot and gunner collective pitch controls have a rotating grip-type throttle.

Tail Rotor Pitch Control Pedals

9. Tail rotor pitch control pedals alter the pitch of the tail rotor blades and thereby provide the means for directional control. The force trim system is connected to the directional controls and is operated by the force trim switch on the cyclic control grip.

Stability and Control Augmentation System

10. The SCAS is a three-axis, limited-authority, rate-referenced stability augmentation system. It includes an electrical input which augments the pilot mechanical control input. This system permits separate consideration of airframe displacements caused by external disturbances from displacements caused by pilot input. The SCAS is integrated into the fore, aft, lateral and directional flight controls to improve the stability and handling qualities of the helicopter. The system consists of electro-hydraulic servo actuators, control motion transducers, a sensor/amplifier unit and a control panel. The servo actuator movements are not felt by the pilot. The actuators are limited to a 25-percent authority and will center and lock in case of an electrical and/or a hydraulic failure.

ENGINE

Engine Description

11. The T53-L-13 engine, rated at 1400 shp, is a successor to the T53-L-11 engine. The additional power has been achieved with no change in the basic T53-L-11 engine envelope mounting and connection points and with a 6-percent increase in basic engine weight.

12. The performance gain is accomplished thermodynamically by the mechanical integration of a modified axial compressor, a two-stage compressor turbine and a two-stage power turbine into the T53-L-11 engine configuration.

13. Replacement of the first two compressor stators and changing of the first two stages of compressor rotor blades and discs results in an approximate 20-percent increase in mass air flow through the engine. This is accomplished without the use of inlet guide vanes.

14. An inlet flow fence, located on the outer wall of the inlet housing in the area of the previously used inlet guide vanes, provides the desired inlet conditions for the transonic compression during acceleration at low speeds. At compressor speeds up to 70 percent, the fence is in the extended position. Above 70 percent, the flow fence is retracted into the outer wall of the inlet housing. Similar to a piston ring, the circumference of the flow fence is changed by the action of a piston actuator powered by compressor discharge pressure.

15. The specification for this engine allows the use of JP-4 or JP-5 fuel for satisfactory operation throughout the engine's operating envelope. During this program, JP-4 fuel was used.

Engine Power Control System

16. The fuel control for the T53-L-13 engine is a hydro-mechanical type of fuel control. It consists of the following main units:

a. Dual-element fuel pump.

b. Gas producer speed governor.

c. Power turbine speed topping governor.

d. Acceleration and deceleration control.

e. Fuel shut-off valve.

f. Transient air bleed control.

17. An air bleed control is incorporated within the fuel control to provide for opening and closing the compressor interstage air bleed in response to the following signals present in the power control:

a. Gas producer speed.

b. Compressor inlet air temperature.

c. Fuel flow.

18. The fuel control is designed to be operated either automatically or in an emergency mode. In the emergency position, fuel flow is terminated to the main metering valve and is routed to the manual (emergency) metering and dump valve assembly. While in the emergency mode, fuel flow to the engine is controlled by the position of the manual metering valve which is connected directly to the power control (twist grip). During the emergency operation, there is no automatic control of fuel flow during acceleration and deceleration; thus, engine acceleration and exhaust gas temperature (EGT) must be pilot monitored.

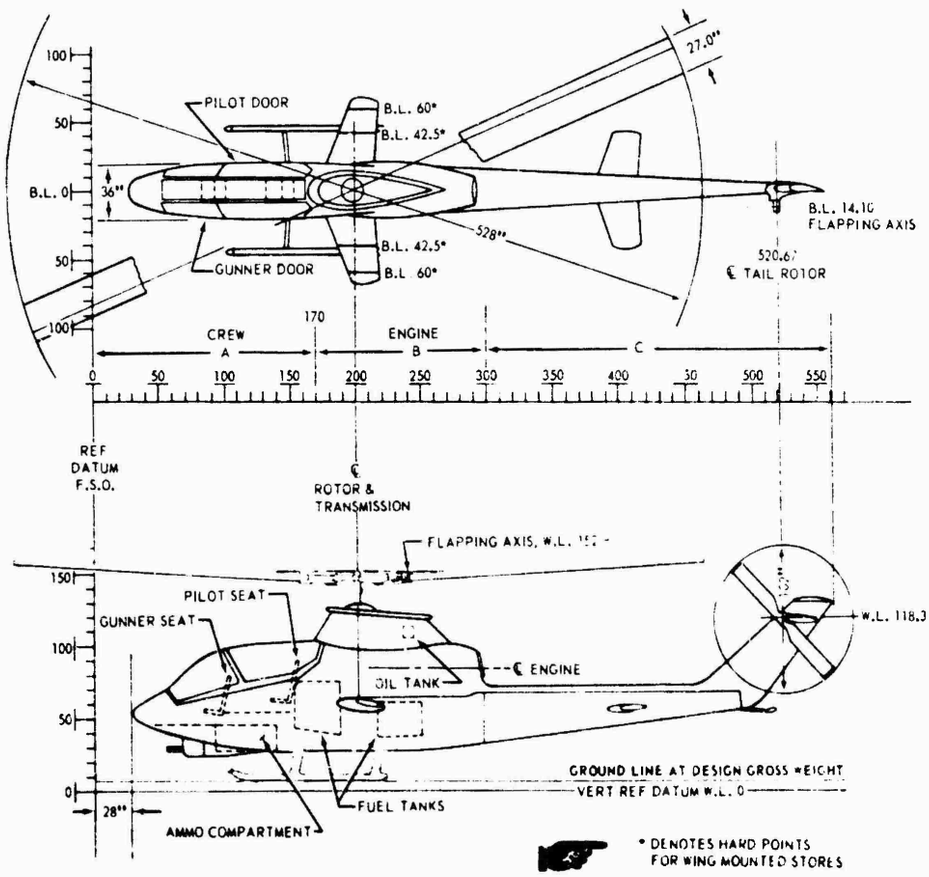

BASIC AIRCRAFT INFORMATION

Airframe Data

Overall length (rotor turning)	637.2 in.
Overall width (rotor trailing)	124.0 in.
Centerline of main rotor to centerline of tail rotor	320.7 in.
Centerline of main rotor to elevator hinge line	198.6 in.
Elevator area (total)	15.2 sq ft
Elevator area (both panels)	10.9 sq ft
Elevator airfoil section	Inverted Clark Y
Vertical stabilizer area	18.5 sq ft
Vertical stabilizer airfoil section	Special camber
Vertical stabilizer aerodynamic center	Fuselage station (FS) 499.0
Wing area:	
Total	27.8 sq ft
Outboard of butt line (BL) 18.0 (both sides)	18.5 sq ft
Wing span	10.33 ft
Wing airfoil section:	
Root	NACA 0030
Tip	NACA 0024
Wing angle of incidence	14 deg

Main Rotor Data	
Number of blades	2
Diameter	44 ft
Disc area	1520.5 sq ft
Blade chord	27 in.
Rotor solidity	0.0651
Blade area (both blades)	99 sq ft
Blade airfoil	9.33 percent symm special section
Linear blade twist	-0.455 deg/ft
Hub precone angle	2.75 deg
Rotor inertia	2900 slug-ft^2
Antitorque Rotor Data	
Number of blades	2
Diameter	8.5 ft
Disc area	56.74 sq ft
Blade chord	8.41 in.
Rotor solidity	0.105
Blade airfoil	NACA 0010 modified
Blade twist	Zero deg
Transmission Drive System Ratios	
Engine to main rotor	20.383:1.0
Engine to antitorque rotor	3.990:1.0
Engine to antitorque drive system	1.535:1.0

Test Aircraft Control Displacements

Longitudinal cyclic control:

Full forward to full aft with SCAS nulled	9.07 in.

Lateral cyclic control:

Full left to full right with SCAS nulled	10.00 in.

Directional (pedal) control:

Full left to full right with SCAS nulled	7.07 in.

Collective control:

Full up to full down with SCAS nulled	9.30 in.

OPERATING LIMITATIONS

Limit Airspeed

Any configuration with XM159 rocket pods:

180 KCAS below a 3000-foot H_D; decrease 8 KCAS per 1000 feet above 3000 feet

All other configurations:

190 KCAS below a 4000-foot H_D; decrease 8 KCAS per 1000 feet above 4000 feet

Gross-Weight/Center-of-Gravity Envelope

Forward cg limit:

Below 7000 pounds, FS 190.0; linear increase to FS 192.1 at 9500 pounds

Aft cg limit:

Below 8270 pounds, FS 201.0; linear decrease to FS 200 at 9500 pounds

Sideslip Limits

Five degrees at V_L with linear increase to 30 degrees at 50 KCAS

Rotor and Engine Speed Limits (Steady State)	
Power on:	
Engine rpm	6400 to 6600
Rotor rpm	314 to 324
Power off:	
Rotor rpm	294 to 339
Rotor rpm transient lower limit	250
Power on during dives and maneuvers:	
Rotor rpm	314 to 324
Temperature and Pressure Limits	
Engine oil temperature	93°C
Transmission oil temperature	110°C
Engine oil pressure	25 to 100 psi
Transmission oil pressure	30 to 70 psi
Fuel pressure	5 to 20 psi
T53-L-13 Engine Limits	
Normal rated EGT (maximum continuous)	625°C
Military rated EGT (30-minute limit)	645°C
Starting and acceleration EGT (5-second limit)	675°C
Maximum EGT for starting and acceleration	760°C
Torque pressure limit	50 psi

APPENDIX III. DATA REDUCTION METHODS

NONDIMENSIONAL METHOD

1. Helicopter performance results may be generalized through the use of nondimensional coefficients which can be used to define performance at other than the specified test conditions. In the first portion of the test program, the maximum sustained load factor for constant-speed, fixed-altitude coordinated turns was used to establish a base line from which the effects of the deficient aircraft total energy could be investigated. Equivalent thrust and power (as defined in paragraph 25 of the Results and Discussion section of this report) were employed to normalize the data.

2. The following nondimensional coefficients were used to generalize test results obtained during the test program:

$$\text{Equivalent Power Coefficient} = C_{P_{equiv}} = \frac{P_{equiv}}{\rho A\ (\Omega R)^3} \qquad (1)$$

$$\text{Equivalent Thrust Coefficient} = C_{T_{equiv}} = \frac{nW}{\rho A\ (\Omega R)^2} \qquad (2)$$

$$\text{Advance Ratio} = \mu = \frac{1.689\ V_T}{\Omega R} \qquad (3)$$

$$\text{Main Rotor Tip Mach Number} = M_{tip} = \frac{1.689\ V_T + \Omega R}{a} \qquad (4)$$

Where: ρ = Air density (slug/ft^3)

A = Main rotor disc area (ft^2)

ΩR = Main rotor tip speed (ft/sec)

n = Normal load factor (g)

W = Gross weight (lb)

V_T = True airspeed (kt)

a = Speed of sound in air (ft/sec)

3. The 1962 *US Standard Atmosphere* was used to define density, pressure, and temperature used in the nondimensionalizing process.

INSTRUMENTATION CALIBRATION

4. All data were acquired by means of sensitive test instrumentation which were calibrated before and after the test program. Where possible, the instrumentation was selected to have a linear output over the range of interest for this test program.

5. The calibration data were curve fitted using least square fit techniques, and standard deviations from the fits were derived. These standard deviations are tabulated in appendix IV and may be used to assess the validity of the curve fits and the overall significance of the data. The curve fits were used during the data reduction phase to expedite conversions from trace deflections to engineering units.

WEIGHT AND BALANCE

6. The cg of the test aircraft was controlled and checked prior to each test flight, and ballast was either added or removed to maintain the aft cg.

7. Before and after each flight, the specific gravity and temperature of the fuel were recorded. These data, when used in conjunction with external sight gage readings of the calibrated fuel cell, enabled the volume and weight of fuel consumed during the flight to be calculated. Fuel used in flight was determined from a calibrated fuel counter system installed on the engineer panel.

AIRSPEED CALIBRATION

8. The test airspeed indicator system (high-speed swivel-head probe designed by Lockheed and mounted on a 6-foot nose boom) was calibrated using the ground speed course at Edwards Air Force Base. An airspeed calibration from 30 KTAS to V_H with zero sideslip angle was performed to determine the position error. The calibration was then repeated introducing sideslip angle to determine its effect on position error.

9. The results of the sideslip calibration indicated that the probe position error remained essentially constant (+4 knots) throughout the AH-1G airspeed envelope at any vector sum of the angle of attack and angle of sideslip not exceeding ±30 degrees.

ENGINE POWER DETERMINATION

10. The engine torquemeter is essentially a piston; the pressure on which is proportional to the power output of the engine. The relationship between engine shaft horsepower and torquemeter indication was obtained from the engine manufacturer's test cell calibration curves.

AERODYNAMIC ANGLES AND AIRCRAFT ATTITUDES

11. Angles of attack and sideslip were measured by a pair of vanes mounted on the pitot-static boom approximately 5 feet from the nose of the aircraft. Angle-of-attack data used in the calculations for theoretical bank angle (para 21, Results and Discussion section) were not adjusted for main rotor wake effects. Pitch, roll and yaw attitudes were measured by attitude gyros mounted in the rear of the ammunition bay. Comparison of the integrated rate gyro data with the attitude gyro outputs revealed the former to be in error because of an 11-degree phase lag induced in the rate gyro circuit by a dampening capacitor. Assuming the rate gyro to behave like a damped second order system, close agreement between rate and attitude gyro data can be obtained when the phase lag is mathematically reduced to 4 degrees (typical for the gyros employed). The data shown in this report, however, have not been corrected in the above manner.

BANK ANGLE, LOAD FACTOR RELATIONSHIP

12. The relationship between bank angle and normal load factor (introduced in paragraph 21 of the Results and Discussion section of this report) is derived as follows:

The analysis starts with Euler equations for roll, pitch and yaw velocity (ref 22, app I):

$$p = \dot{\phi} - \dot{\psi} \sin \Theta \tag{5}$$

$$q = \dot{\Theta} \cos \phi + \dot{\psi} \cos \Theta \tag{6}$$

$$r = \dot{\psi} \cos \Theta \cos \phi - \dot{\Theta} \sin \phi \tag{7}$$

Where: p = Roll velocity Θ = Pitch attitude

q = Pitch velocity ϕ = Roll attitude

r = Yaw velocity ψ = Yaw attitude

Figure I illustrates the axes employed.

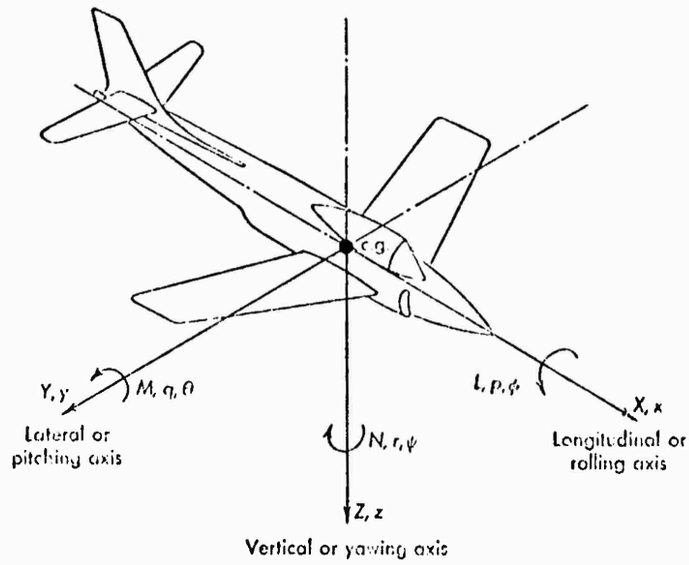

Figure I. Airplane-Body Axes.

Next, the aircraft is assumed to turn only about a vertical axis, hence $\dot{\theta}$ and $\dot{\phi}$ are zero.

Equations 5 through 7 become:

$$p = -\psi \sin \Theta \tag{8}$$

$$q = \dot{\psi} \cos \Theta \sin \phi \tag{9}$$

$$r = \dot{\psi} \cos \Theta \cos \phi \tag{10}$$

These rates are then substituted into the generalized equations of force equilibrium (ref 22):

$$X - mg \sin \Theta = m (\dot{u} + qw - ru) \tag{11}$$

$$Y + mg \cos \Theta \sin \phi = m (\dot{v} + ru - pw) \tag{12}$$

$$Z + mg \cos \Theta \cos \phi = m (\dot{w} + pv - qu) \tag{13}$$

Where: X = Force on vehicle in X direction

Y = Force on vehicle in Y direction

Z = Force on vehicle in Z direction

m = Aircraft mass

u = Velocity in X direction

v = Velocity in Y direction

w = Velocity in Z direction

With the substitutions of equations 8, 9 and 10, and with the further assumption that for coordinated flight the side force (Y) is zero and that all accelerations are zero, equation 12 becomes:

$$g \cos \Theta \sin \phi = u \dot{\psi} \cos \phi + w \dot{\psi} \sin \Theta \tag{14}$$

Since by definition:

$$\tan \alpha = \frac{w}{u} \tag{15}$$

$$\tan \beta = \frac{v}{u} \tag{16}$$

Equation 14 becomes:

$$g \cos \Theta \sin \phi = u \dot{\psi} (\cos \Theta \cos \phi + \sin \Theta \tan \alpha) \tag{17}$$

Rearranging:

$$\frac{u \dot{\psi}}{g} = \frac{\tan \phi}{1 + K} \tag{18}$$

Where: $$K = \frac{\tan \Theta \tan \alpha}{\cos \phi} \tag{19}$$

Equation 13 is then solved for Z/mg which is identically -n, the load factor:

$$\frac{Z}{mg} = - n = \frac{pv}{g} - \frac{qu}{g} - \cos\Theta \cos\phi \tag{20}$$

$$n = - u \frac{\dot{\psi} \sin\Theta \tan\beta}{g} - u \frac{\dot{\psi} \cos\Theta \sin\phi}{g} - \cos\Theta \cos\phi \tag{21}$$

Substituting equation 18 and multiplying by $\cos\phi$:

$$n \cos\phi = \cos\Theta \cos^2\phi + \cos\Theta \frac{\sin^2\phi}{1 + K} + \frac{\sin\phi . \tan\beta \sin\Theta}{1 + K} \tag{22}$$

Equation 22 is the result cited in paragraph 21 of the Results and Discussion section of this report. This derivation was suggested by Mr. C. L. Livingston of the Bell Helicopter Company.

ENERGY MANEUVERABILITY

13. Figures 3 and 4, appendix V, were obtained using the relationship introduced in paragraph 25 of the Results and Discussion section of this report:

$$P_{equiv} = P_{eng} - mV \frac{dV}{dt} - W \frac{dh}{dt} - I\Omega \frac{d\Omega}{dt} \tag{23}$$

If P_{eng} is specified, and Ω is held constant:

$$- W \frac{dh}{dt} - mV \frac{dV}{dt} = P_{equiv} - P_{eng} \tag{24}$$

When the airspeed is held constant, the rate of sink required to sustain the load factor (fig. 3) is calculated from:

$$-\frac{dh}{dt} = \frac{P_{equiv} - P_{eng}}{W} \tag{25}$$

Where P_{equiv} is obtained from figure 2 for the $C_{T_{equiv}}$ corresponding to load factor times the selected gross weight and to advance ratio.

Correspondingly, the deceleration required to sustain the load factor at a constant altitude is calculated from:

$$-\frac{dV}{dt} = \frac{P_{equiv} - P_{eng}}{mV} \tag{26}$$

LOAD PARAMETERS DURING BANKED TURNS

14. Mean and peak-to-peak vibratory components of several load parameters are plotted in figures 5 through 14, appendix V. Fairings represent discrete levels of equivalent main rotor thrust. Symbols shown on the plots are unflagged for the 9200-pound grwt data and flagged for the 8000-pound grwt data. Data obtained during this test program were compared with existing data, where available, and fairings selected accordingly.

TIME HISTORY DATA

15. Time history data from simulated operational maneuvers appears in figures 17 through 23b, appendix V. The main rotor bending moments are plotted in the following manner: Mean flapwise and chordwise bending are indicated by a short horizontal line. The one-half peak-to-peak envelope of the vibratory flapwise and chordwise bending constitutes the vibratory trace. This is illustrated in figure II.

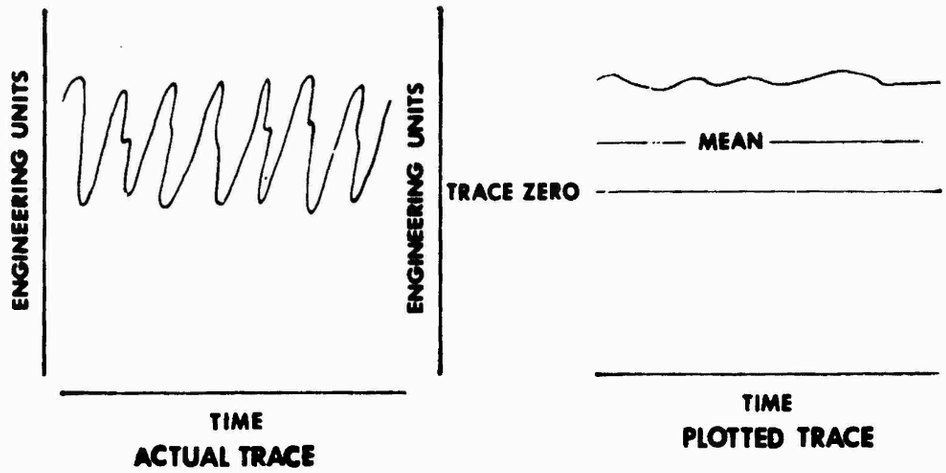

Figure II. Mean Flapwise and Chordwise Bending.

Push-rod and pitch link load data and control forces are shown as a shaded envelope, the extremity of which is defined by the peak oscillatory value of the parameter. Where the envelope appears steady, it is recognized that the harmonic content of the trace is of high frequency. This is illustrated in figure III.

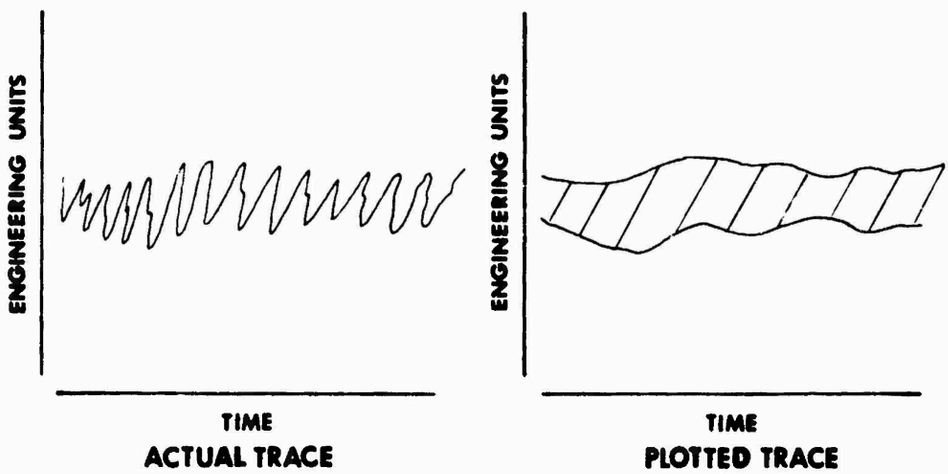

Figure III. Load Data and Control Forces.

APPENDIX IV. INSTRUMENTATION

1. All instrumentation was installed in the test helicopter prior to the start of the test program. All instrumentation was calibrated. The flight test instrumentation was installed and maintained by the Instrumentation and Calibration Division, USAASTA. The cockpit instruments listed below were provided for pilot and engineering reference in establishing test points and checking the oscillograph instrumentation.

PILOT PANEL

Parameter	Range of Interest	Desired Accuracy
Airspeed (boom system)	Zero to 200 KIAS	±1 knot
Altitude (boom system)	Zero to 10,000 ft	±10 ft
Rate of climb (ship)	±3000 fpm	±50 fpm
Rotor rpm	250 to 350 rpm	±1 rpm
Gas producer speed, N_1 (ship)	6000 to 7000 rpm	±1/2 percent
Power turbine speed, N_2 (ship)	70 to 101.5 percent	±10 rpm
Engine torque pressure (ship)	Zero to 80 psid	±1/2 psi
Exhaust gas temperature	300° to 800°C	±10°C
Longitudinal control position	Zero percent full aft, 100 percent full fwd	±1 percent
Lateral control position	Zero percent full left, 100 percent full right	±1 percent
Pedal control position	Zero percent full left, 100 percent full right	±1 percent
Collective control position	Zero percent full down, 100 percent full up	±1 percent
CG normal acceleration	-0.5 to 2.5g	±0.02g
Angle of sideslip	±30 deg	±1/2 deg

Outside air temperature	-30° to +50°C	±1/2°C
Fuel-flow indicator	30 to 130 gal/hr	±1 gal/hr
Oscillograph control panel:		
Paper speed	Hi-Low-Off	
Jam lights		
Gyro uncage light	Uncage with oscillograph on	

ENGINEER PANEL

Parameter	Range of Interest	Desired Accuracy
Outside air temperature	-30° to +50°C	±1/2°C
Fuel-flow indicator	30 to 130 gal/hr	±1 gal/hr
Oscillograph control panel:		
Paper speed	Hi-Low-Off	
Jam lights		
Gyro uncage light	Uncage with oscillograph on	
Altitude (boom system)	Zero to 10,000 ft	±10 ft
Airspeed (boom system)	Zero to 200 KIAS	±1 kt
Rotor rpm	250 to 350 rpm	±1 rpm

OSCILLOGRAPH

2. A 50-channel oscillograph was employed as the primary data recording device. The oscillograph parameters, ranges, desired accuracies, sensitivities, readability, calibration standard deviations and sensor locations are listed on the following pages. The calibration standard deviation can be compared with the readability for each channel to evaluate the maximum significance. This can be compared with the desired accuracy specified at the beginning of the test program. Readability is defined by 0.01 inch of trace deflection. The calibration standard deviations are obtained as a by-product of fitting the calibration data with a least squares fit.

OSCILLOGRAPH PARAMETERS	Range of Interest	Desired Accuracy
Longitudinal control position	Zero percent full aft, 100 percent full forward	±1 percent
Lateral control position	Zero percent full left, 100 percent full right	±1 percent
Directional control position	Zero percent full right, 100 percent full left	±1 percent
Collective control position	Zero percent full down, 100 percent full up	±1 percent
Longitudinal control force	-25 pounds pull, +25 pounds push	±1/2 pound
Lateral control force	-25 pounds left, +25 pounds right	±1/2 pound
Directional control force	-100 pounds right, +100 pounds left	±2 pounds
Longitudinal SCAS position	Zero percent full aft, 100 percent full forward	±1 percent
Lateral SCAS position	Zero percent full left, 100 percent full right	±1 percent
Directional SCAS position	Zero percent full right, 100 percent full left	±1 percent

Sensitivity	Readability	Calibration Standard Deviation	Sensor Location
47.7 percent per inch	0.48 percent	0.37 percent	Potentiometer in control linkage at FS 105.0, WL 50.0, BL -16.0
48.0 percent per inch	0.48 percent	0.44 percent	"
50.0 percent per inch (nominal-nonlinear)	0.5 percent	Not computed	Potentiometer in control linkage at FS 138.0, WL 45.0, BL 0.0
49.6 percent per inch	0.50 percent	0.69 percent	Potentiometer in control linkage at FS 124.0, WL 50.0, BL -16.0
25.4 pounds per inch	0.25 pound	0.29 pound	Strain gage at base of stick at FS 115.0, WL 54.0, BL 0.0
22.7 pounds per inch	0.23 pound	0.32 pound	"
102 pounds per inch	1.0 pound	1.9 pounds	Load cell on pedal face at FS 103.0, WL 54.0, BL ±5.0
48.8 percent per inch	0.48 percent	0.00 percent	Potentiometer at SCAS output at FS 210.0, WL 32.0, BL 10.0
47.3 percent per inch	0.47 percent	0.00 percent	Potentiometer at SCAS output at FS 210.0, WL 32.0, BL -10.0
50.0 percent per inch	0.50 percent	0.00 percent	Potentiometer at SCAS output at FS 270.00, WL 32.0, BL -10.0

OSCILLOGRAPH PARAMETERS	Range of Interest	Desired Accuracy
Pitch attitude	±45 degrees	±0.5 degree
Roll attitude	±90 degrees	±0.5 degree
Yaw attitude (uncage gyro with oscillograph ON switch)	Zero to 360 degrees	±2 degrees
Pitch rate	±45 deg/sec	±0.5 deg/sec
Roll rate	±100 deg/sec	±0.5 deg/sec
Yaw rate	±45 deg/sec	±0.5 deg/sec
CG normal acceleration	-0.5 to 2.5g's	±0.02g
Angle of attack	±20 degrees	±0.5 degree
Angle of sideslip	±30 degrees	±0.5 degree
Airspeed (boom system), differential pressure transducer	Zero to 200 KIAS	±1 knot
Altitude (boom system), absolute pressure transducer	Zero to 10,000 feet	±10 feet

Sensitivity	Readability	Calibration Standard Deviation	Sensor Location
21.4 degrees per inch	0.21 degree	0.06 degree	Gyro at FS 103.5, WL 32.0, BL -7.5
43.0 degrees per inch	0.43 degree	0.14 degree	Gyro at FS 103.5, WL 32.0, BL -7.5
44.9 degrees per inch	0.45 degree	0.25 degree	Gyro at FS 103.0, WL 33.7, BL -1.0
23.0 deg/sec per inch	0.23 deg/sec	0.13 deg/sec	Gyro at FS 157.3, WL 79.6, BL 0.0
57.8 deg/sec per inch	0.58 deg/sec	0.13 deg/sec	Gyro at FS 161.3, WL 79.6, BL 2.5
23.8 deg/sec per inch	0.24 deg/sec	0.12 deg/sec	Gyro at FS 157.3, WL 79.6, BL 3.0
0.962g per inch	0.0096g	0.0000g	Accelerometer at FS 198.0, WL 79.0, BL 14.0
14.3 degrees per inch	0.14 degree	0.16 degree	Vane on nose boom at FS -23.5, WL 50.0, BL 3.0
28.1 degrees per inch	0.28 degree	0.45 degree	Vane on nose boom at FS -26.0, WL 50.0, BL 0.0
50 knots per inch at 100 knots (nonlinear)	0.50 knot	0.04 knot	Battery compartment at FS 61.0, WL 64.0, BL 4.0
1866 feet per inch	19 feet	11 feet	Battery compartment at FS 61.0, WL 64.0, BL 0.0

OSCILLOGRAPH PARAMETERS	Range of Interest	Desired Accuracy
Pilot event	Spike	N/A
Engineer event	Spike	N/A
Rotor rpm (blip)	Spike	N/A
Rotor rpm (linear)	250 to 350 rpm	±1 rpm
Gas producer speed, N_1 (linear)	70 to 101.5 percent	±1/2 percent
Engine torque pressure (differential)	Zero to 60 psid	±1/2 psi
Copilot lateral vibration	±1.0g	±1 percent
Copilot vertical vibration	±1.0g	±1 percent
Rotor thrust link	Zero to 20,000 pounds	±100 pounds
Longitudinal control rod load	±4000 pounds	±100 pounds
Lateral control rod load	±4000 pounds	±100 pounds

Sensitivity	Readability	Calibration Standard Deviation	Sensor Location
N/A	N/A	N/A	N/A
N/A	N/A	N/A	N/A
N/A	N/A	N/A	Magnetic pickup
21.7 rpm per inch	0.21 rpm	0.14 rpm	Tachometer at FS 203.0, WL 71.0, BL 0.0
9.85 percent per inch	0.10 percent	0.09 percent	Tachometer at FS 244.5, WL 80.0, BL 8.0
16.25 psi per inch	0.16 psi	Unknown	Pressure transducer at FS 240.5, WL 80.0, BL 9.0
1.05g's per inch	0.01g	0.02g	Accelerometer at FS 80.75, WL 59.0, BL 10.0
1.05g's per inch	0.01g	0.02g	Accelerometer at FS 82.0, WL 57.75, BL 10.0
9567 pounds per inch	96 pounds	30 pounds	Strain gage at FS 200.0, WL 71.0, BL 0.0
4120 pounds per inch	41 pounds	65 pounds	Strain gage at FS 186.0, WL 103.0, BL 10.0
3968 pounds per inch	40 pounds	50 pounds	Strain gage at FS 186.0, WL 103.0, BL -10.0

OSCILLOGRAPH PARAMETERS	Range of Interest	Desired Accuracy
Collective control rod load	±4000 pounds	±100 pounds
Rotor blade chordwise bending at station 135	±400,000 in.-lb	±5 percent
Rotor blade flapwise bending at station 46	±200,000 in.-lb	±5 percent
Rotor blade flapwise bending at station 60	±150,000 in.-lb	±5 percent
Drag brace axial load	±50,000 pounds	±5 percent
Pitch link axial load	±14,000 pounds	±5 percent
Main rotor teeter angle	Stop to stop	±1 degree

Sensitivity	Readability	Calibration Standard Deviation	Sensor Location
3921 pounds per inch	39 pounds	43 pounds	Strain gage at FS 214.0, WL 103.0, BL -10.0
200,000 in.-lb per inch	2000 in.-lb	Unknown	Strain gages at leading and trailing edges of blade
100,000 in.-lb per inch	1000 in.-lb	Unknown	Strain gages at blade quarter chord, top and bottom
75,000 in.-lb per inch	750 in.-lb	Unknown	Strain gages at blade quarter chord, top and bottom
25,000 pounds per inch	250 pounds	Unknown	Strain gage on brace
7,000 pounds per inch	70 pounds	Unknown	Strain gage on link
10.1 degrees per inch	0.10 degree	0.10 degree	Potentiometer at teetering hinge

APPENDIX V. TEST DATA

Subject	Figure Number
Bank Angle/Load Factor Relationships	1
Equivalent Power Required in Maneuvering Flight	2
Rate of Sink Required to Sustain Load Factor	3
Deceleration Required to Sustain Load Factor	4
Thrust Link Load	5 and 6
Flapwise Bending Moment	7 and 8
Chordwise Bending Moment	9 and 10
Rotating Pitch Link Load	11 and 12
Longitudinal Push-Rod Loads	13 and 14
Return-to-Target Maneuvers	15 and 16
Engine Torque Oscillation	17 through 19
Control Force Feedback Characteristics	20 and 21
Symmetrical Pull-up	22 and 23

FIGURE 1

BANK ANGLE / LOAD FACTOR RELATIONSHIPS

THEORETICAL VS TEST

AH-1G USA S/N 66-15247

C.G.	DENSITY ALT FT	GROSS WT LB	CONFIG.	ROTOR RPM
AFT	5560	9000	HEAVY HOG	324

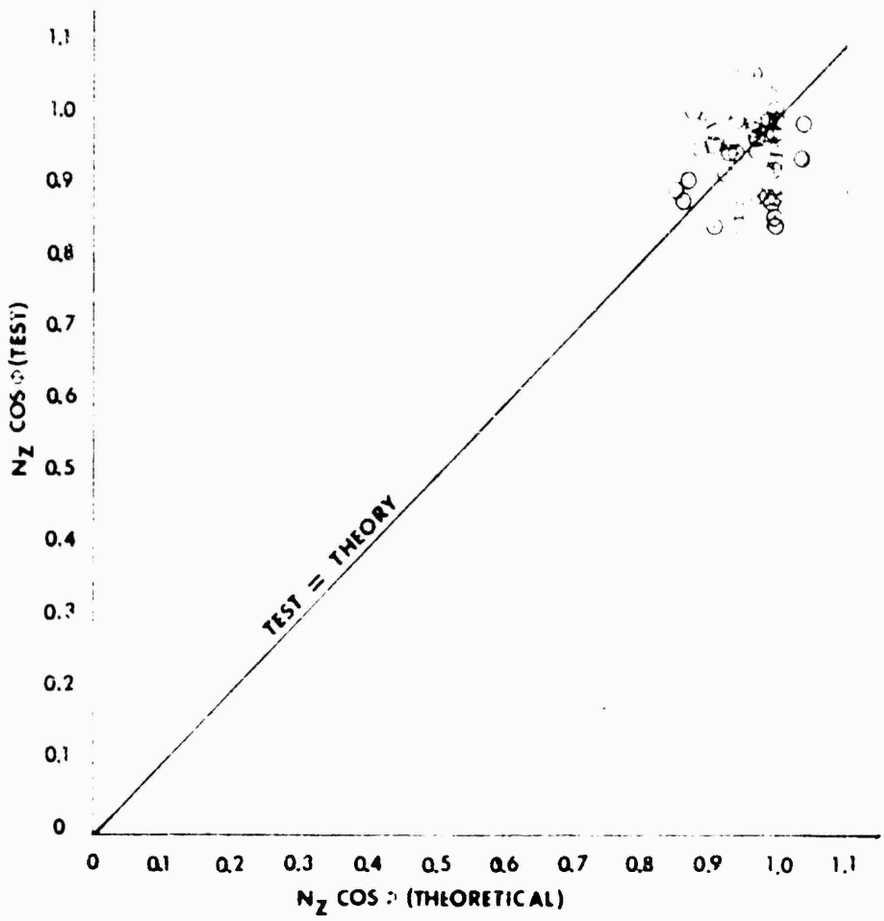

$$N_Z \cos\Phi \text{ (THEORETICAL)} = \cos\theta \cos^2\Phi + \cos\theta \frac{\sin^2\Phi}{1+K} + \frac{\sin\Phi \tan\Phi \sin\theta}{1+K}$$

$$K = \frac{\tan\theta \tan\alpha}{\cos\Phi}$$

N_Z NORMAL LOAD FACTOR

Φ - ROLL ANGLE

θ - PITCH ANGLE

β - ANGLE OF SIDESLIP

α - ANGLE OF ATTACK

FIGURE 2
EQUIVALENT POWER REQUIRED IN MANEUVERING FLIGHT
AH-1G USA S N 66 15247
HEAVY HOG CONFIGURATION
AFT C.G.

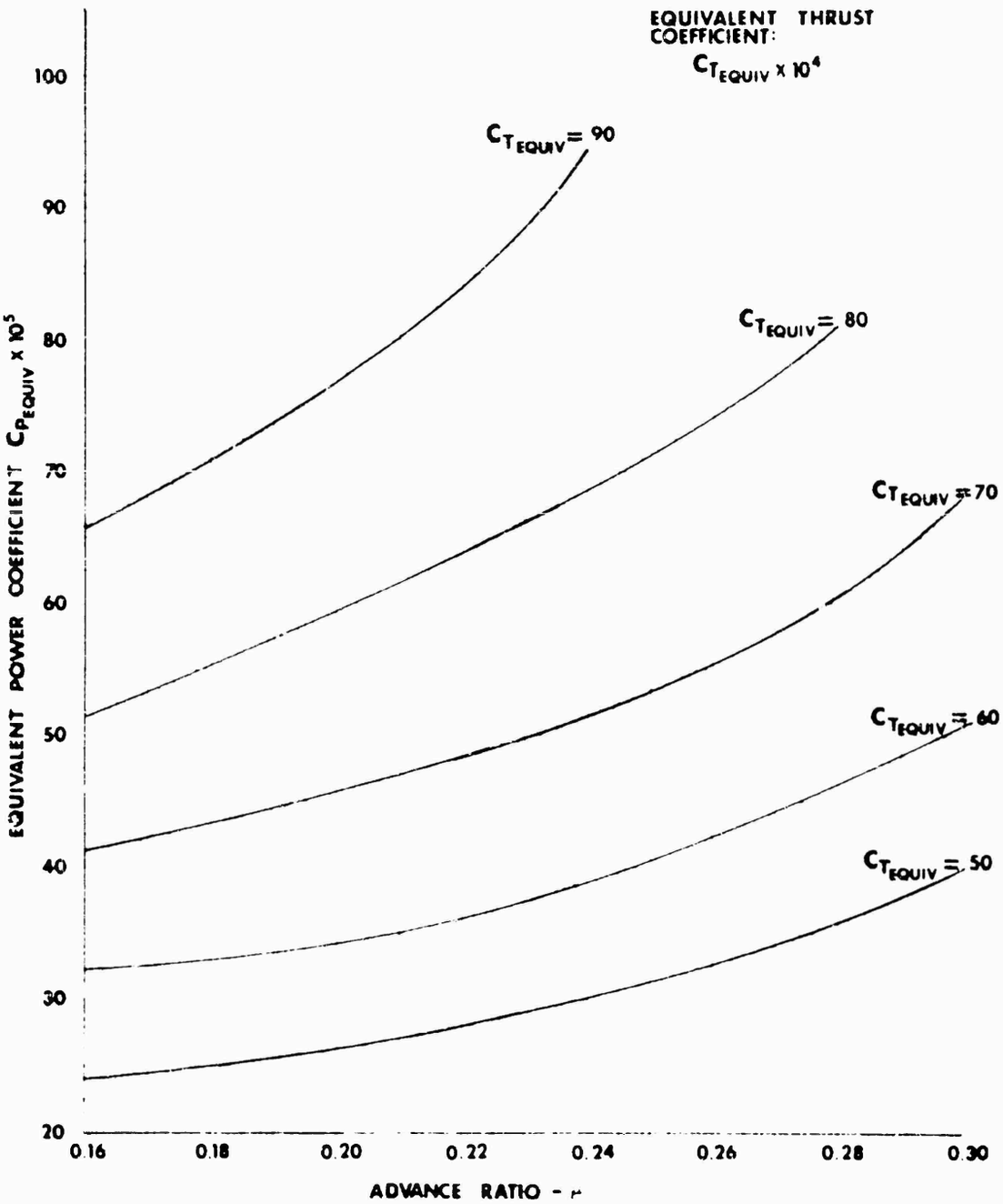

FIGURE 3
RATE OF SINK REQUIRED TO SUSTAIN LOAD FACTOR
AT CONSTANT AIRSPEED
AH-1G USA S/N 66-15247

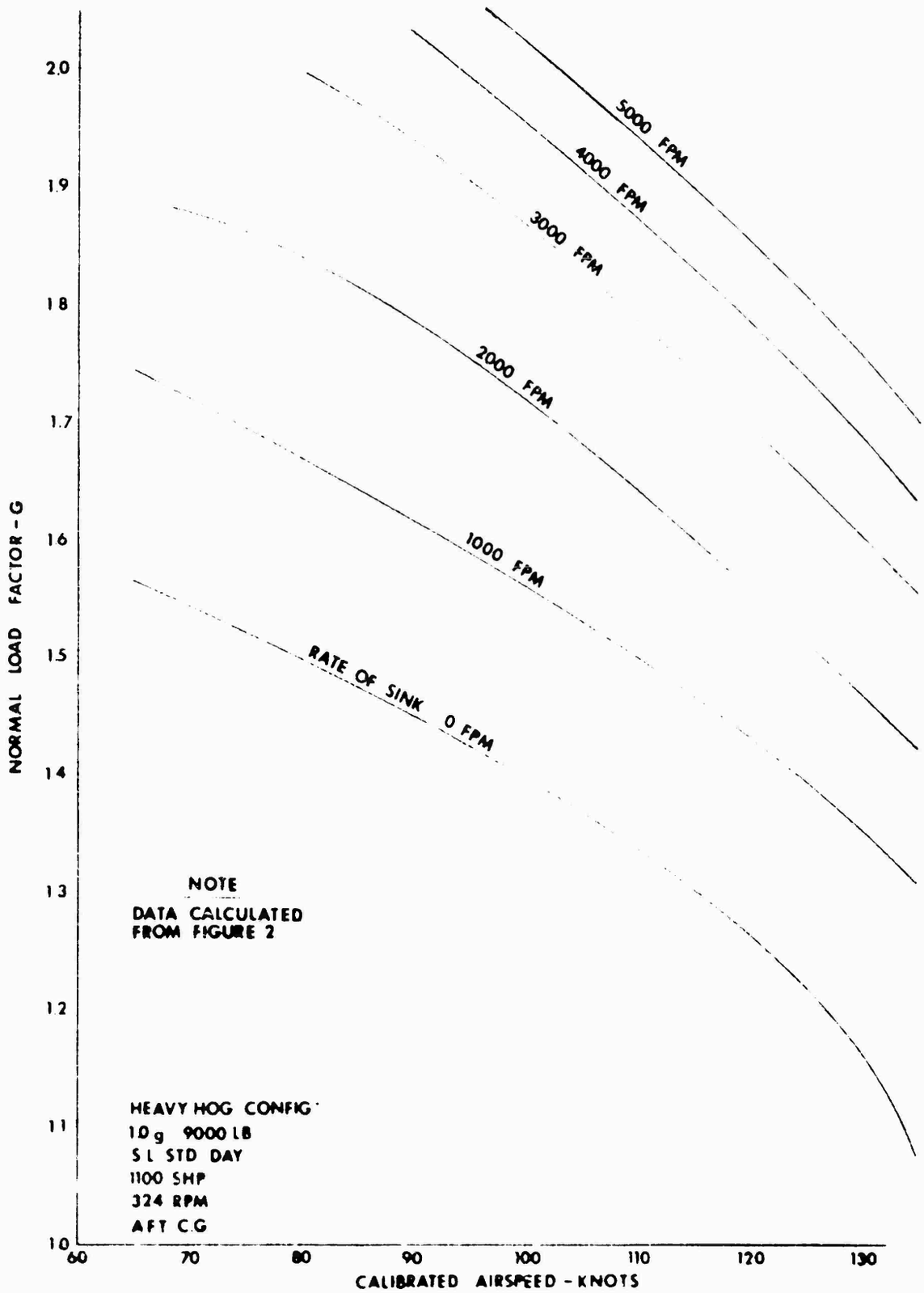

FIGURE 4
DECELERATION REQUIRED TO SUSTAIN LOAD FACTOR
AT CONSTANT ALTITUDE
AH-1G USA S/N 66-15247

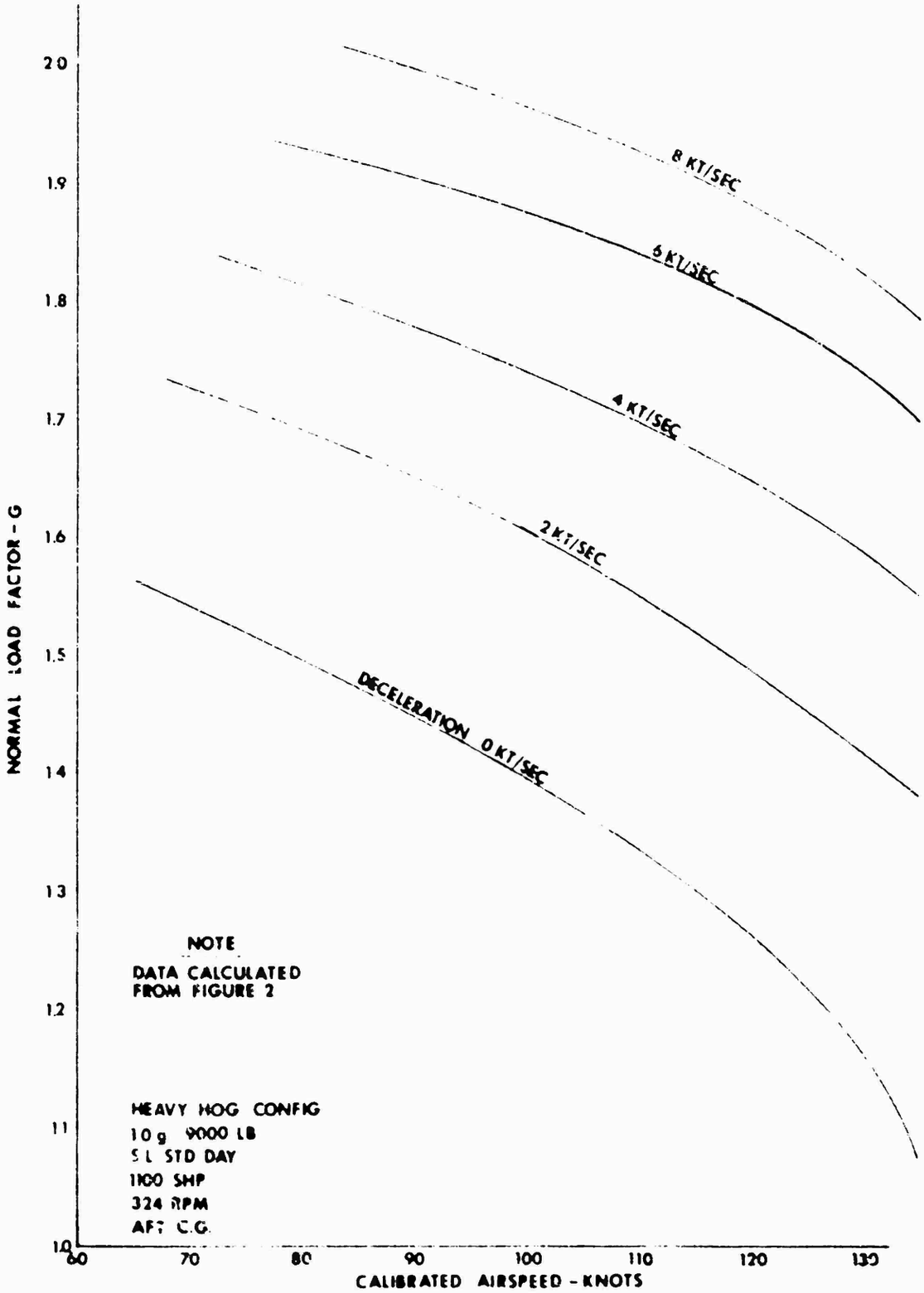

FIGURE 5
THRUST LINK AXIAL LOAD
AH-1G USA S/N 66-15247

SYMBOL	DENSITY ALT (FT)	GROSS WT (LB)	C.G. STATION (IN)	ROTOR RPM	CONFIG.
UNFLAGGED	5000	9200	200.2 (AFT)	324	HEAVY HOG
FLAGGED	5000	8000	201.0 (AFT)	324	CLEAN

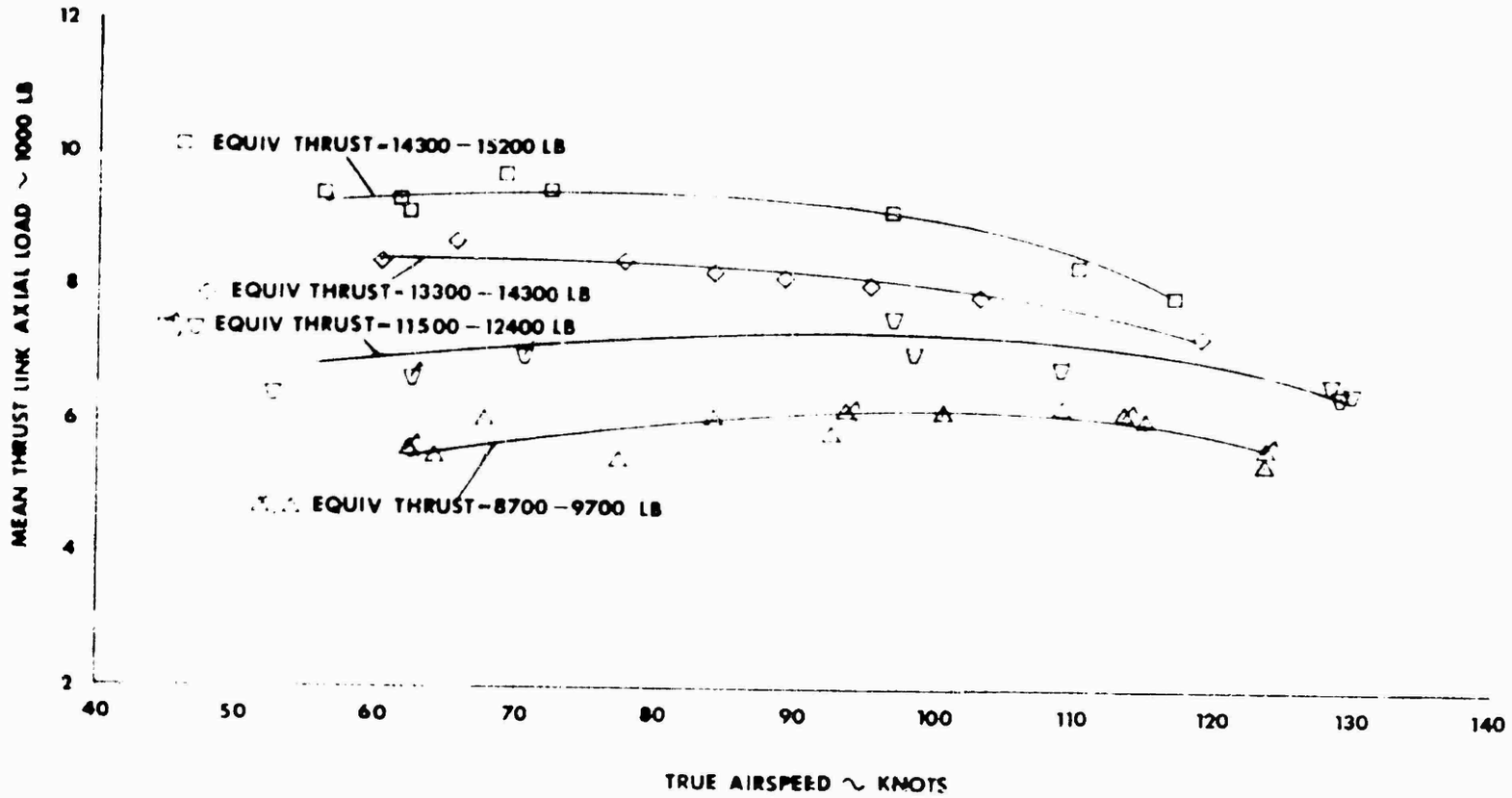

FIGURE 6
THRUST LINK AXIAL LOAD
AH-1G USA S/N 66-15247

SYMBOL	DENSITY ALT (FT)	GROSS WT (LB)	C.G. STATION (IN.)	ROTOR RPM	CONFIG.
UNFLAGGED	5000	9200	200.2 AFT	324	HEAVY HOG
FLAGGED	5000	8000	201.0 AFT	324	CLEAN

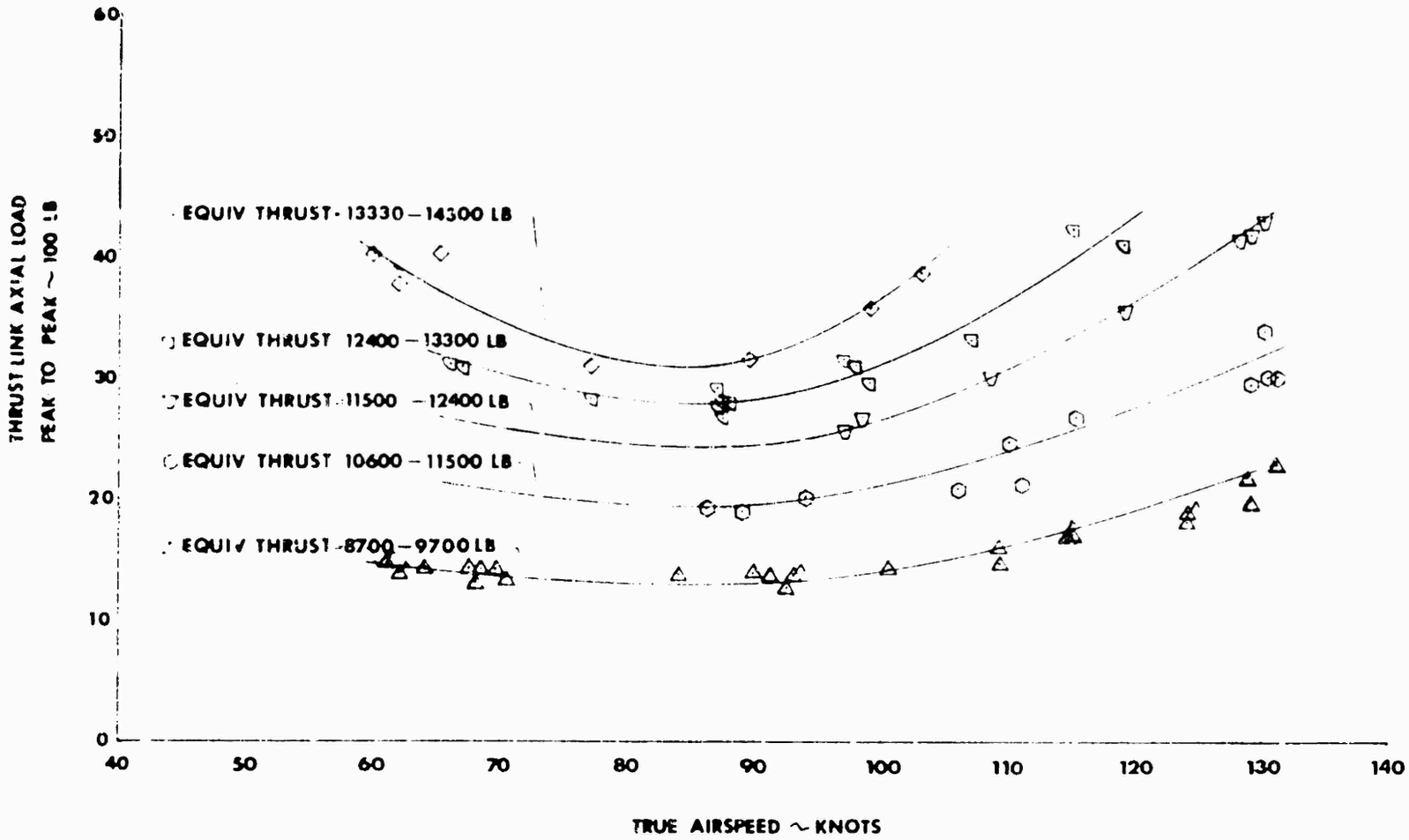

FIGURE 7
STATION 46 FLAPWISE BENDING MOMENT
AH-1G USA S/N 66-15247

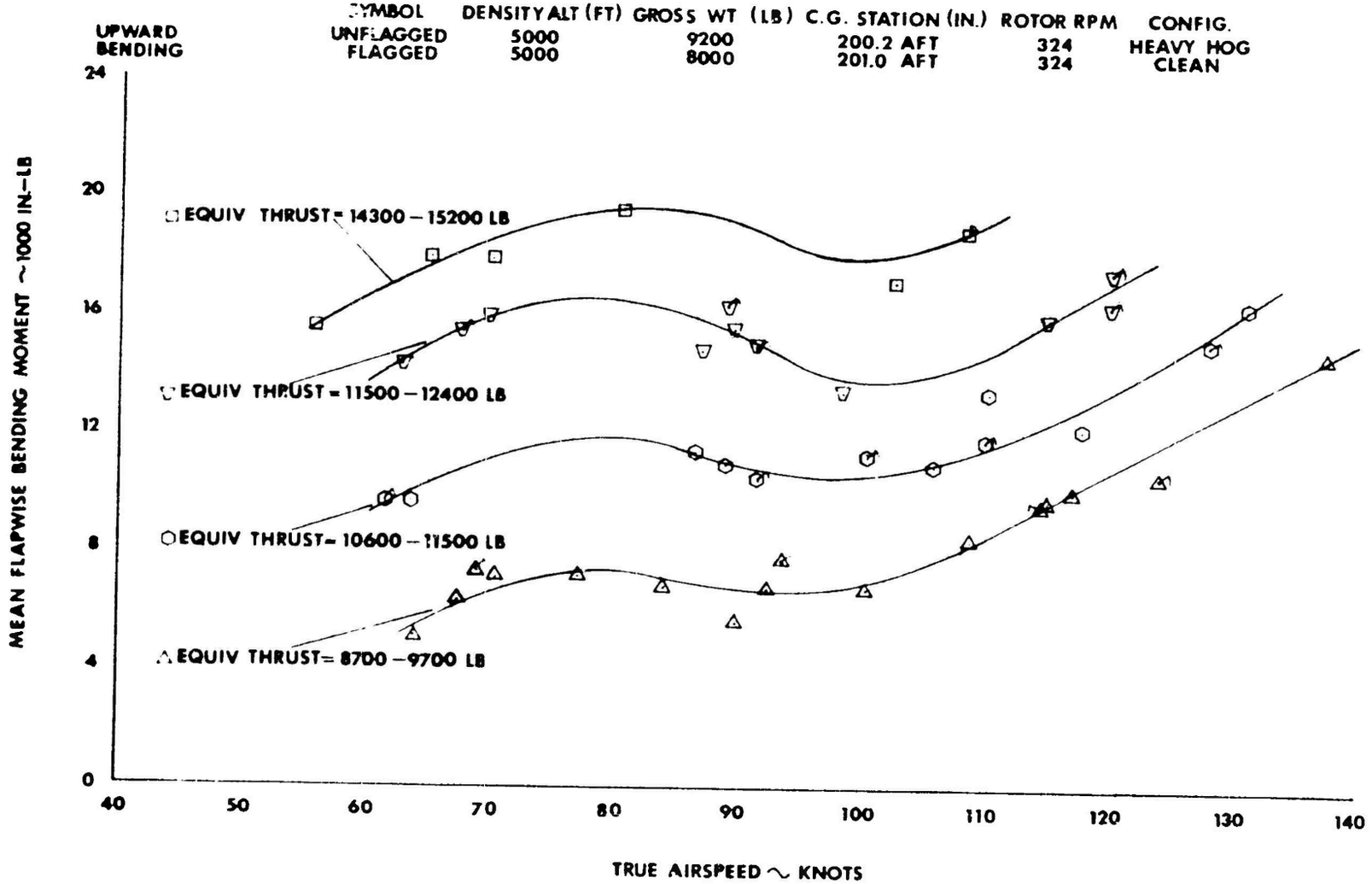

FIGURE 8
STATION 46 FLAPWISE BENDING MOMENT
AH–1G USA S/N 66–15247

SYMBOL	DENSITY ALT (FT)	GROSS WT (LB)	C.G. STATION (IN.)	ROTOR RPM	CONFIG.
UNFLAGGED	5000	9200	200.2 AFT	324	HEAVY HOG
FLAGGED	5000	8000	201.0 AFT	324	CLEAN

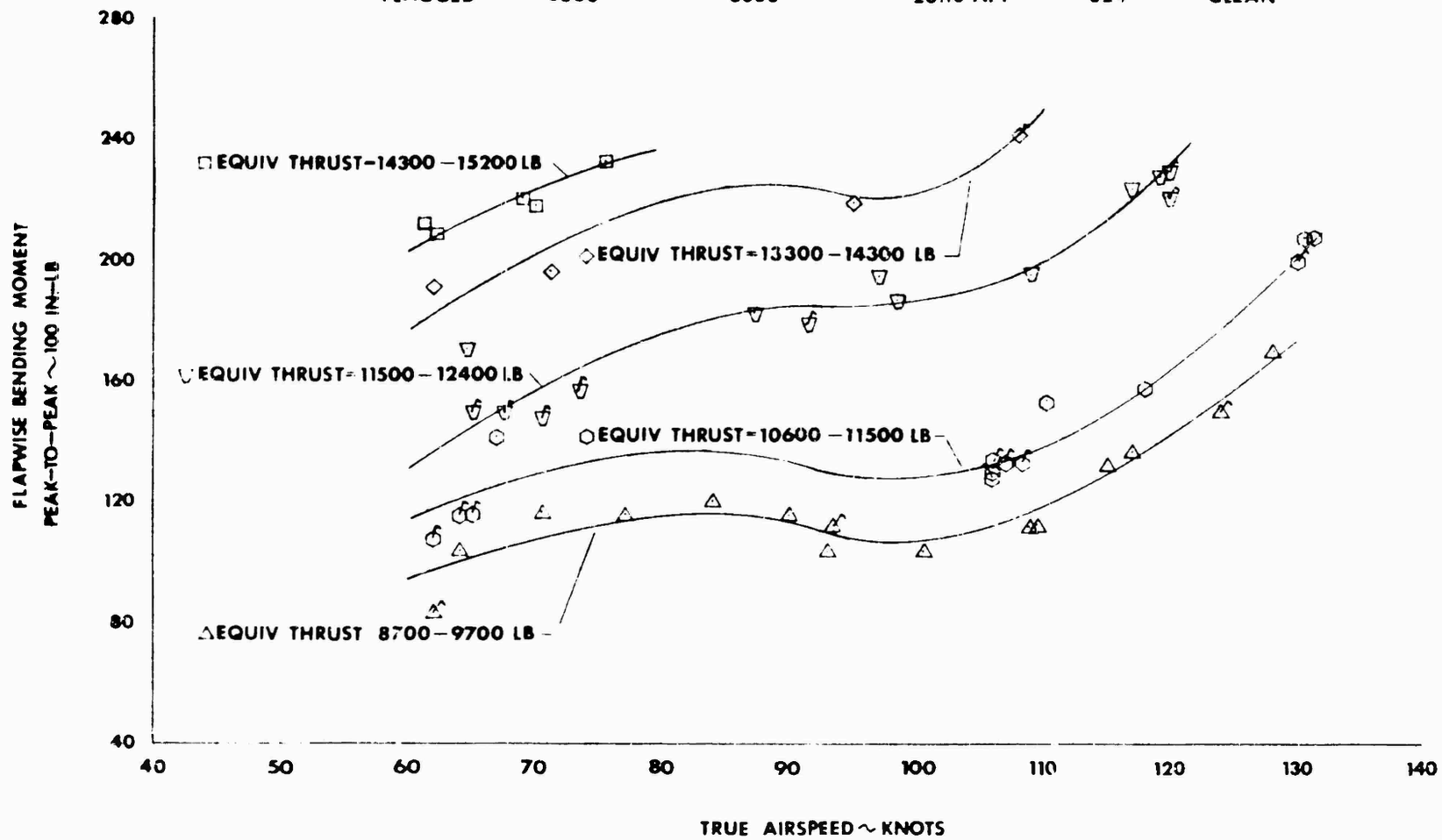

FIGURE 9
STATION 135 CHORDWISE BENDING MOMENT
AH-1G USA S/N 66-15247

SYMBOL	DENSITY ALT (FT)	GROSS WT (LB)	C.G. STATION (IN.)	ROTOR RPM	CONFIG.
UNFLAGGED	5000	9200	200.2 AFT	324	HEAVY HOG
FLAGGED	5000	8000	201.0 AFT	324	CLEAN

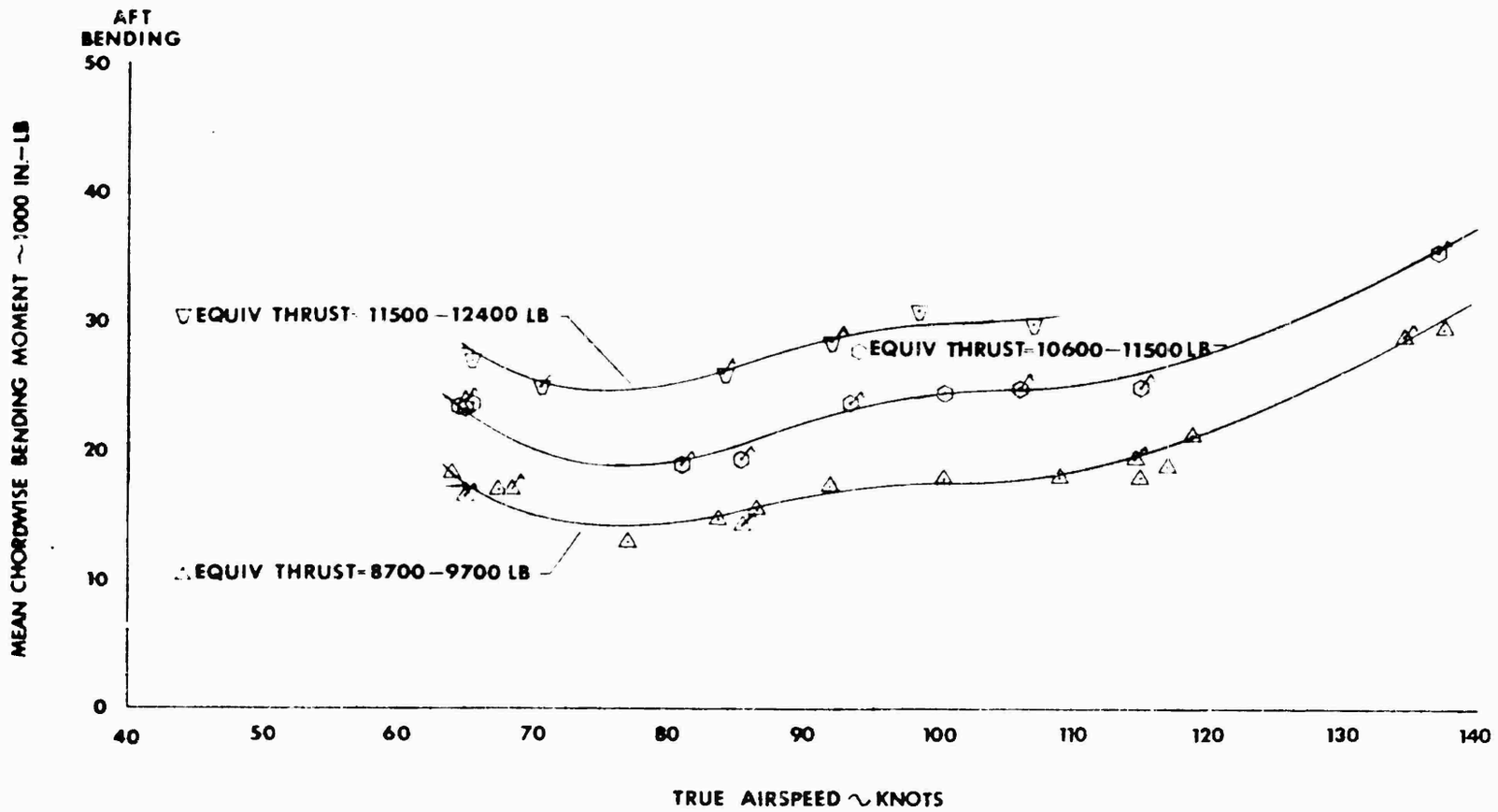

FIGURE 10
STATION 135 CHORDWISE BENDING MOMENT
AH-1G USA S/N 66-15247

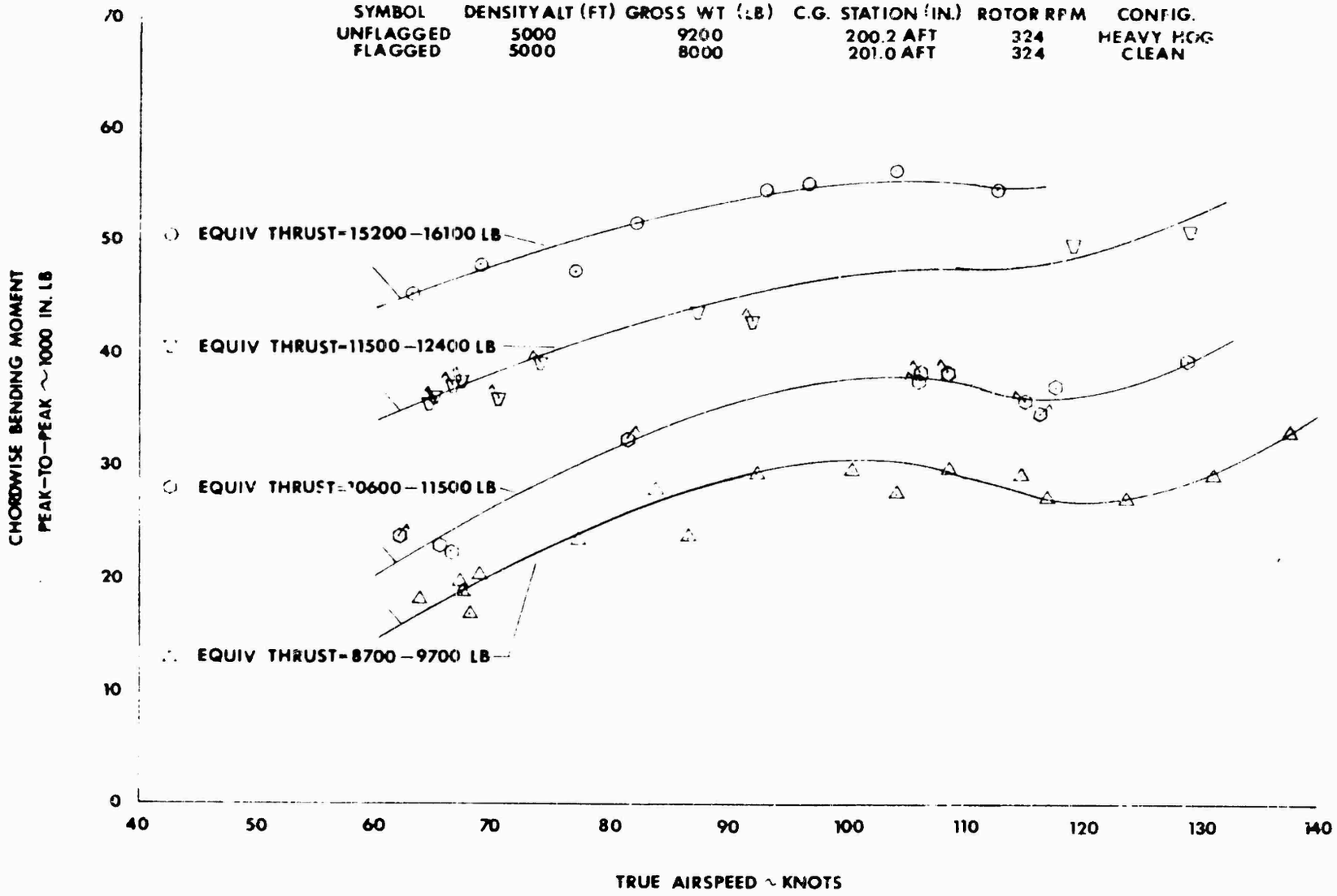

FIGURE 11
MAIN ROTOR ROTATING PITCH LINK AXIAL LOAD
AH-1G USA S/N 66-15247

SYMBOL	DENSITY ALT (FT)	GROSS WT (LB)	C.G. STATION (IN.)	ROTOR RPM	CONFIG.
UNFLAGGED	5000	9200	200.2 AFT	324	HEAVY HOG
FLAGGED	5000	8000	201.0 AFT	324	CLEAN

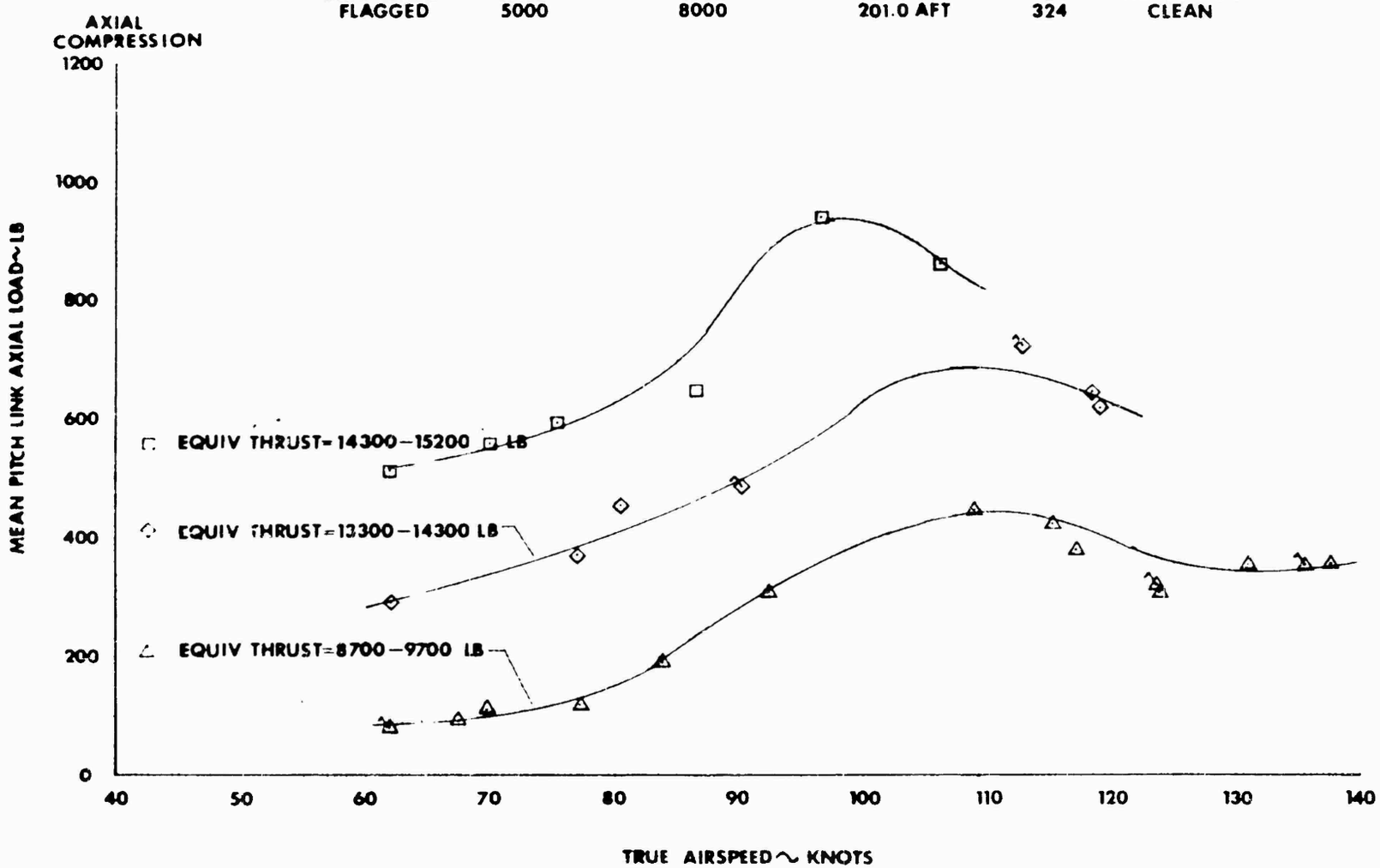

FIGURE 12
MAIN ROTOR ROTATING PITCH LINK AXIAL LOAD
AH-1G USA S/N 66-15277

SYMBOL	DENSITY ALT (FT)	GROSS WT (LB)	C.G. STATION (IN.)	ROTOR RPM	CONFIG.
UNFLAGGED	5000	9200	200.2 AFT	324	HEAVY HOG
FLAGGED	5000	8000	201.0 AFT	324	CLEAN

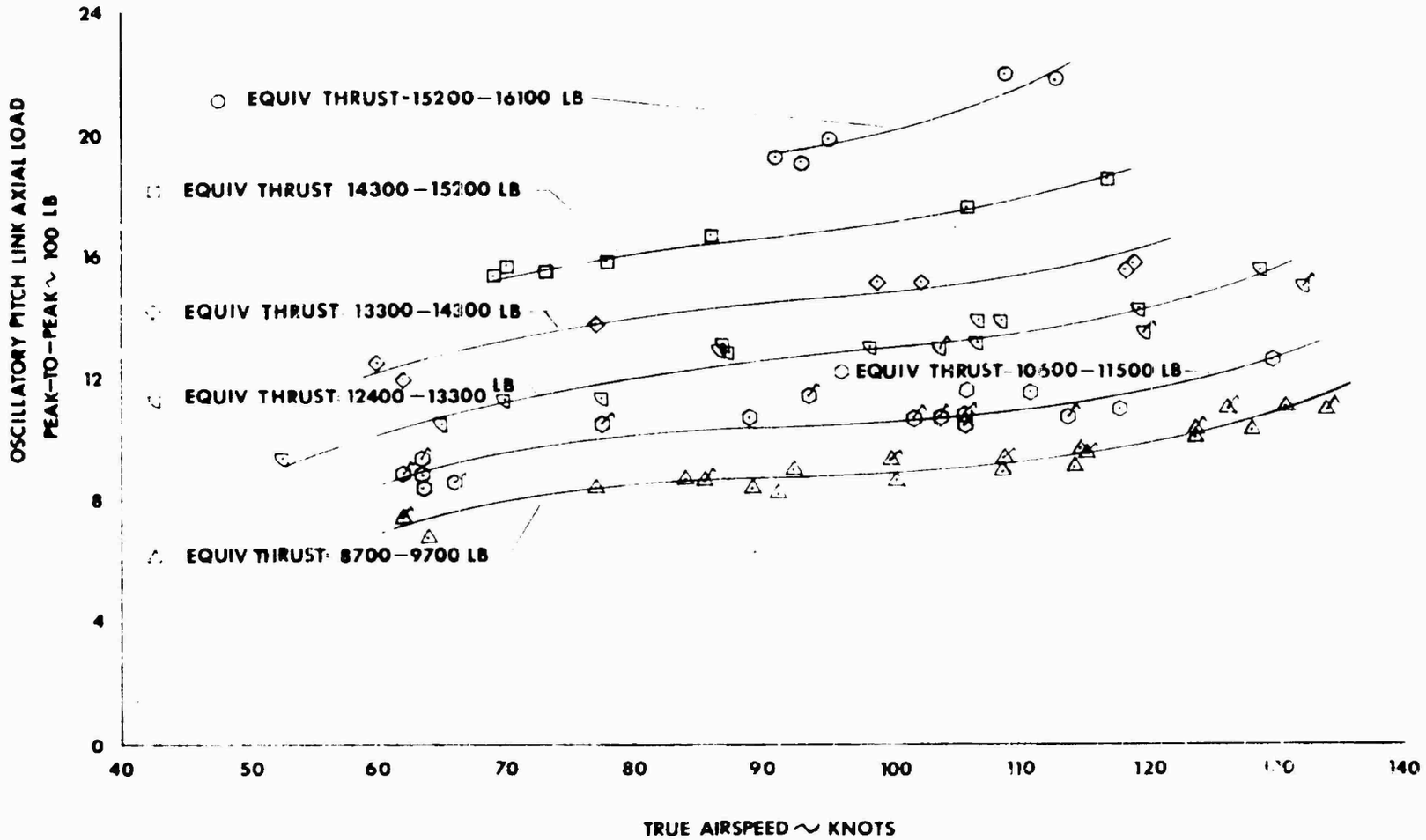

FIGURE 13
LONGITUDINAL PUSHROD AXIAL LOAD
AH-1G USA S/N 66-15247

SYMBOL	DENSITY ALT (FT)	GROSS WT (LB)	CG STATION (IN)	ROTOR RPM	CONFIG.
UNFLAGGED	5000	9200	200.2 AFT	324	HEAVY HOG
FLAGGED	5000	8000	201.0 AFT	324	CLEAN

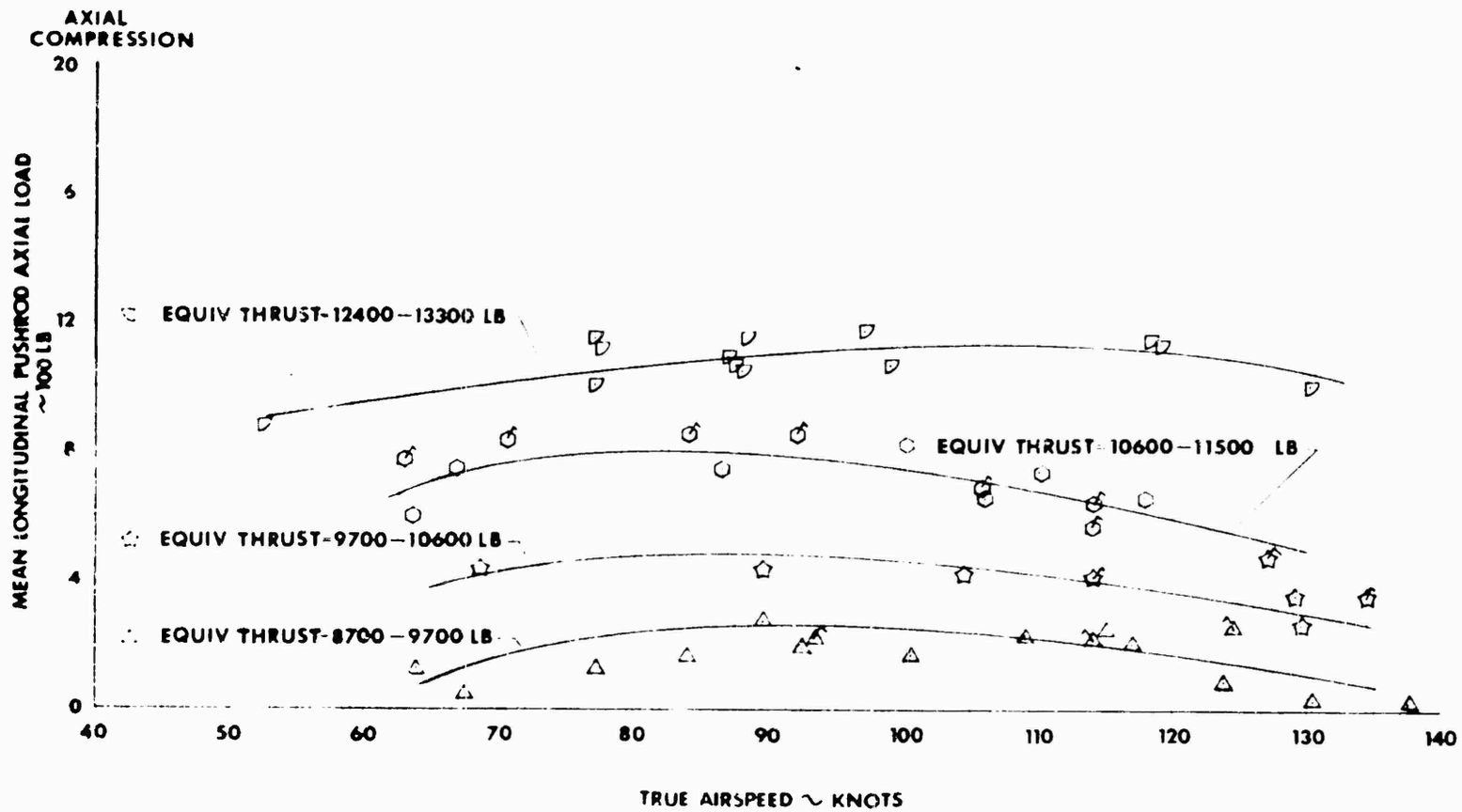

FIGURE 14
LONGITUDINAL PUSHROD AXIAL LOAD
AH-1G USA S/N 66-15247

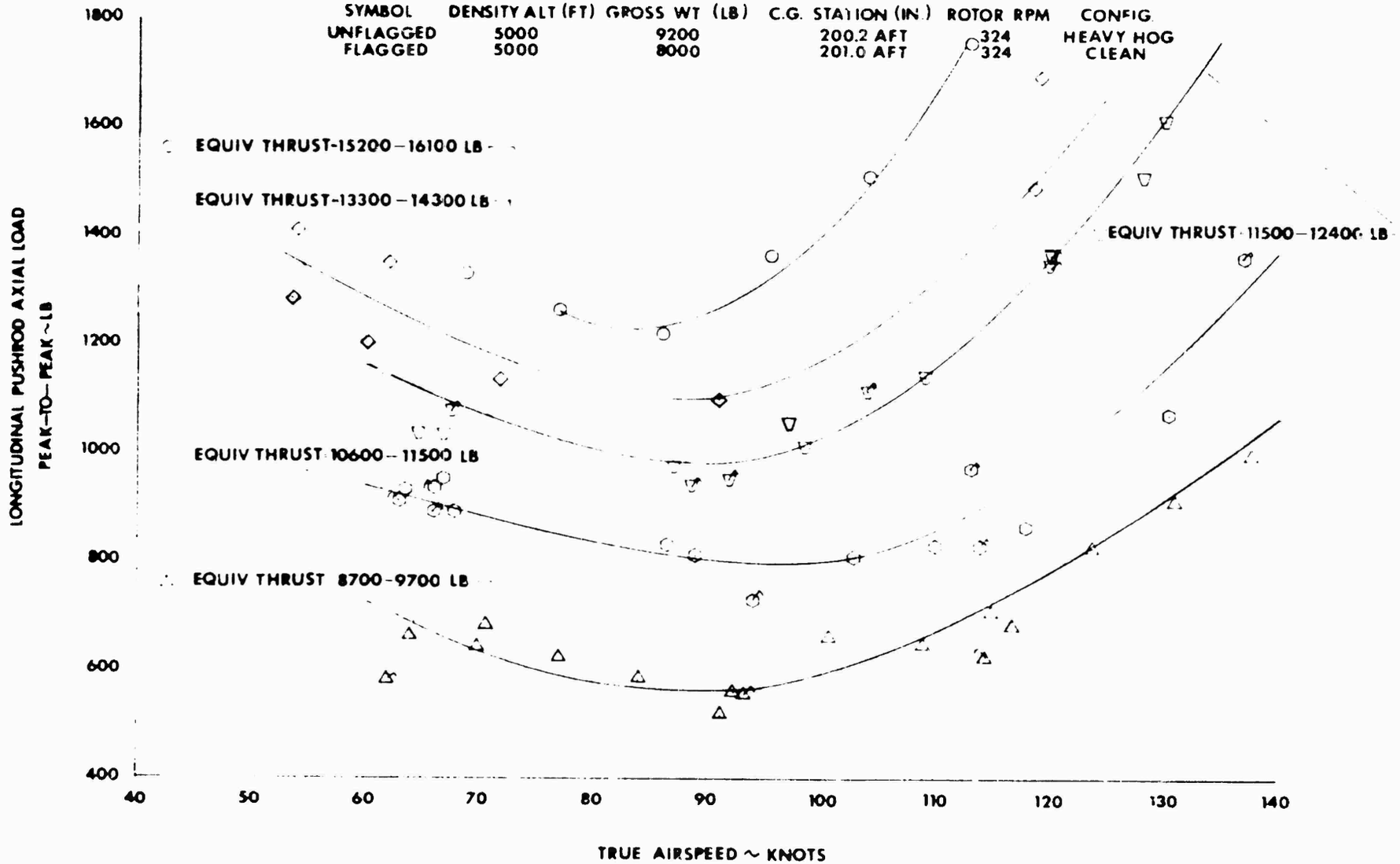

FIGURE 15
RETURN TO TARGET MANEUVERS
AH-1G USA S/N 66-15247

C G STATION	ROTOR RPM	CONFIG
AFT	324	HEAVY HOG

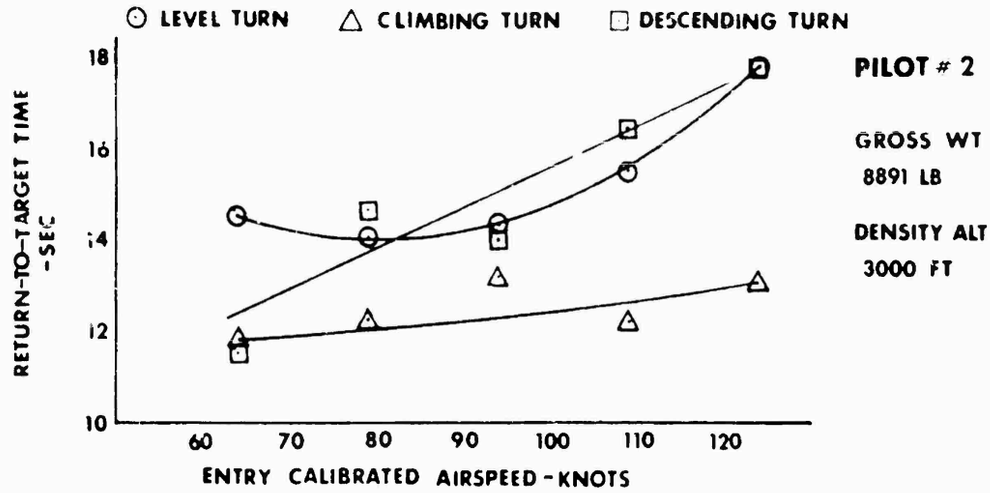

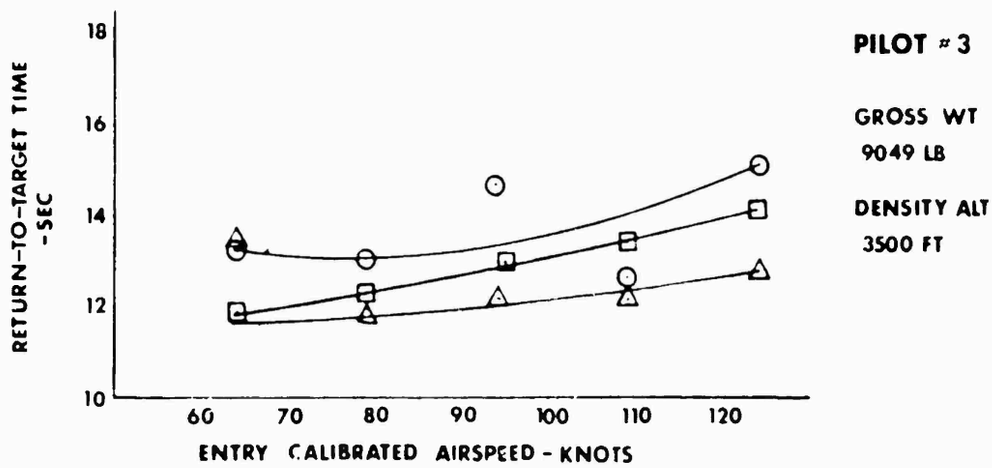

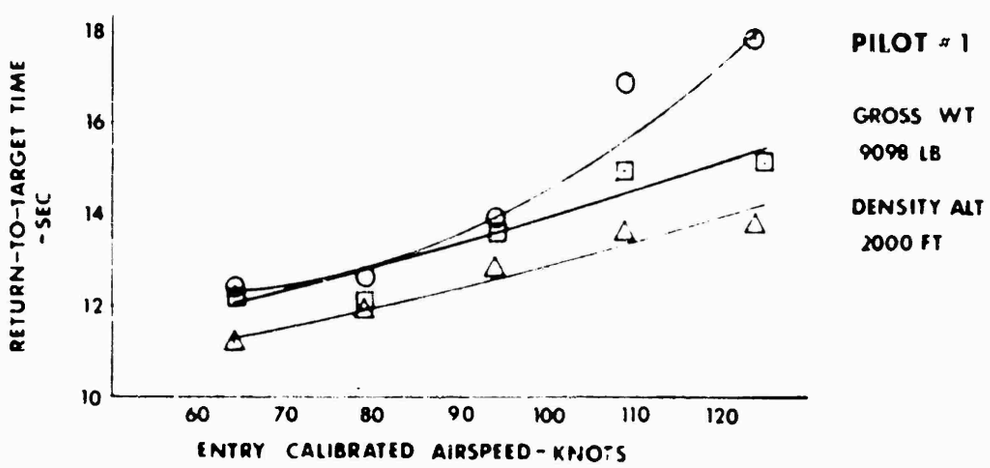

FIGURE 16
RETURN TO TARGET MANEUVERS
AH-1G USA S/N 66-15247

DENSITY ALT (FT)	GROSS WT (LB)	C.G. STATION (IN.)	ROTOR RPM	CONFIG.
2800	9000	AFT.	324	HEAVY HOG

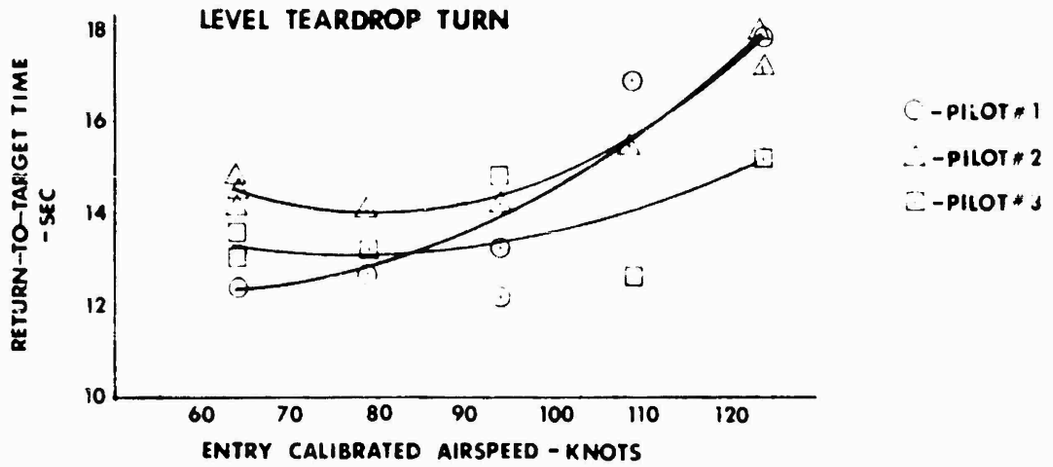

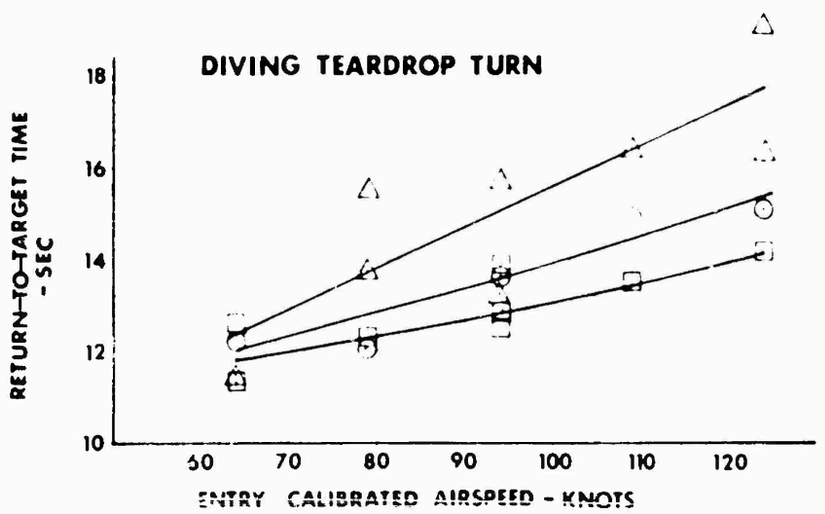

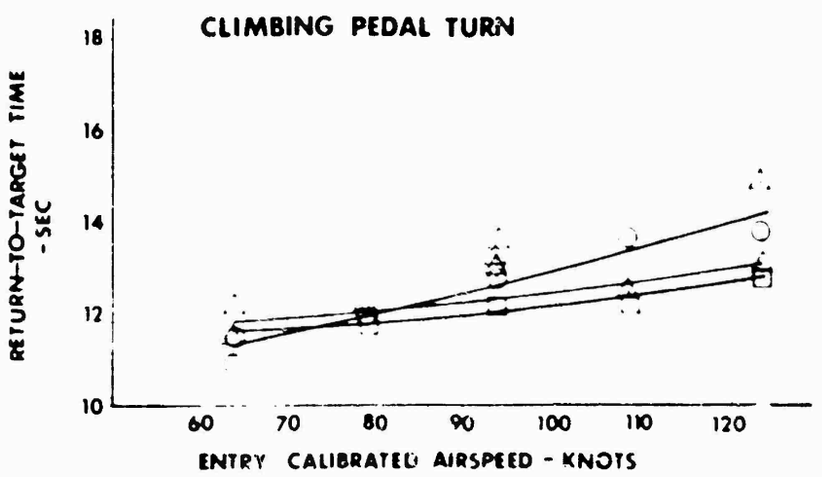

FIGURE 17
ENGINE TORQUE OSCILLATION
AH-1G USA S/N 66-15247

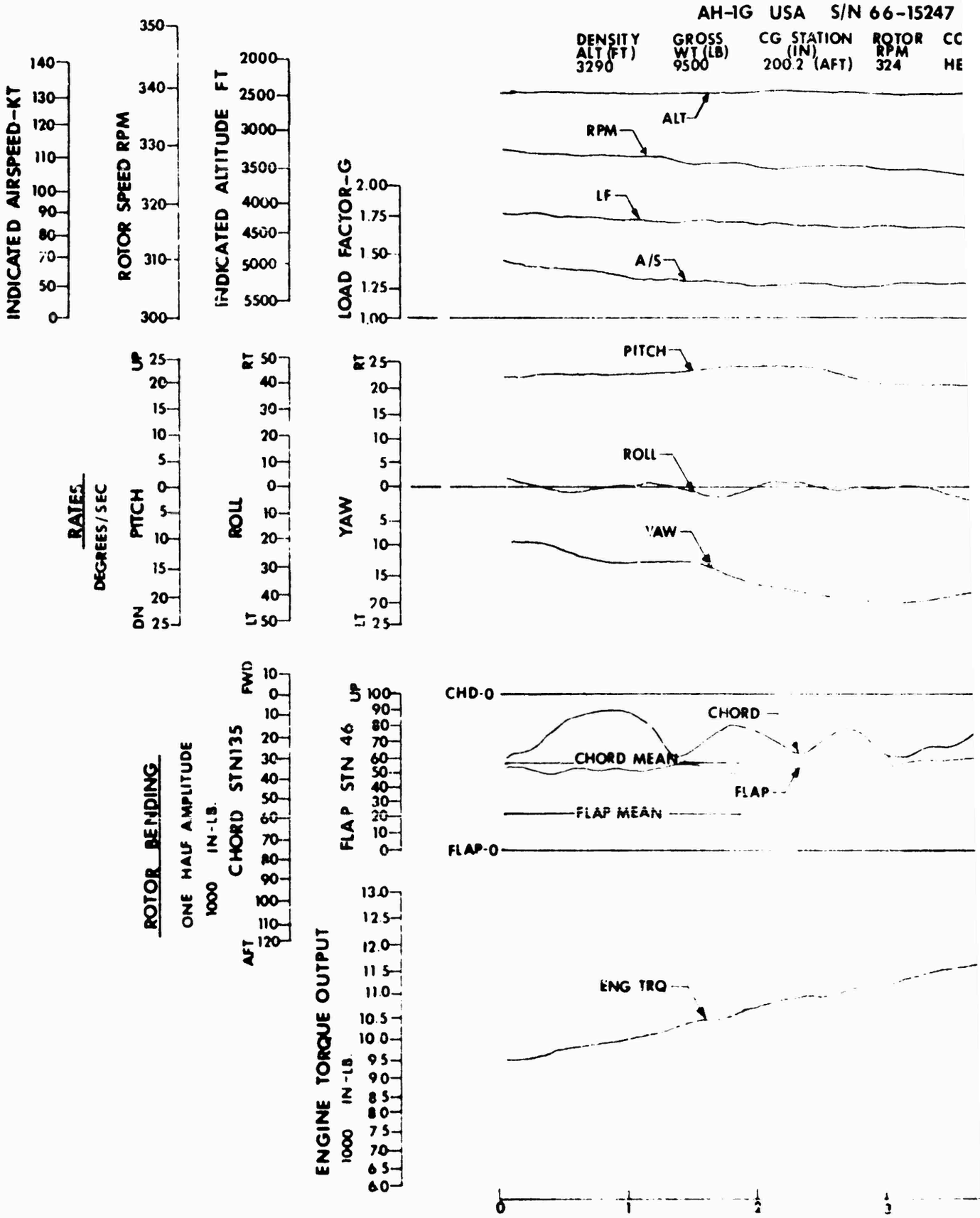

GURE 17
RQUE OSCILLATION
SA S/N 66-15247

STATION (IN)	ROTOR RPM	CONF'G
0.2 (AFT)	324	HEAVY HOG

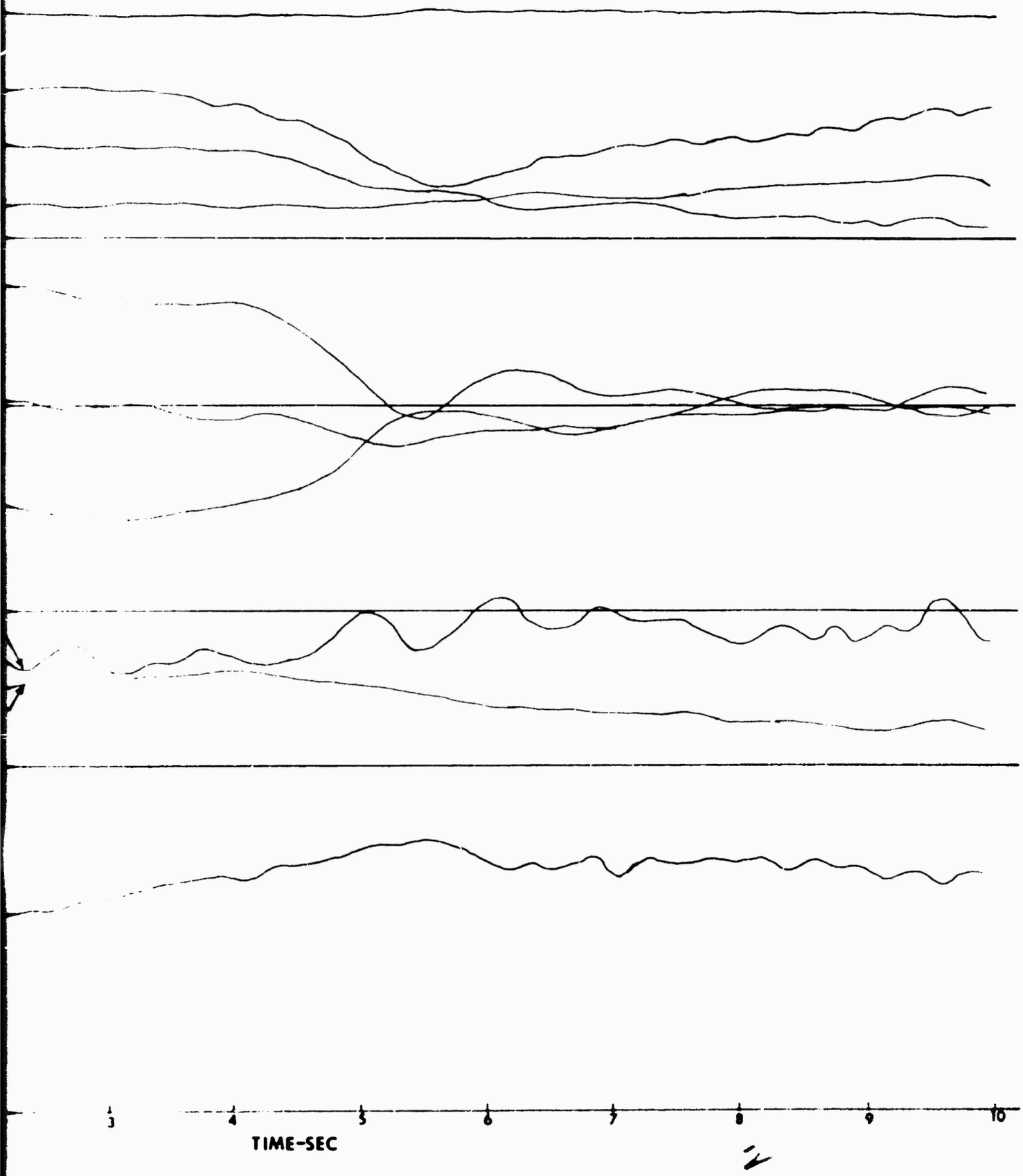

FIGURE 18
ENGINE TORQUE OSCILLATION
AH-1G USA S/N 66-15247

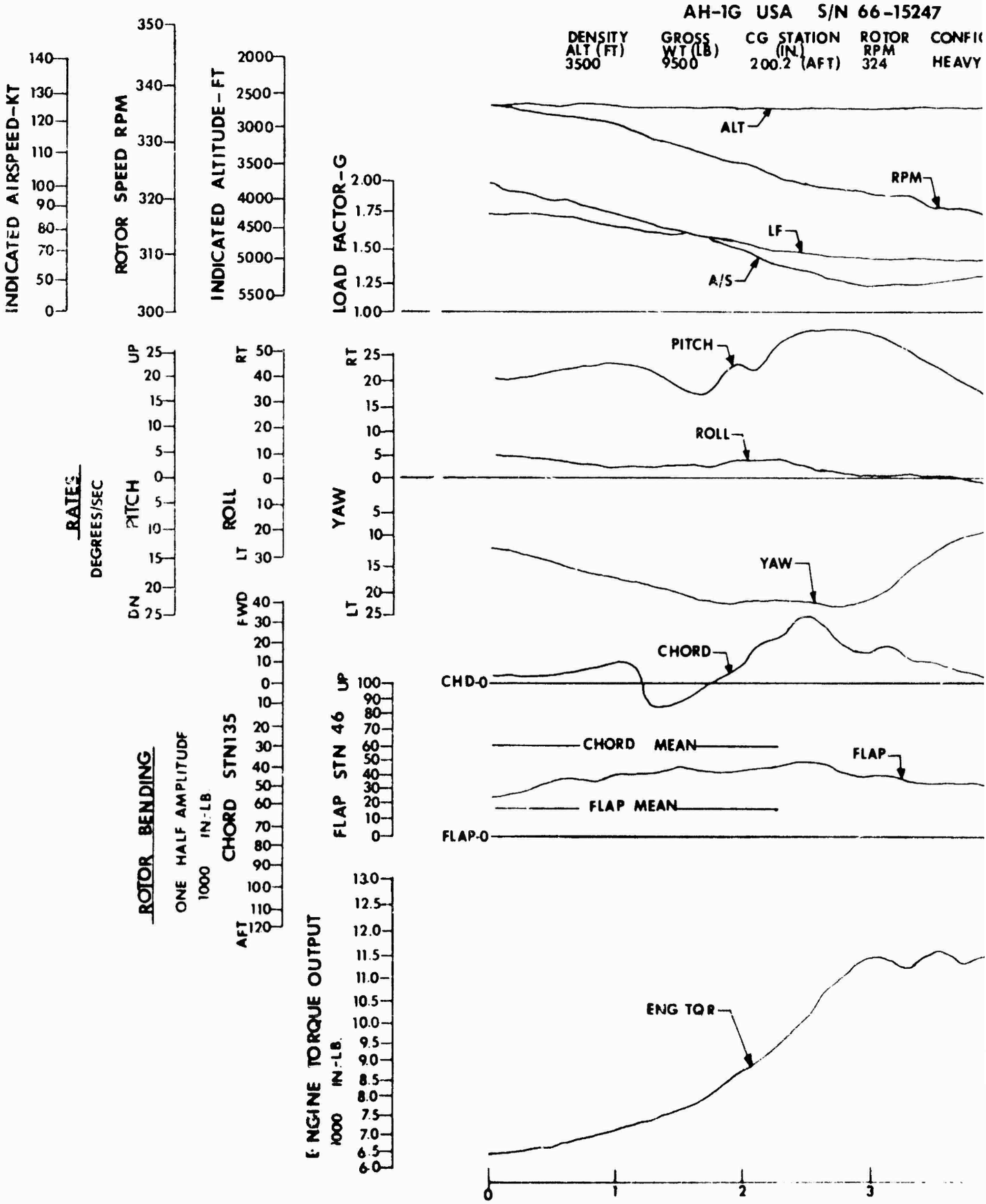

URE 18
QUE OSCILLATION
A S/N 66-15247

STATION (IN.)	ROTOR RPM	CONFIG
.2 (AFT)	324	HEAVY HOG

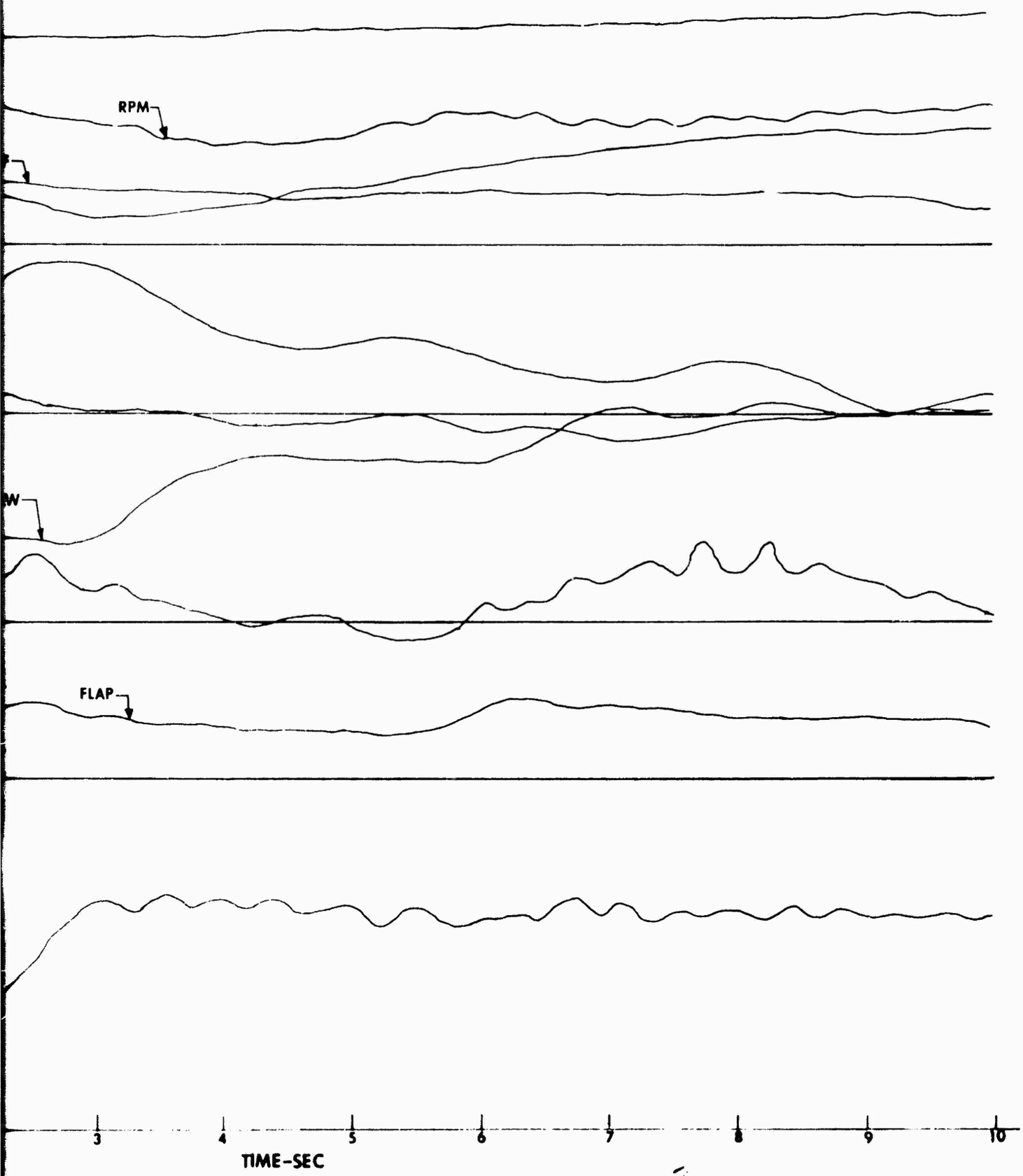

FIGURE 19
ENGINE TORQUE OSCILLATI
AH-1G USA S/N 66-1524

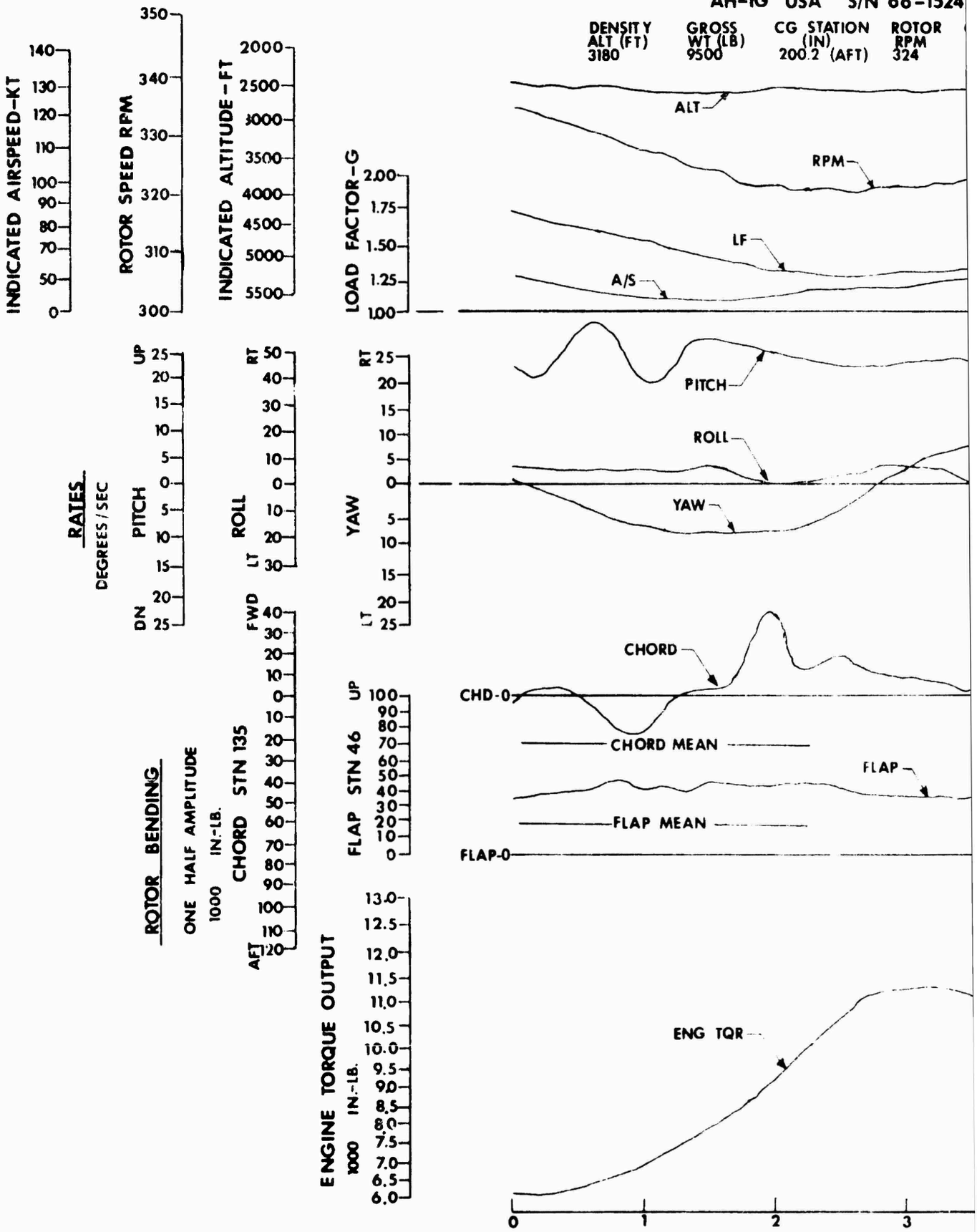

FIGURE 19
TORQUE OSCILLATION
USA S/N 66-15247

CG STATION (IN)	ROTOR RPM	CONFIG
200.2 (AFT)	324	HEAVY HOG

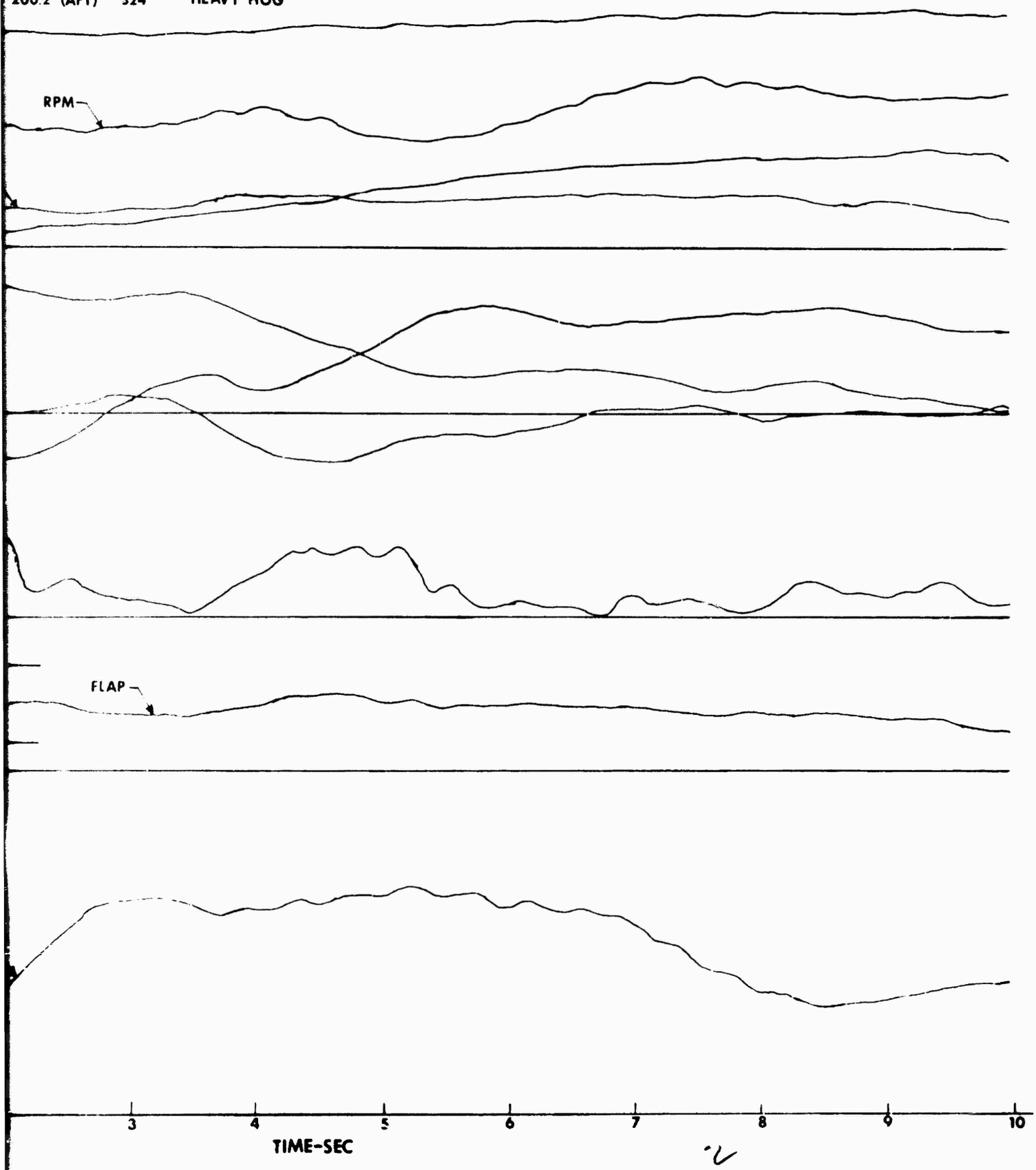

FIGURE 20a

CONTROL FORCE FEEDBACK CHARACTERISTICS

AH-1G USA S/N 66-15247

DENSITY ALT (FT)	GROSS WT (LB)	CG STATION (IN)	ROTOR RPM	CONFIG.
2080	9200	200.2 (AFT)	324	HEAVY HOG

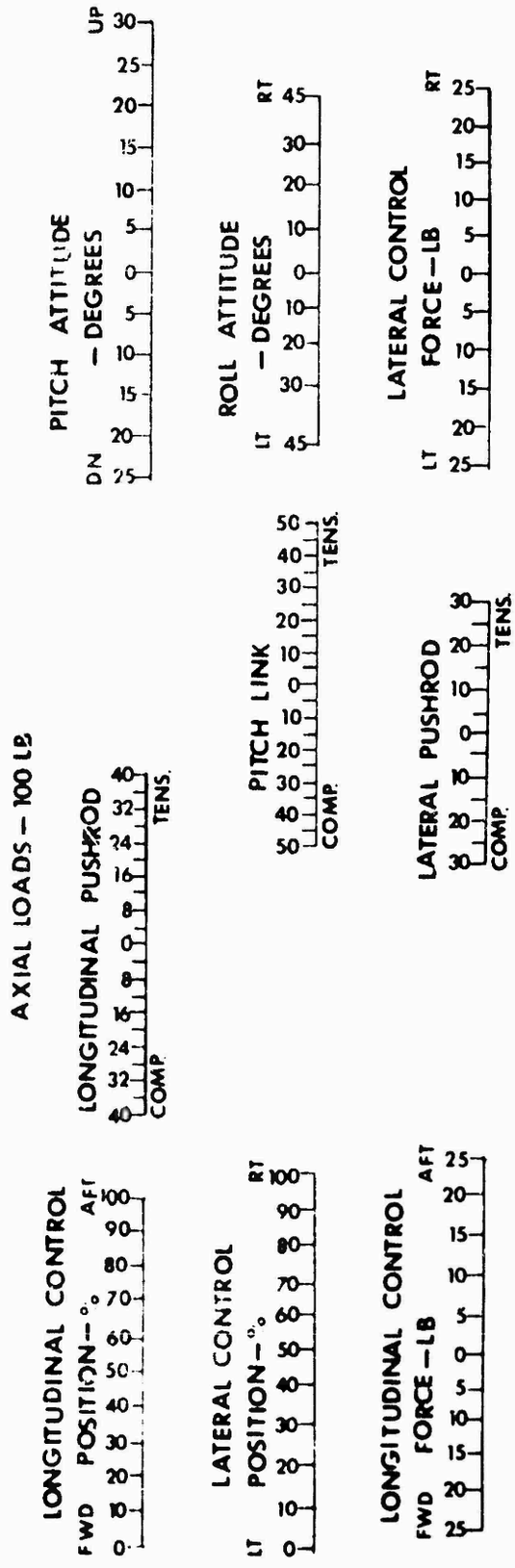

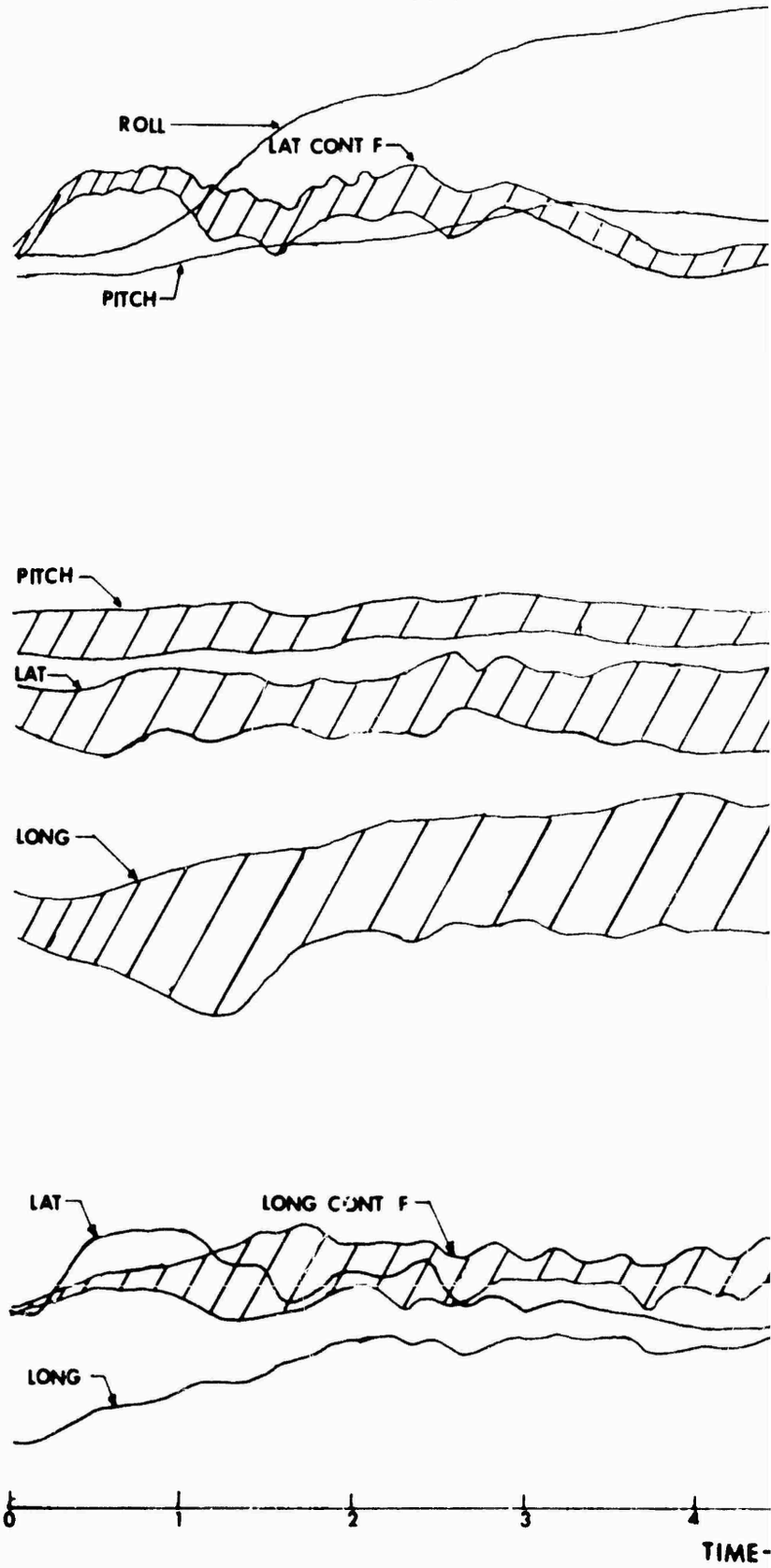

RE 20a

EDBACK CHARACTERISTICS

S/N 66-15247

TION	ROTOR RPM	CONFIG.
FT)	324	HEAVY HOG

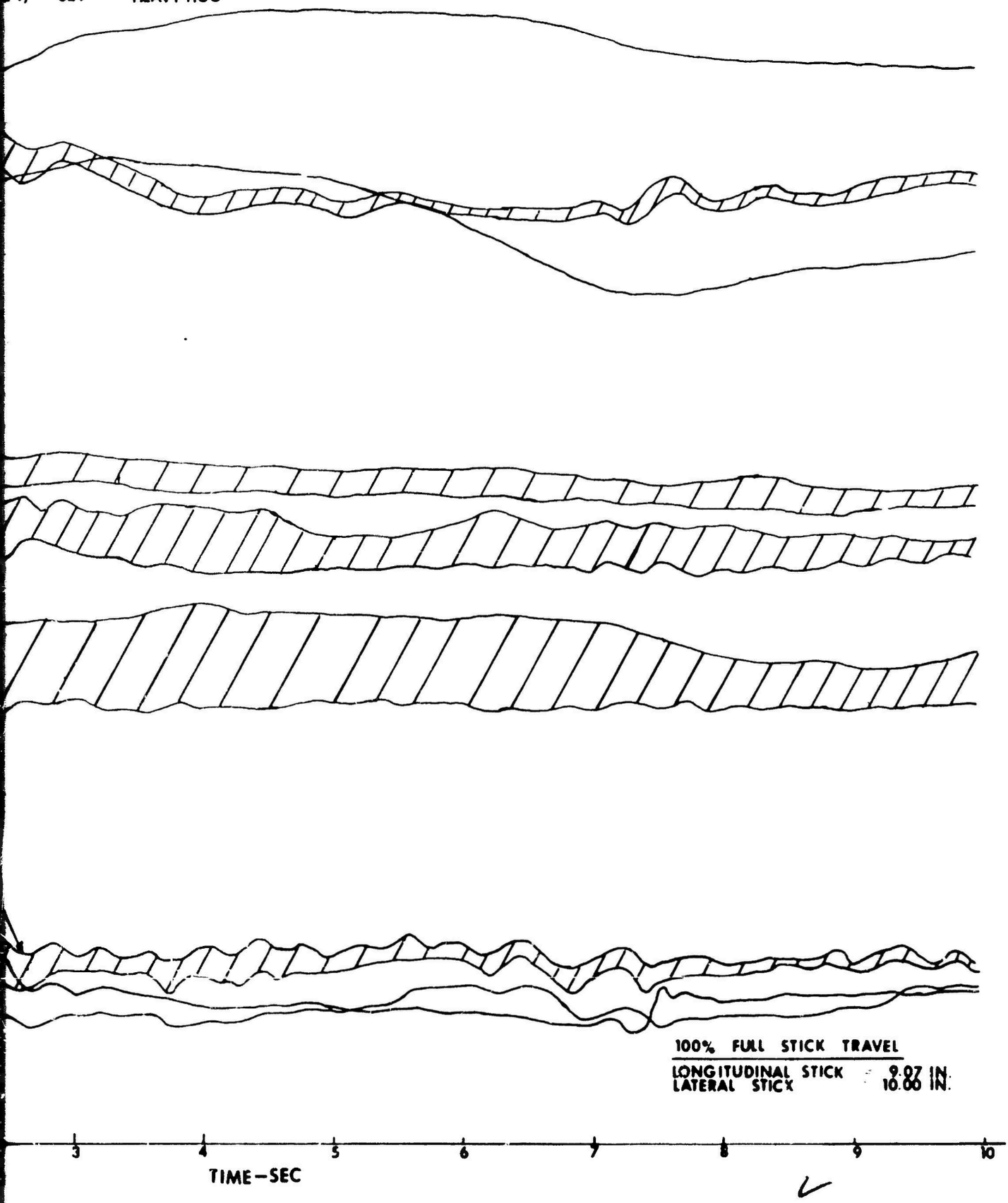

FIGURE 20b

CONTROL FORCE FEEDBACK CH

AH-1G USA S/N 66-1

DENSITY ALT (FT)	GROSS WT (LB)	CG STATION (IN)	ROTOR RPM
2080	9200	200.2 (AFT)	324

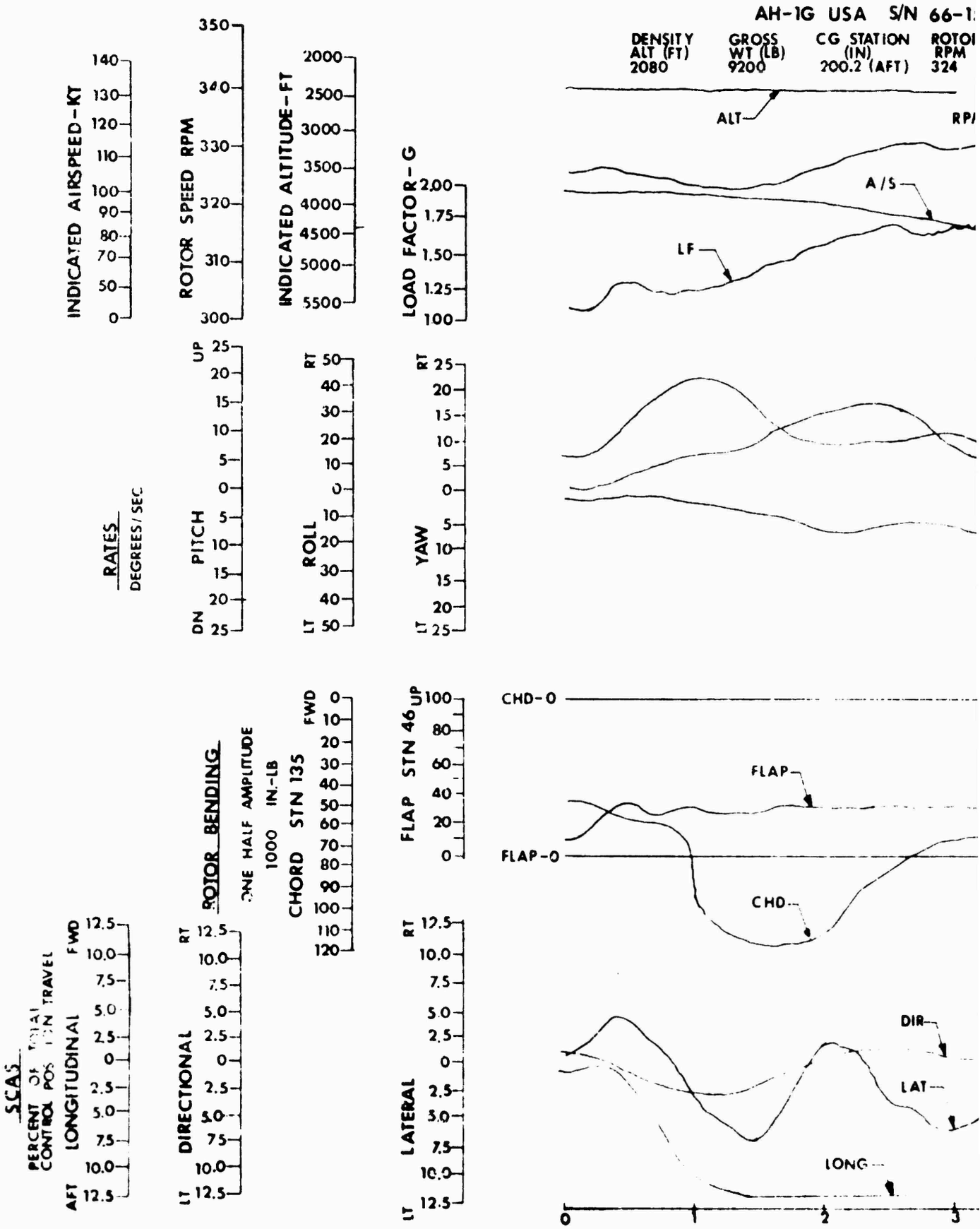

FIGURE 20b

CE FEEDBACK CHARACTERISTICS

USA S/N 66-15247

CG STATION (IN)	ROTOR RPM	CONFIG.
200.2 (AFT)	324	HEAVY HOG

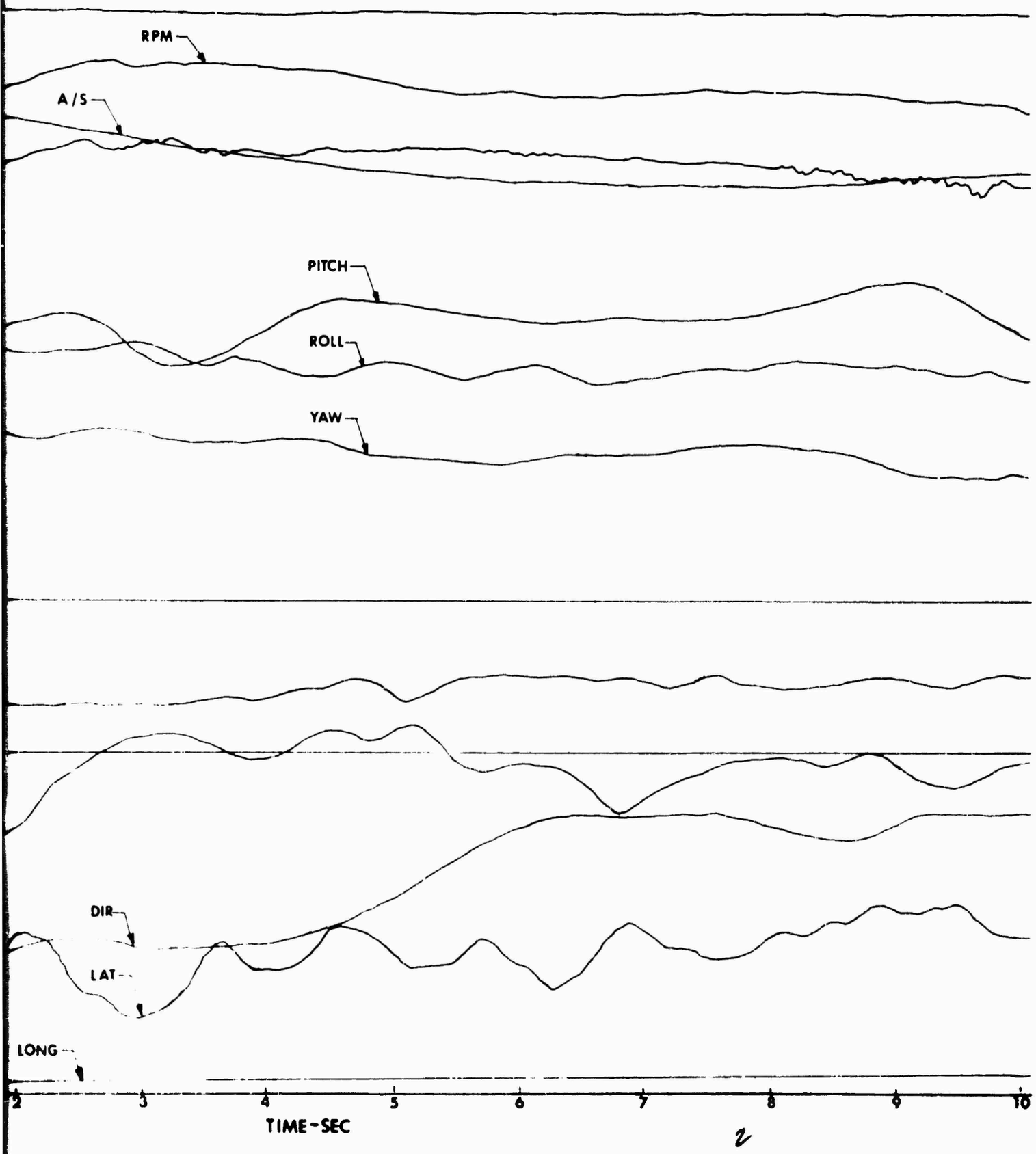

2

FIGURE 21a

CONTROL FORCE FEEDBACK CHARACTERISTICS

AH-1G USA S/N 66-15247

DENSITY ALT. (FT)	GROSS WT (LB)	CG STATION (IN)	ROTOR RPM	CONFIG.
2060	9200	200.2 (AFT)	324.	HEAVY HOG

RE 21a

EDBACK CHARACTERISTICS

S/N 66-15247

TION	ROTOR RPM	CONFIG.
FT)	324.	HEAVY HOG

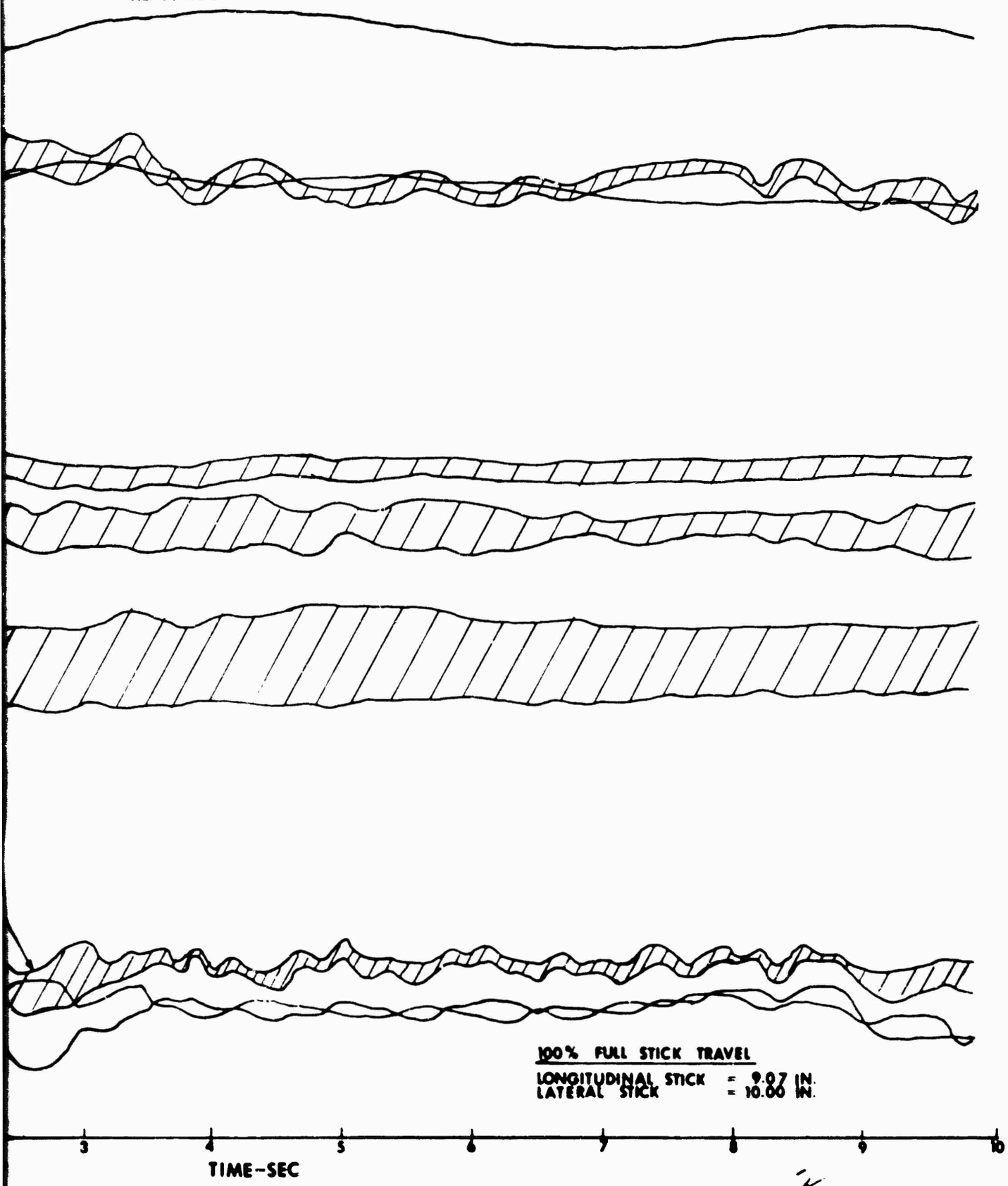

FIGURE 21b

CONTROL FORCE FEEDBACK CH

AH-1G USA S N 66-1

FIGURE 21b

E FEEDBACK CHARACTERISTICS

USA S N 66-15247

CG STATION (IN)	ROTOR RPM	CONFIG.
300.2 (AFT)	324	HEAVY HOG

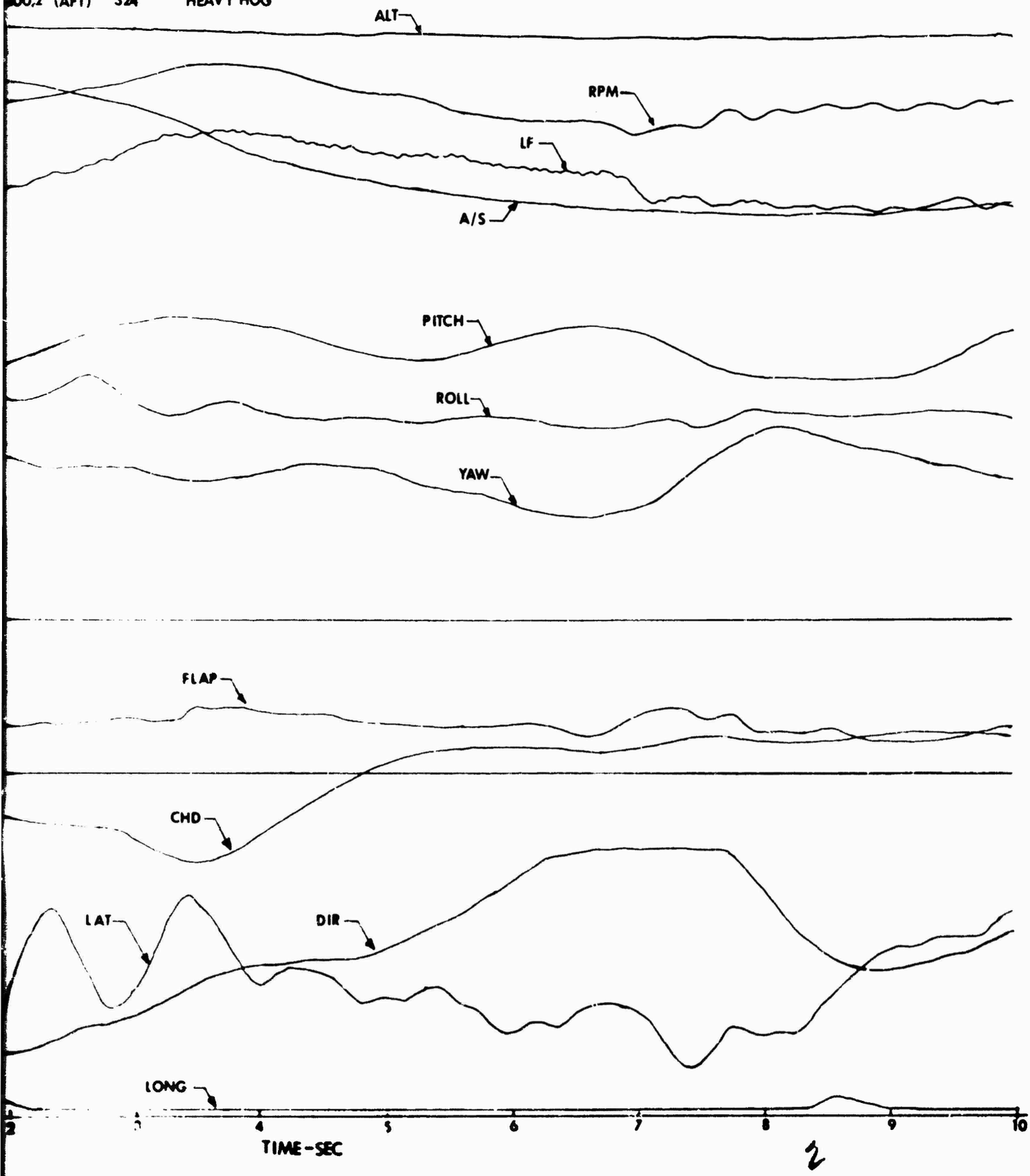

2

FIGURE 22
SYMMETRICAL PU
AH 1G USA S

DENSITY ALT (FT)	GROSS WT (LB)	RO RI
5535	9500	32

FIGURE 22a
SYMMETRICAL PULL-UP
AH 1G USA S/N 66 15247

DENSITY ALT (FT)	GROSS WT (LB)	ROTOR RPM	CONFIGURATION	C. G.
5535	9500	324	HEAVY HOG	AFT

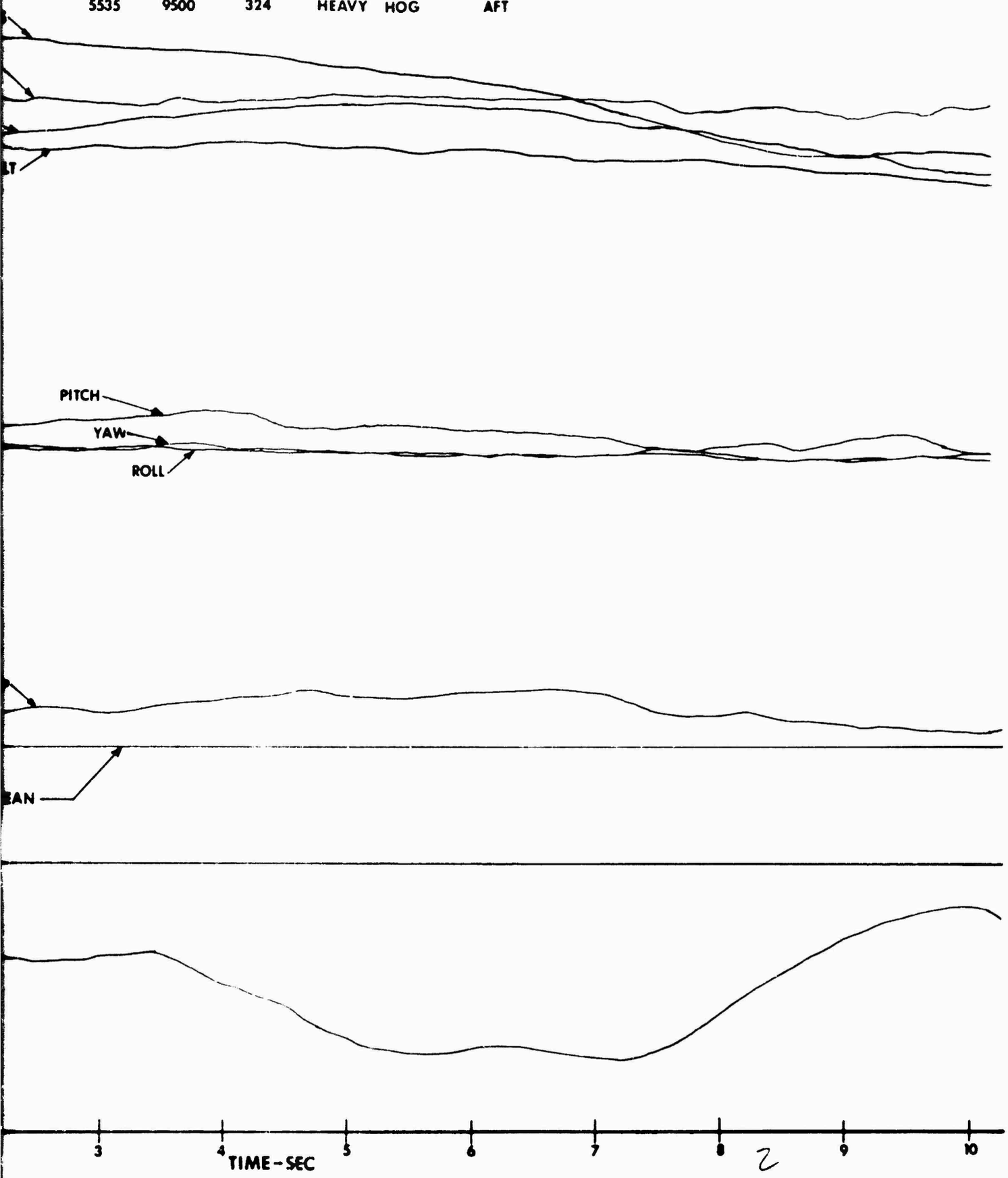

2

F
SYMMET
AH-1G U

DENSITY ALT (FT)	GR WT
5535	95

FIGURE 22b

SYMMETRICAL PULL-UP

AH-1G USA S/N 66-15247

DENSITY ALT (FT)	GROSS WT (LB)	ROTOR RPM	CONFIGURATION	C. G.
5535	9500	324	HEAVY HOG	AFT

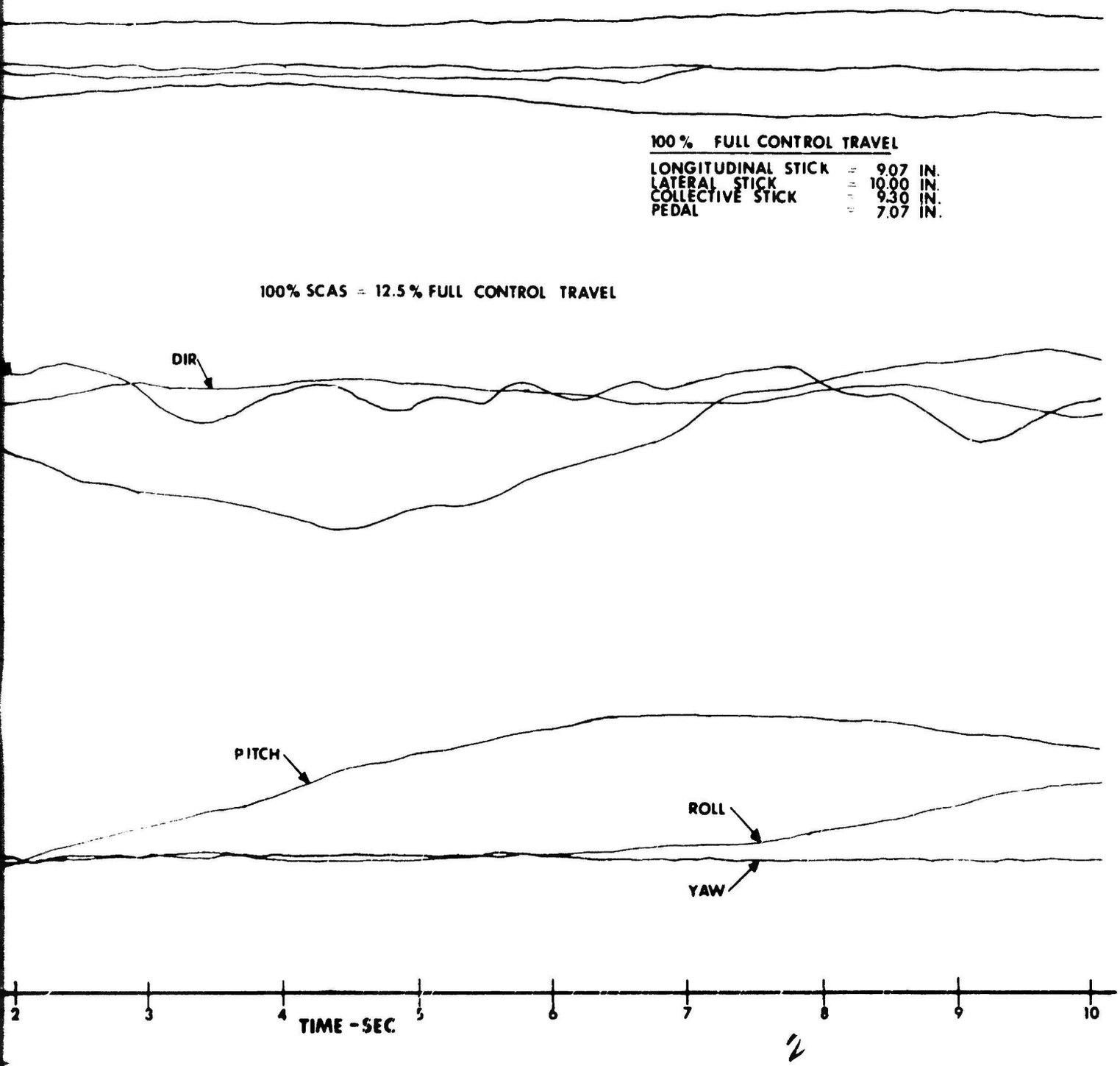

2

FIGURE 23a
SYMMETRICAL PULL
AH-1G USA S/N 6

DENSITY ALT (FT)	GROSS WT (LB)	ROTOR RPM
5535	9500	324

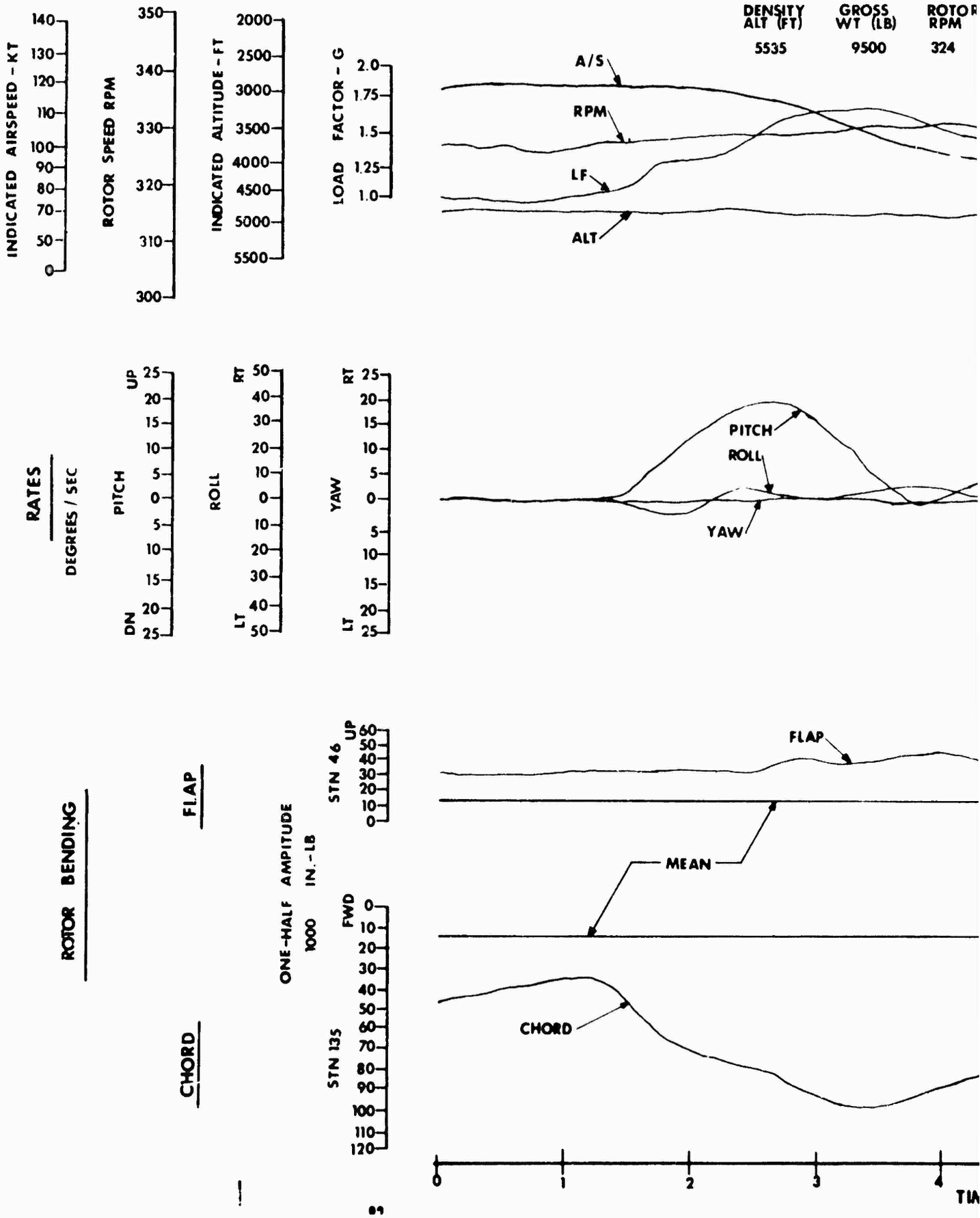

FIGURE 23a

SYMMETRICAL PULL-UP

AH-1G USA S/N 66-15247

DENSITY ALT (FT)	GROSS WT (LB)	ROTOR RPM	CONFIGURATION	C. G.
5535	9500	324	HEAVY HOG	AFT

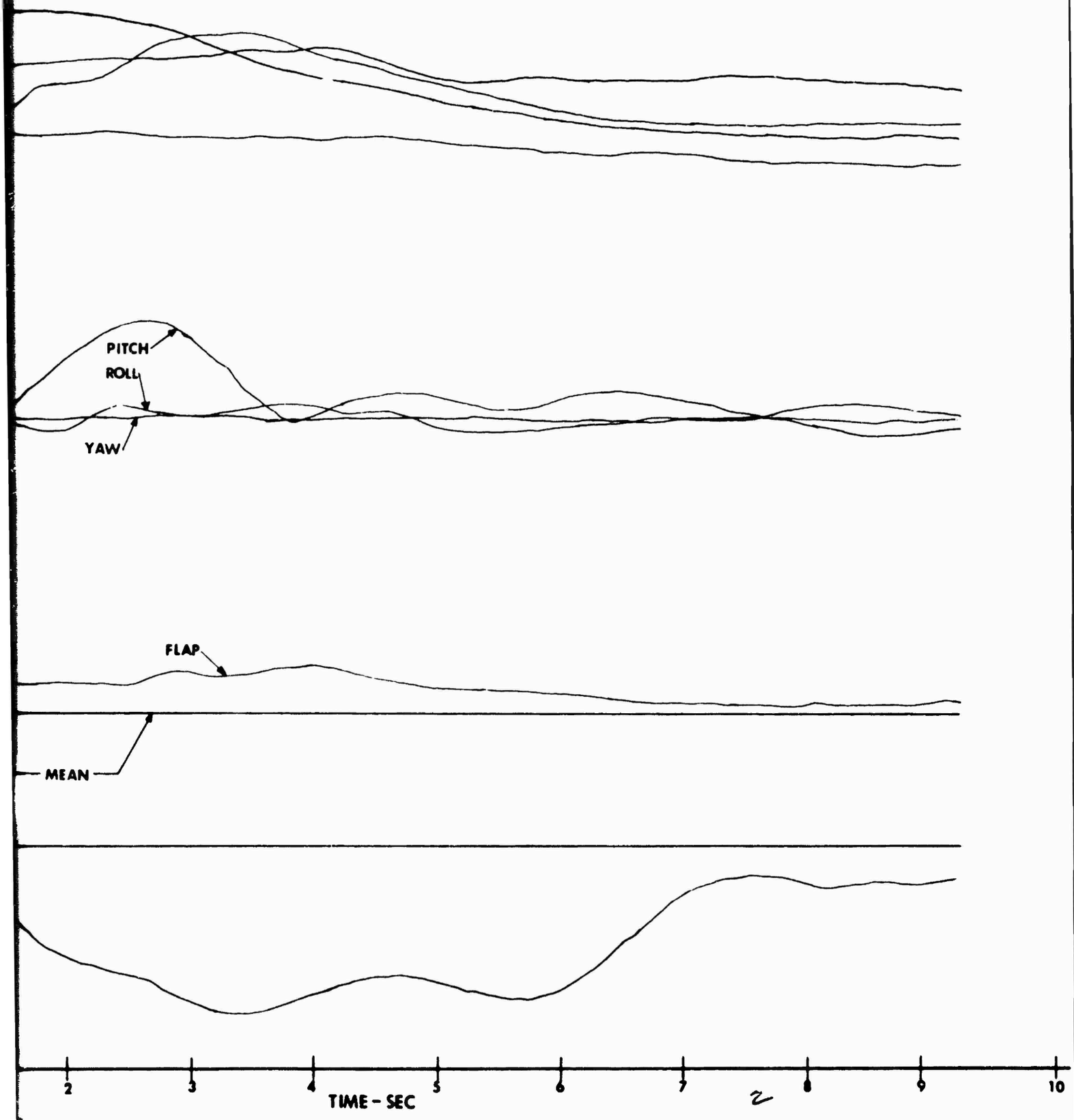

SY
AH
DENSITY
ALT (FT)
3535
CONTROL POSITION - %
LONGITUDINAL
FWD
AFT
LATERAL
LT
RT
DIRECTIONAL
LT
RT
COLLECTIVE
DN
UP
LAT
LONG
SCAS
PERCENT OF TOTAL
CONTROL POSITION TRAVEL
LONGITUDINAL
AFT
FWD
LATERAL
LT
RT
DIRECTIONAL
LT
RT
LAT
DIR
LONG
ATTITUDE - DEGREES
PITCH
DN
UP
ROLL
LT
RT
YAW
LT
RT
PITCH
0
1
2
3

FIGURE 23b

SYMMETRICAL PULL-UP

AH-1G USA S/N 66-15247

DENSITY ALT (FT)	GROSS WT (LB)	ROTOR RPM	CONFIGURATION	C.G.
5535	9500	324	HEAVY HOG	AFT

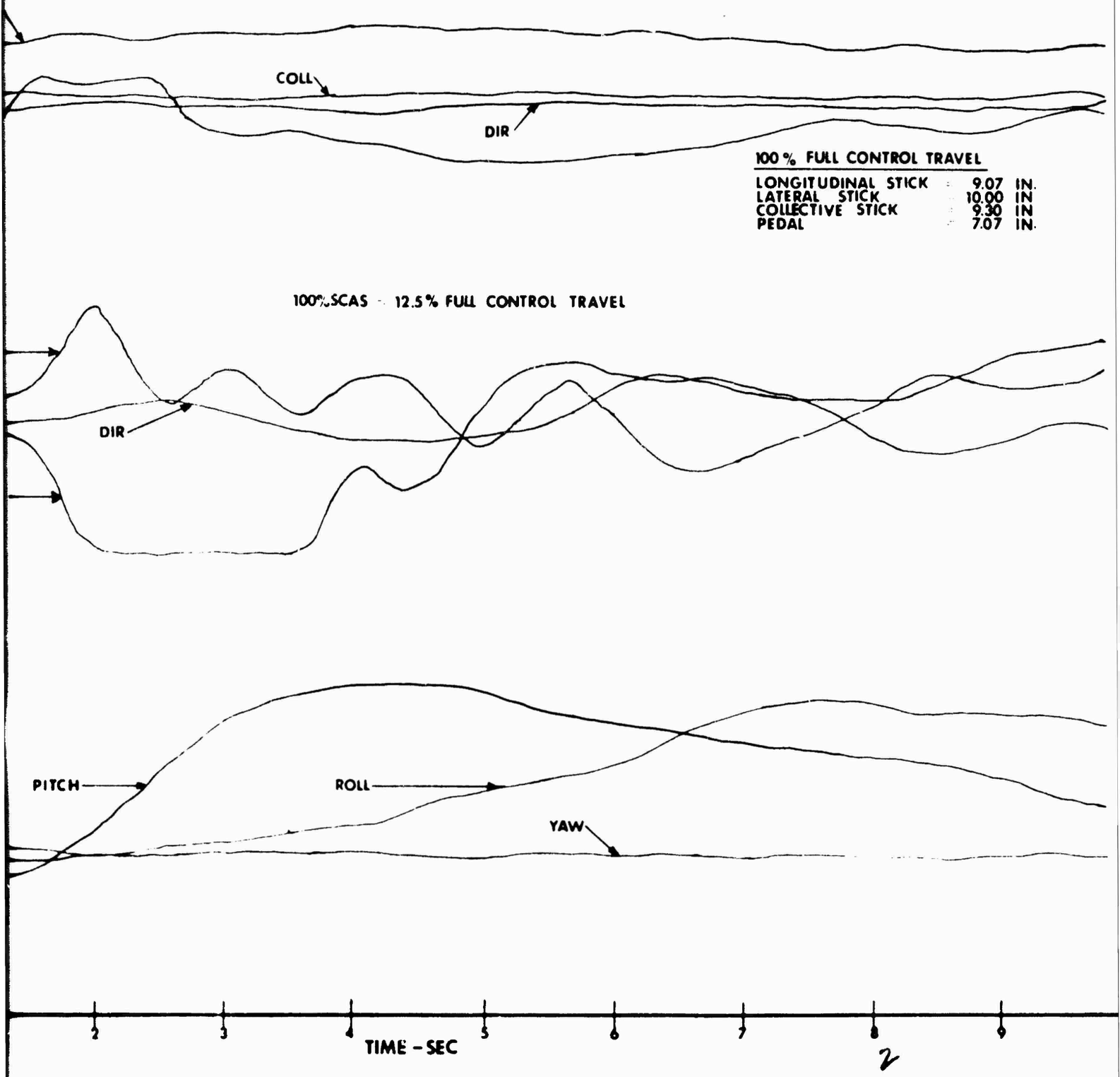

2

UNCLASSIFIED
Security Classification

DOCUMENT CONTROL DATA - R & D

(Security classification of title, body of abstract and indexing annotation must be entered when the overall report is classified)

1. ORIGINATING ACTIVITY *(Corporate author)*
US ARMY AVIATION SYSTEMS TEST ACTIVITY
EDWARDS AIR FORCE BASE, CALIFORNIA 93523

2a. REPORT SECURITY CLASSIFICATION
UNCLASSIFIED

2b. GROUP

3. REPORT TITLE
ENGINEERING FLIGHT TEST
AH-1G HELICOPTER (HUEYCOBRA)
MANEUVERING LIMITATIONS

4. DESCRIPTIVE NOTES *(Type of report and inclusive dates)*
Final Report, September 1969 through December 1970

5. AUTHOR(S) *(First name, middle initial, last name)*
RICHARD B. LEWIS, II, Project Officer/Engineer
EDWARD E. BAILES, Project Engineer
RANDY D. McCLELLAN, Engineer
MARVIN W. BUSS, Project Pilot
WILLIAM J. CONNOR, CW4, AV, US Army, Project Pilot
JOHN A. JOHNSTON, LTC, TC, US Army, Project Pilot
JOHN D. CLAXTON, CPT, TC, US Army, Project Pilot

6. REPORT DATE
MARCH 1971

7a. TOTAL NO. OF PAGES
87

7b. NO. OF REFS
22

8a. CONTRACT OR GRANT NO.
RDTE PROJECT NO. 1X141807D174

b. PROJECT NO.
USAAVSCOM PROJECT NO. 69-11

c.
USAASTA PROJECT NO. 69-11

d.

9a. ORIGINATOR'S REPORT NUMBER(S)
USAASTA PROJECT NO. 69-11

9b. OTHER REPORT NO(S) *(Any other numbers that may be assigned this report)*
N/A

10. DISTRIBUTION STATEMENT
This document may be fu[redacted] approval of the CG, USAAVSCOM, ATTN: AMSAV-R-[redacted] 63166.

11. SUPPLEMENTARY NOTES

12. SPONSORING MILITARY ACTIVITY
US ARMY AVIATION SYSTEMS COMMAND
ATTN: AMSAV-R-F
PO BOX 209, ST. LOUIS, MISSOURI 63166

13. ABSTRACT

The AH-1G helicopter maneuvering limitations flight test program was conducted at Edwards Air Force Base, California, between 13 March and 4 May 1970. The purpose of the test program was to study in detail the characteristics of maneuvering flight and to identify any limitations required to improve flight safety. The program included investigation of steady-state turns, three types of return-to-target maneuvers, and simulated operational maneuvers. Repeated instances of untorquing of the tail rotor retention nut were encountered during flight and constituted a safety-of-flight deficiency. Four shortcomings were noted: 1) undesirable cyclic control force characteristics, 2) transient torque surge, 3) insufficient main rotor rpm overspeed margin, 4) lateral stability and control augmentation system instability. It was concluded that the maneuvering characteristics of the AH-1G are generally excellent and are suitable for operational use. A number of maneuvering characteristics should be emphasized during pilot training, and the information should be incorporated into the operator's manual. Several additions to the cockpit instrumentation are proposed, and further maneuverability testing is recommended.

DD FORM 1 NOV 65 1473 REPLACES DD FORM 1473, 1 JAN 64, WHICH IS OBSOLETE FOR ARMY USE.

UNCLASSIFIED
Security Classification

14. KEY WORDS	LINK A ROLE	LINK A WT	LINK B ROLE	LINK B WT	LINK C ROLE	LINK C WT
AH-1G helicopter						
Maneuvering limitations flight test program						
Study characteristics						
Identify limitations						
Untorquing						
Cyclic						
Transient						
Overspeed						
Augmentation instability						
Pilot training						
Additions						
Further testing						